High-resolution hydraulic modelling as an approach to planning rehabilitation interventions in unchanneled valley-bottom palmiet wetlands: a case study of the Kromme River

A thesis submitted in fulfilment of the requirements for the degree of

MASTER OF SCIENCE

Of

Rhodes University

By

Wiebke Langner

ORCID ID: https://orcid.org/0000-0001-6057-9657

2022

ABSTRACT

This study employs high-resolution hydraulic modelling techniques to inform the planning of rehabilitation interventions in unchanneled valley-bottom palmiet wetlands, using the upper Kromme River wetlands as a case study. It investigates the impact of geomorphic processes on the morphology of the valley, how changes in valley morphology affect the flow characteristics (velocity, stream power, depth) of the river, and how these changes affect the geomorphic dynamics of the wetlands. An aerial LiDAR survey was conducted for a 23km-long reach of the upper Kromme River where the wetlands are situated. A high-resolution (5 m) DTM was created from the LiDAR data to examine the valley morphology. Focusing on three major wetland basins, the relationship between valley morphology and geomorphic processes was examined using high-resolution imagery that accompanied the LiDAR survey and Google Satellite imagery. The hydraulic modelling software HEC-RAS was used to investigate the spatial variation in velocity, stream power, and water depth down the surveyed length of the river. The model outputs provide insight into the effect of valley morphology on flow characteristics. The river appears to have a graded longitudinal profile, such that there is a systematic reduction in slope down its length. Water flowing down the river works, through the processes of erosion and deposition, to control the longitudinal slope, channel planform, and geometry to create a valley with a gentle longitudinal slope (approximately 1%) and a broad, near-horizontal valley-bottom in the mountainous landscape of the Cape Fold Mountains. The overall form of the Kromme River valley and wetlands is primarily a consequence of repeated cycles of cutting and filling. Tributary alluvial fans control the initiation of gully erosion in the wetlands, but their effect is diminished in a downstream direction. Despite a 10-fold increase in discharge down the 23km length of river for a given flood magnitude, there is no significant increase in flow velocity, stream power, or depth in a downstream direction. Consequently, the kinetic energy of the water in the lower wetland basin is surprisingly low. These conditions favour the establishment of palmiet. Flows in eroded reaches are much higher than in non-eroded reaches where discharge is spread across a broad valley bottom. In terms of palmiet establishment and regeneration, this means that areas dominated by depositional processes are best suited to the establishment of palmiet. Based on this information, optimal sites to trial new wetland rehabilitation strategies that employ palmiet were selected. This work supports the importance of understanding the role of geomorphology in wetland structure and dynamics when approaching wetland rehabilitation and is likely to be more sympathetic to natural processes than current interventions.

PREFACE

The research described in this thesis was carried out at the Department of Geography, Rhodes University, Grahamstown, from January 2015 to December 2016, under the supervision of Professor W.N. Ellery.

This study represents the original work by the author. Where use has been made of the work of others it is duly acknowledged in the text.

Name: Wiebke Langner

Student Number: G15L2822

Signed:

ACKNOWLEDGEMENTS

This research would not have been possible without the generous support of the following people and organizations:

I would like to thank my supervisor, Professor W.N. Ellery, sincerely for inspiring, encouraging, and helping me throughout my Master's journey. His vast knowledge of the complexities of wetlands and his endless curiosity to understand the natural world further will always stay with me.

I thank the South African National Biodiversity Institute for funding this research.

I'm grateful to the farmers and landowners in the Langkloof for allowing me access to the wetlands.

Lastly, I would like to thank my partner, Matthew Sephton, and my family for giving me the love, strength, and care I needed to persevere through my Master's journey.

TABLE OF CONTENTS

LIST OF FIGURES

LIST OF TABLES

CHAPTER 1: INTRODUCTION

1.1 Background

Traditionally, wetland formation has been conceptualized as being driven by hydrological factors (Gosselink and Turner, 1978, Mitsch and Gosselink, 2015). Rainfall, surface water and groundwater flow into a basin and contribute in site-specific ways to shallow flooding of the soil for extended periods. This creates flooded soils that rapidly become anaerobic; conditions that promote radical alteration of soil biogeochemistry, leading to changes in soil morphology and their suitability for life. In order to survive such conditions, plants need to adapt in order to transport oxygen into the root zone, while animals spending parts of their life cycle in shallow soils need to have adaptations to ensure that they have access to oxygen (Mitsch and Gosselink, 2015). These interactions between the hydrological regime, soil biogeochemistry and biota, are central to the ways that wetland scientists and managers think about wetlands. In terms of wetland rehabilitation, the mantra is that modification of hydrological conditions that led to wetland degradation, need to be reinstated in for a wetland to be rehabilitated.

However, in addition to hydrological conditions, geomorphological factors are increasingly becoming recognized as central to wetland formation, structure, and dynamics (Tooth *et al.*, 2002, Tooth *et al.*, 2004, Grenfell *et al.*, 2010, McCarthy *et al.*, 2011). The characteristics of wetlands that are central to the shallow flooding of soils in a landscape are 1) the presence of a near-horizontal valley cross-section and 2) the presence of a gentle longitudinal slope (typically less than 2 %, depending on wetland size; Tooth *et al.*, 2002, Tooth *et al.*, 2004, Ellery *et al.*, 2009, 2016). Such valley-bottom characteristics are the product of geomorphic processes that shape landscape morphology: erosion and deposition. It seems appropriate to say that wetland scientists and managers have been slow to embrace these ideas and incorporate them into wetland rehabilitation practices. This may be largely due to the fact that the incorporation of geomorphology into wetland management makes wetland rehabilitation far more difficult than are modifications to the wetland to improve its hydrological conditions. It would be fair to say that incorporation of geomorphic processes in wetland rehabilitation requires interventions that are often contrary to those that simply focus on reinstating the "natural" hydrological regime. For example, if erosion has taken place in a wetland (a geomorphic response to water flow), the focus of wetland rehabilitation based on hydrology, may be to ensure natural hydrological conditions are reinstated in that part of the wetland that has not been eroded. In contrast, the approach of scientists and managers that base decisions on geomorphic processes may be to focus on maintaining the natural geomorphic dynamic and focus rehabilitation efforts on accelerating natural recovery of the eroded reach from below the eroded gully. It is clear

that these two approaches are at loggerheads, and it may be that appropriate measures lie somewhere between these two conflicting viewpoints.

Geomorphic processes of erosion and deposition are the outcome of interactions between hydrological processes (discharge and the associated velocity and stream power), longitudinal slope, surface roughness and characteristics of the valley cross-section (hydraulic radius). In this respect the "hydrological regime" shapes valley morphology to accommodate the available flow, and over great lengths of time, distribute energy uniformly down the valley.

1.2 Palmiet

Palmiet (*Prionium serratum*) is a wetland plant that is endemic to the southern and south-eastern regions of South Africa. Many valley-bottom wetlands in the Cape Fold Mountains are dominated by palmiet, including the Kromme River wetlands. Palmiet significantly influences hydrogeomorphic characteristics because it limits erosion, resulting in wetlands that have an above-average slope relative to their size and flow. In palmiet-dominated wetlands, the plant seems to regulate the hydrological characteristics in the system (Rebelo 2012, Rebelo *et al.* 2015, Rebelo 2018, Rebelo *et al.*, 2018). For this reason, palmiet is considered an ecosystem engineer (Sieben 2012, Sieben *et al.,* 2018). It seems that palmiet plays a key role in stabilizing the valley bottom because it rapidly colonizes exposed sediments and then persists for long periods. It may be valuable for new wetland rehabilitation strategies to make use of palmiet's functional characteristics.

1.3 Hydraulic modelling

Hydraulic modelling techniques present a useful method to investigate the link between landscape morphology, geomorphic processes, and the hydraulic characteristics of the system (velocity, stream power, and depth). The hydraulic modelling undertaken in this research was intended to characterize the Kromme River valley based on typical flows in the system, and to characterize the hydraulics of the system, particularly the flow velocity and stream power (a general measure of the water's capacity to erode). Based on the premise that palmiet regenerates most effectively in low-energy settings, hydraulic modelling can reveal sites that are most suitable for trialling new rehabilitation strategies that employ palmiet.

1.4 Research aim and objectives

This study investigated relationships between geomorphic processes and flow characteristics down a 20 km reach of the upper Kromme River wetlands using hydrodynamic modelling. With this understanding it is hoped that an approach to wetland rehabilitation that incorporates hydrological and associated geomorphic processes will be achieved, to suggest a set of rehabilitation interventions more sympathetic with natural processes.

The specific research question is:

What are the optimal locations to trial novel wetland rehabilitation interventions that favour the establishment of palmiet in unchanneled valley-bottom palmiet wetlands using the Kromme River as a case study?

This study aims to use hydraulic modelling techniques to determine locations most likely to be favourable for novel wetland rehabilitation strategies in unchanneled valley-bottom palmiet wetlands to be put to the test, using the Kromme River as a case study.

To achieve the aim of this study, the objectives were the following:

1. Analyse the valley morphology in relation to geomorphic features and processes.
2. Apply the model and analyse hydraulic modelling outputs to determine the effect of valley morphology on stream hydraulics.
3. Select sites for trialling new wetland rehabilitation strategies that employ palmiet.

CHAPTER 2: LITERATURE REVIEW

2.1 Palmiet

Palmiet is a common riparian wetland species that is endemic to the southern and south-western regions of South Africa (Rebelo, 2012). It occurs in the valley-bottom wetlands of the Cape Fold Mountains, as well as catchments dominated by quarzitic lithologies Natal Group sandstones that are contemporaneous with the lower quartzitic lithologies of the Cape Supergroup (Peninsula and Skurweberg Formations) (Sieben *et al.,* 2018). Palmiet thrives in permanently flooded valley-bottom wetlands in the Cape Fold Mountains, and many valley-bottom wetlands in the region are dominated by palmiet. The Kromme wetlands contain extensive, dense stands of palmiet, especially in the upper Krugersland and Kompanjiesdrift wetlands. Wetlands such as these that are dominated by palmiet are referred to as palmiet wetlands (Rebelo, 2018).

Adapted to growing in permanently flooded soils, this semi-aquatic, evergreen plant grows to a height of about 3 m and reproduces clonally to form large, monospecific stands on river floodplains and open water areas along river edges (Barclay, 2017). Palmiet's long, pale-green leaves are stiff and leathery. During flood events, they drape down over the stems, shielding them from moving rocks (Boucher and Withers, 2004, Job, 2014). Their flexible stems allow them to bend sideways against the channel banks or prostrate on the valley floor during very high flows, shielding the banks and bed from erosion (Gull, 2012). Palmiet wetlands generally exist on slopes that are relatively steep for their size and flow because they limit erosion (Ellery *et al.,* 2009).

Palmiet is considered an ecosystem engineer because it exerts control on geomorphic processes and valley morphology (Sieben, 2012, Barclay, 2017, McNamara, 2017, Pulley *et al.,* 2018, Sieben *et al.*, 2018). The fibrous remains of old leaves remain attached to the plant, covering the main stem (Barclay, 2017). Its extensive root system and network of stems trap significant amounts of sediment (Gull, 2012). The growth of palmiet and the sedimentation it causes alter a wetland's morphology and hydrology (Rebelo 2012, Rebelo *et al.,* 2015, Rebelo 2018, Rebelo *et al*., 2018). It colonizes open bodies of water, growing from channel banks and floating islands into river channels, slowing the flow and ultimately blocking the channel (Job, 2014). Diffuse flow through the large, dense stands of palmiet, helps to create sufficiently low-energy hydrological conditions favourable to peat formation (Job, 2014).

It is widely accepted that palmiet wetlands need to be conserved, and the Kromme River palmiet wetlands are regarded nationally as important palmiet wetlands (Rebelo *et al*., 2015). However, there is a limited understanding of palmiet's recruitment and regeneration ecology, besides that it

reproduces both sexually and vegetatively. Conservation efforts can be much more effective if we better understand how this plant colonizes suitable habitats.

It is becoming evident (van Eck, 2022, In Prep.) that habitats suited to palmiet recruitment and establishment are eroded gullies and depositional features that form after cycles of valley-floor cutting and filling, as described by Pulley *et al*. (2018). Field observations indicate that palmiet colonizes newly exposed sediments on gully beds, sandy depositional features, like floodouts and bars (van Eck, 2022, In Prep.), and areas of open water adjacent to channel banks (Job, 2014). Palmiet also occurs in wetlands that have not been disturbed by erosion for decades to centuries, like the Krugersland and Kompanjiesdrift wetlands.

The fact that palmiet dominates both geomorphically stable wetlands, as well as recently disturbed sediments presents an interesting dichotomy. It seems that palmiet is adapted to exploiting periodic disturbance events, such as those described in the Kromme wetlands by Pulley *et al.* (2018). However, it rapidly colonizes exposed sediments and then persists for long periods, promoting the stability of the valley floor.

The typical rehabilitation strategy implemented in palmiet wetlands involves the installation of structures designed to halt erosion, thereby "protecting" upstream stands of palmiet. But because palmiet actively colonizes newly exposed sediments from erosional events, it may be that these natural geomorphic dynamics are central to the plant's persistence in these wetlands. Current rehabilitation interventions might, therefore, be counterproductive.

2.2 Wetlands and fluvial geomorphology

Wetlands form where there is a positive water balance and an excess supply of surface water, such that soils are flooded for extended periods and become anaerobic, causing plants to adapt.

The factors influencing the water balance in valleys are summarized by the following equation (Mitsch and Gosselink, 2015):

$$\Delta V/\Delta t = Pn + Si + Gi - ET - So - Go$$

Where:

- ΔV represents the change in volume of surface water in a valley,
- Δt is the period of time,
- Pn is the input from precipitation,
- Si is the input from surface water inflow from hillslopes or an inflowing river,
- Gi is the input from groundwater discharge,

- ET is the water loss via evapotranspiration,
- So is the water loss to surface outflows along a river,
- Go is the loss of surface water to groundwater as groundwater recharge.

The climate in southern Africa is semi-arid, and the rate of evaporation is greater than that of precipitation. This negative net water balance means that most large wetlands in this region are primarily fed by rivers, not by rainfall. Because southern African wetlands are part of fluvial systems, their structure, functioning, and dynamics must be viewed in the context of fluvial geomorphology (Tooth and McCarthy, 2007).

Wetlands in southern Africa's highly incised landscape are integrally linked to fluvial networks (Tooth and McCarthy, 2007, Ellery *et al*., 2009). These fluvial wetlands are fed primarily by stream flow, with precipitation and groundwater seepage acting as supplementary water sources (Tooth *et al.,* 2002, Ellery *et al.,* 2009, Job, 2014, Ellery *et al.,*2022, In Prep).

Because of the link between wetlands and fluvial networks, fluvial geomorphology has been increasingly recognised as a theoretical framework for understanding the origin, dynamics, and threats to wetlands in southern Africa. Fluvial geomorphology as a field aims to understand how water flowing in streams and rivers has influenced the form and evolution of landscapes (King, 1963, Leopold *et al.,* 1964, Edwards *et al.,* 2009). Tooth *et al* (2002, 2004), Tooth and McCarthy, (2007), Grenfell *et al.,* (2008, 2009, and 2010), and Ellery *et al.,* (2009, 2013) have studied various wetlands in South Africa employing this approach.

While southern African wetlands are generally linked to fluvial networks, it must be noted that the hydrological characteristics of these wetlands are different than those of streams and rivers (Ellery *et al.,* 2009). Streams are higher energy systems with faster flow, compared to wetlands, that are low energy systems with slower flows that cause prolonged flooding (Ellery *et al.,* 2009).

Wetlands do not simply form when pre-existing landscapes are flooded for an extended period of time. Wetlands form in valleys where fluvial processes contribute to the reduction of longitudinal slope through erosion, and where processes that laterally plane the valley floor dominate over vertical erosion (Tooth *et al.,* 2002, Tooth *et al.,* 2004; Ellery *et al.,* 2009). Streams work to produce environments that are broad, flat, and gently sloping, where wetland systems can form (Ellery *et al.,* 2009).

2.3 Wetland classification

One of the first things that wetland rehabilitation practitioners must know when they prepare to begin work in a wetland is what type of wetland it is. This supports effective wetland management and conservation because the type of wetland informs the rehabilitation approach.

There are many different wetland classification systems that categorise wetlands based on their landscape setting, ecology, hydrology, or substrate composition. These classification systems are useful to support wetland inventory, but do not account for long-term landscape processes. Therefore, they provide no indication of a wetland's origin, functioning, and dynamics.

A new genetic geomorphic classification for wetlands was developed by Grenfell *et al.* (2019). It aims to categorize wetlands based on the fundamental landscape processes that resulted in their formation. The system divides wetlands into four macrotypes based on their sediment source – colluvial, alluvial, aeolian, and geochemical. The macrotypoes are sub-divided into eight wetland types based on the location of a wetland within a landscape, the morphology (cross-section and longitudinal slope) of the wetland, and the geomorphic features and processes that occur in the wetland. The eight wetland types are: hillslope seep, floodplain, valley-bottom, plain, blocked-valley, alluvial fan, aeolican depression, and geochemical depression (Grenfell *et al*., 2019).

According to the genetic geomorphic classification system, these wetland types are further divided into sub-types based on the presence or absence of a discontinuous channel outflow, the presence or absence of a river channel, indicators of lateral channel migration, or the type of underlying bedrock (Grenfell *et al*., 2019).

The wetlands in this study are classified as alluvial unchanneled valley-bottom wetlands because they have a discernible valley boundary, the valley floor is broad and near-horizontal cross-section, the longitudinal slope is steeper than a typical floodplain wetland, the elevation of the thalweg decreases with distance downstream, and the wetland is densely vegetated such that flow across the wetland is diffuse and there is no channel (Grenfell *et al*., 2019).

2.4 Geomorphic origin and development of fluvial wetlands

There is growing consensus that geomorphology cannot be neglected as a key driver of wetland formation and that it has a key influence on wetland structure, functioning, and short-term changes in wetland systems (Tooth *et al.,* 2002, McCarthy *et al.,* 2011). Geomorphic processes are affected by climate, and the interaction of these controls the hydrology of a landscape and its ecology.

Geomorphic processes that contribute to the formation of a landscape wherein a wetland can exist need to be considered if wetland origin, structure, functioning, and dynamics are to be understood

(Pulley *et al.,* 2018). The two major geomorphic processes associated with changes in landscape morphology are erosion and deposition. Erosion is a slope lowering process, while deposition increases the slope (Ellery, *et al.,* 2009). These processes affect how water is distributed in a landscape, and this influences the ecological structure and functioning of a wetland ecosystem. Wetland rehabilitation practitioners require a holistic understanding of how wetland systems formed, their structure, functioning, and dynamics so that rehabilitation interventions can bring about positive effects (Ellery, *et al.,* 2009).

Growth in our understanding of the importance of geological controls and geomorphological processes leading to wetland formation, structure, and dynamics started following decades of work in the Okavango Delta, as captured in McCarthy and Ellery (1995) and spelled out in much more detail in subsequent publications involving these two authors (McCarthy *et al.,* 1993, McCarthy and Ellery, 1995, McCarthy *et al.,* 1997, Gumbricht *et al.,* 2001, McCarthy *et al.,* 2002, Ellery and Ellery, 2022). In these publications, the overall control of the Okavango Delta ecosystem was recognized as being a consequence of rifting associated with the south-western extension of the East African Rift Valley (McCarthy and Ellery, 1995), with clastic sedimentation within the rift valley leading to a large alluvial fan that gives the Okavango its overall morphology (Gumbricht *et al.,* 2001).

A number of conceptual models that explain the origin and dynamics of southern African wetlands have been posited.

2.4.1 Geological controls on wetland formation

One of the most well-known models for the formation of wetlands was developed by Tooth *et al*. (2002) following their research in the Klip River floodplain near Memel on the Highveld of the eastern Free State (Tooth *et al.,* 2002, 2004). This model suggests that underlying geology exerts a key control on the development of floodplain wetlands, such as those in the upper Klip River.

In valleys where there is an erosion-resistant lithology, like a dolerite sill or dyke, downstream of a less erosion-resistant lithology, such as sandstone or shale, the resistant lithology acts as a local base level. Upstream from this base level, the stream incises vertically until its gradient is appropriate for its discharge and sediment load, after which it erodes laterally via a meandering channel. The lateral erosion widens and planes the valley, creating a broad, flat landscape where a wetland can form (Tooth *et al.,* 2002, 2004). Geomorphic features that characterize floodplain wetlands that have formed in this manner include elevated alluvial ridges, oxbow lakes, and back swamps (Tooth *et al.,* 2002, 2004).

The catchment of the Klip River is on shale, which weathers easily. After flowing across tens of kilometers of shale, the river crosses a dolerite dyke, which is extremely resistant to erosion. This

lithology acts as a local base level, upstream of which the Klip River erodes its bed to the slope beyond which it cannot erode further, at which point the stream starts to meander and carve the valley laterally, creating a floodplain with a near-horizontal cross-section and a very gentle longitudinal slope (Tooth *et al.,* 2002). Lateral channel migration occurs when there is a large sediment supply (Tooth *et al.,* 2010).

2.4.2 Wetland formation related to trunk-tributary interactions

Further work on the Nyl River wetland in Limpopo Province by McCarthy *et al*. (2011) and Wakkerstroom Vlei in Mpumalanga Province (Joubert and Ellery, 2013) revealed the role of tributary alluvial fans across the trunk valley, lowering trunk valley slope in an upstream direction, leading to wetland formation. In cases where the lowering of the slope is sufficient to lead to prolonged flooding, peat forms.

Models of the origin of valley bottom wetlands suggest that geomorphic processes controlled by trunk and tributary stream interactions create a landscape where a wetland can form (Grenfell *et al.,* 2008, Grenfell *et al.,* 2010, McCarthy *et al.,* 2011, Ellery *et al.,* 2012). Key factors in these models are the rates of sediment deposition and the capacity of the trunk stream relative to the tributary stream (Grenfell *et al.,* 2010).

In trunk valleys with tributaries from smaller, less erosive catchments, the trunk stream's rate of sedimentation may be higher than that of the tributaries (Grenfell *et al.,* 2008, Grenfell *et al.,* 2010). In this case, the more rapid aggradation in the trunk stream can create a blockage of the tributary stream (Grenfell *et al.,* 2008). The blockage acts as a local base level, so the tributary stream incises in an upstream direction to lower its slope (Grenfell *et al.,* 2008, Grenfell *et al.,* 2010). The reduction in slope creates conditions where a valley bottom wetland can form (Grenfell *et al.,* 2008).

In trunk valleys where steep tributary streams from large, erosive catchments join the trunk stream, they deposit large amounts of sediment on the trunk valley floor (McCarthy *et al.,* 2011, Joubert and Ellery, 2013). If the trunk stream's capacity and rate of sedimentation are lower than that of the tributary, the trunk valley can become blocked by tributary sediment, either fully or partially (McCarthy *et al.,* 2011, Joubert and Ellery, 2013). Along the trunk stream, the blockage acts as a local base level, creating accommodation space upstream where sedimentation occurs and flows become more diffuse (McCarthy *et al.,* 2011). Conditions that promote prolonged flooding are created, and a wetland can form in the blocked trunk valley (Grenfell *et al.,* 2010, McCarthy *et al.,* 2011). This model of wetland formation seems to apply to the Nyl River floodplain wetland in Limpopo Province, South Africa.

2.4.3 Cut-and-fill cycles as a mechanism for wetland formation

A number of studies in the Kromme River valley suggest that repeated cycles of gully cutting and filling have laterally planed the bedrock and led to the evolution of a broad valley with a near-horizontal floor that can host a wetland (Lagesse, 2017, Schlegel, 2017, Pulley *et al.,* 2018). Valleys in the Cape Fold Mountains are generally narrow due to the faulting and folding of the mountains. Therefore, the Kromme River valley must have been widened and planed through geomorphic processes. Erosion seems to be a process that is intrinsic to the landscape.

Pulley *et al*. (2018) proposed a model to explain the role that gully erosion has played in creating a valley with a near-horizontal cross-section and a gentle longitudinal slope that can host a wetland. In this model, repeated cut and fill cycles associated with gully erosion laterally plane a valley, leading to valley widening and lowering of the longitudinal slope, creating a landscape suitable for wetland formation.

Steeply sloping tributary streams flow into the Kromme River valley from adjacent catchments. Where the tributaries join the trunk stream, they deposit large amounts of sediment onto the valley floor in the form of alluvial fans. These tributary alluvial fans reduce the width of the trunk valley and locally steepen the longitudinal slope of the trunk valley (Pulley *et al.,* 2018). This results in flows being concentrated, increasing the chance of gully erosion being initiated during flood events (Schlegel, 2017).

Once gully erosion has been initiated, the gully propagates upstream along the trunk valley. It incises down to bedrock, and the coarse sediment that is produced at the head of the gully is deposited directly downstream at the toe of the gully, filling it in an upstream direction (Lagesse, 2017). When the gully is completely infilled, the resulting depositional feature is elevated in the center of the valley relative to the margins. These depressions along the valley margins are where flows are concentrated and where future cycles of erosion are initiated (Lagesse, 2017).

With each cycle of cutting and filling, the Kromme River valley is widened, and the longitudinal slope is lowered. Over tens of thousands of years, these geomorphic processes created a valley that is suitable to host a wetland.

Cycles of cutting and filling are not unique to the Kromme system. They have been observed and investigated in many different landscape settings in North America (Antevs, 1952, Patton and Schmm, 1975, Womack and Schumm, 1977), South America (Bekkaddour *et al*., 2014), Australia (Brierley and Fryirs, 1999), South Africa (Botha et al., 1994), and Zambia (Burrough *et al*., 2015). Generally, cut-and-fill cycles, are defined as alternating phases of incision via gully erosion followed by phases of filling via deposition of sediment within previously eroded gullies (Nanson and Croke,

1992, Brierley and Fryirs, 1999). A discontinuous stream network is a common trend in fluvial systems characterized by cut-and-fill cycles (McNamara, 2017).

2.5 Geomorphic processes affect stream hydraulics

Understanding the geomorphic processes that control a trunk valley and wetland's morphology can provide insight into the hydrodynamics of the system. As channel planform and geometry are altered by erosional and depositional processes, so are flow characteristics, like velocity and stream power. Rivers accommodate a given discharge by adjusting channel width, depth, and longitudinal slope (Ellery *et al.,* 2009). When slope and bed roughness are constant, flow velocity and stream power are greater in narrow, deep channels than in broad, shallow channels. When bed roughness and channel geometry are constant, flow velocity and stream power are greater on steep slopes than on gentle slopes. For example, where large tributary alluvial fans impinge the trunk valley bottom and the valley is narrowed, the river accommodates the discharge across a narrower cross-section, and the depth of flow increases. Therefore, flow velocity and stream power are greater in these reaches during flood events. This type of understanding of the relationship between geomorphic processes, valley morphology, and stream hydrodynamics allows researchers to infer where erosion and deposition are most likely to occur during a flood event.

The hydraulics of fluvial systems follow that of open channel flow, wherein discharge, depth, gradient, and bed roughness are all independent variables (Chow, 1959). These variables can change over time, affecting the channel's cross-sectional geometry or longitudinal slope. It can be difficult to determine the flow hydraulics in wetlands (Schlegel, 2017). Wetlands generally have low flow velocities and low gradients, and roughness is highly variable (Schlegel, 2017).

How water flows down a valley is affected by the geomorphic processes that are at work in the system. The geomorphic processes of erosion and deposition alter valley morphology and create geomorphic features, like alluvial fans, floodouts, and gullies. Alluvial fans, which are depositional features, can reduce valley width, steepen the longitudinal slope in a downstream direction, and lower the slope in an upstream direction.

The impact of geomorphic features on stream hydraulics can best be appreciated in hydraulic modelling. In theory, it is expected that where alluvial fans reduce valley width and increase longitudinal slope locally in a downstream direction, the flow velocity is greater than in reaches unconfined by alluvial fans (for a given discharge). Where stream flow is confined to erosional gullies, velocity is greater than in reaches where flow is unconfined and spread across a broad valley bottom.

2.6 The concept of a graded river

When conceptualizing geomorphic processes in fluvially integrated wetlands, it is useful to think of drainage networks as unified systems that are in dynamic equilibrium, where a change in one part of the system leads to changes in other parts (Leopold *et al.*, 1964, Schumm, 1977, Ellery *et al.,* 2009). The most important variables at play in fluvial systems are discharge, velocity, channel planform and cross-sectional geometry, gradient, sediment load, and base level (Leopold and Maddock, 1953, Schumm, 1977, Ellery *et al.,* 2009, Phillips, 2010).

Streams respond to a natural or artificial change in one of these variables by altering one or more of the other variables (Lagesse, 2017). Streams adjust their gradient and channel shape (width and depth) to accommodate a given volume of water (discharge) and sediment such that potential energy is distributed as uniformly as possible down the length of the stream (Ellery *et al.,* 2009).

When a river's channel form and gradient are balanced to transport a given discharge and sediment load such that neither erosion nor deposition occurs, a river is in equilibrium and is referred to as a graded river (Leopold and Bull, 1979, Ellery *et al.,* 2009). Most rivers are continuously working towards this ideal condition, constantly adjusting and evolving as the landscape is gradually lowered by erosion (Ellery *et al.,* 2009).

Drainage networks generally have a concave upward longitudinal profile, from their headwaters to their ultimate base level, the sea (Ellery *et al.,* 2009). A base level is the lowest level to which a river can incise its bed (Leopold and Bull, 1979). Along a river's profile can exist several local base levels, such as, for example, a reach where a tributary stream enters a trunk stream and deposits sediment (Joubert and Ellery, 2013), where the stream flows across a more resistant lithology than upstream (Tooth *et al.,* 2002), or where there is an impoundment along the stream.

Moving water has kinetic energy that performs work. The work mainly involves lifting, transporting, and depositing sediment. Erosion and deposition are the two main processes that rivers use to adjust their gradient and channel form (Ellery *et al.,* 2009). Sediment deposition causes aggradation and an increase in longitudinal slope in a downstream direction, whereas erosion leads to slope reduction (Ellery *et al.,* 2009).

The appropriate longitudinal slope of a stream bed is related to the typical discharge (with a return interval of about 5 years). Where its gradient is too steep for the supplied discharge and sediment, erosion occurs to lower the slope (Ellery *et al.,* 2009). Where a river's gradient is too low for its given discharge and sediment load, deposition occurs to increase the slope (Ellery *et al.,* 2009).

As discharge increases down the length of the river, the appropriate slope of the bed decreases (Ellery *et al.,* 2009). A stream evolves to produce a logarithmic longitudinal slope through the processes of erosion and deposition down the length of the stream. If a stream if graded and the slope is appropriate for the discharge all the way down the stream, the hydraulics should, in theory, be similar all the way down the length of the stream (Leopold and Bull, 1979, Ellery *et al.,* 2009).

2.7 Connectivity

Theoretically, fluvial systems transport water and sediment from landscapes towards the sea. The conceptual framework of landscape connectivity has been around for a long time. It describes how efficiently sediment moves through a fluvial system. Early definitions were based on the fluvial system model that was proposed by Schumm (1981). This model divides fluvial systems into three main zones, each with one dominant geomorphic process:

- The catchment landscape – where processes of hillslope erosion supply the stream channel with sediment.
- The river system – where transport processes move sediment downstream through the catchment.
- The coast – whether depositional processes cause sediment to accumulate.

A shortcoming of this model is that it implies that landscape development occurs in three separate zones down the length of a stream, and that the upper reaches are erosional, the middle reaches are where sediment is transported, and the lower reaches are depositional. Realistically, sediment can be entrained, transported and deposited in any landscape zone within a catchment, and the three processes can happen simultaneously in different zones (Bracken *et al*., 2015, McNamara, 2017).

Fluvial geomorphologists generally agree that within catchments there are localized zones where sediment is either eroded, transported, or deposited (Harvey, 2001, Hooke, 2003, Brierley *et al*., 2006, Fryirs *et al*., 2007, Harvey, 2012, Fryirs, 2013, Bracken *et al*., 2015, McNamara, 2017). Bracken *et al*. (2015) recognized that within a catchment landscape there are sources of sediment and sediment sinks and stores, and that not all sediment that is generated ends up in the sea.

Geomorphic systems' sediment flux varies on a continuum from highly connected (where there is a continuous movement of sediment through a catchment) to disconnected (where sediment entering a system is deposited in local geomorphic features, such as a wetland) (McNamara, 2017).

Sediment cascades and how streams respond to disturbance are dependent on how geomorphic features are configured within and between landscape units (Fryirs *et al.,* 2007). Natural processes, and factors such as sediment grade, trunk-tributary stream interactions, and cycles of erosion, can

enhance or inhibit sediment connectivity, or this may happen due to anthropogenic activities, such as excavation and draining of wetlands or placement of impoundments like weirs in wetlands (Brierley *et al*., 2006, Fryirs *et al*., 2007, Fryirs, 2013).

2.8 Impelling and resisting forces in streams

The potential energy that a river has is a product of the discharge acting on a given slope. Where erosion or deposition occurs is related to the balance between resisting and impelling forces, involving four components: the sediment load being transported, sediment grain size, discharge, and stream slope. This concept was best illustrated by Lane, 1955 (Figure 1).

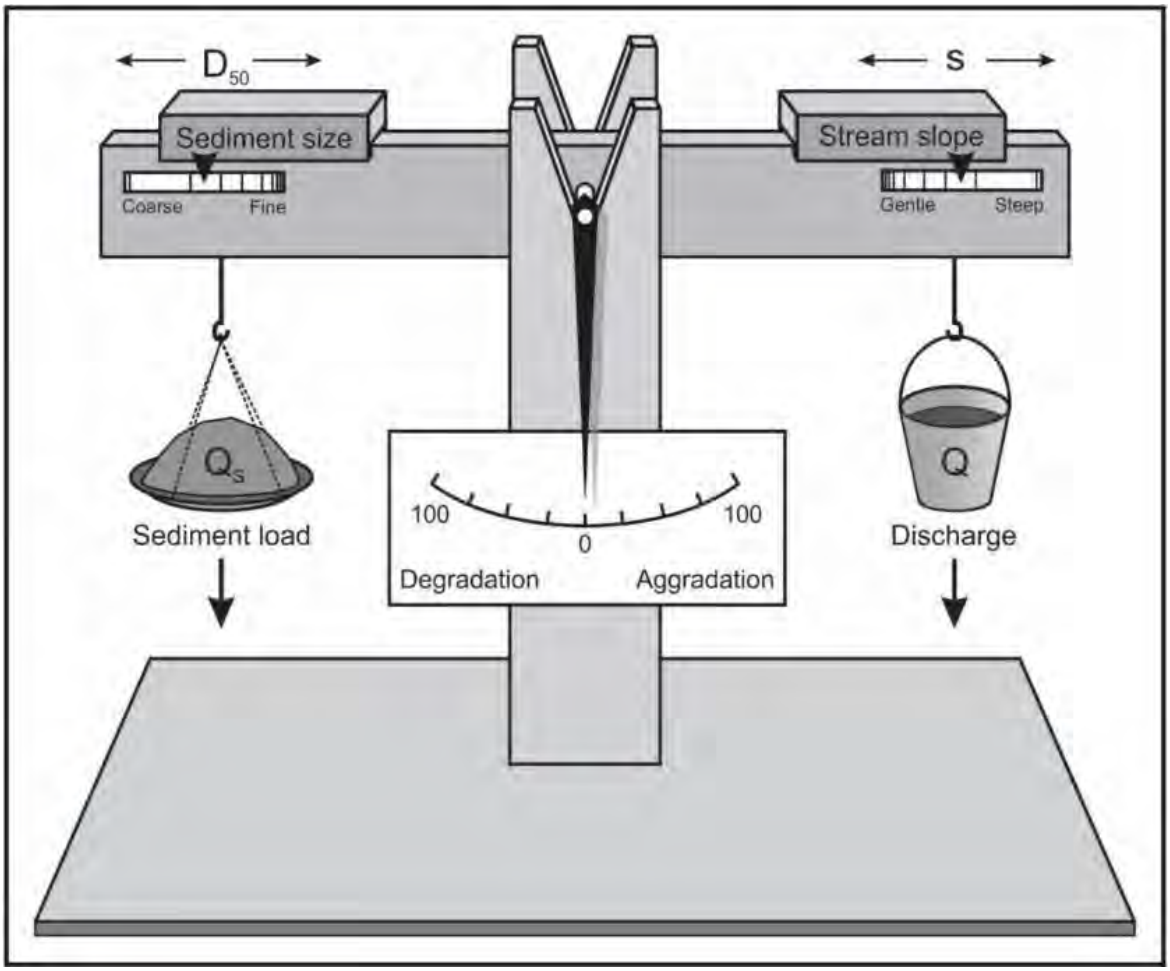

Figure 1: The Lane balance diagram showing how flow and sediment interactions determine the balance of aggradation and degradation in streams (Modified after Lane, 1955).

If a stream has more potential energy than is required to transport its discharge and sediment load, the excess energy causes adjustment of the stream morphology through erosion (Ellery *et al*., 2009). If a stream has less than the required amount of energy to transport its discharge and sediment load, deposition will occur (Ellery *et al*., 2009). The balance between impelling and resisting forces determines whether erosion or deposition will be dominant in a certain reach, which results in

streams performing work to achieve an appropriate longitudinal slope along their entire length for their available discharge and sediment loads (Lane, 1955).

While discharge is the primary variable relating to impelling forces, stream power is the most appropriate outcome of variation in discharge to consider when trying to understand the likelihood of erosion (Fryirs and Brierley, 2012). Another important factor to consider is the roughness of the stream bed as it is a factor that influences the likelihood of erosion. Manning's roughness (n) is, therefore, the most appropriate factor to consider in determining the relationship between discharge and the likelihood of erosion (Fryirs and Brierley, 2012).

2.8.1 Stream power

The concept that sediment entrainment is related to the energy of a stream – a product of river discharge, slope, and gravity – is well established in early work (Gilbert and Murphy, 1914, Rubey, 1933, Knapp, 1938). Bagnold (1966) was the first person to coin the term stream power. He quantified the rate of energy supply to a length of a river using a first-principles approach to investigate how sediment is transported in stream channels, (Bagnold, 1966). Stream power has become a very useful variable, and it has a diverse range of applications. Presently, Bagnold's pivotal 1966 paper is cited over 3200 times on Google Scholar. This demonstrates what a multitude of applications there are for the concept.

Stream power (Ω) was defined as the product of discharge, slope, and the mass of the water:

$$\Omega = \rho\, g\, Q\, S$$

Where p is the density of water (1000 kg/m^3), g is the gravitational constant (9.8 m/s^2), Q is river discharge, and S is the channel slope or energy gradient. Units are in N.m^{-2}.

With improved technology and computing power, as well as new developments in the fields of remote sensing and GIS, stream power is a factor that is increasingly being used by fluvial geomorphologists and engineers because it can be computed remotely, without the need for time-consuming and laborious topographical field surveys (Gartner, 2016). DEM analysis is advancing rapidly, allowing for more detailed investigation of downstream changes in stream power that would otherwise not be possible using field surveys as a way to calculate stream power (Gartner 2016).

Stream power is directly related to sediment transport (Bagnold 1960, 1966, 1977, 1980). This important relationship has been used to investigate geomorphic questions across a wide range of spatio-temporal scales, from the rate of sediment transport in a river cross-section (Bagnold, 1966) to the long-term evolution of longitudinal river profiles (Kirby and Whipple, 2001). Several studies have shown that stream power has a significant influence on channel pattern and form (Chang,

1979, Kondolf *et al*., 2003, Wohl, 2004), bedload sediment grain size (Snyder *et al*., 2013) channel degradation and aggradation (Bull, 1979), sudden geomorphic changes following flood events (Magilligan, 1992, Buraas *et al*., 2014), and floodpain dynamics (Nanson and Croke, 1992).

There is a growing body of research that demonstrates the importance of analysing spatial variation in stream power to investigate channel form (Bizzi and Lerner, 2015) and determine the locations of erosion and deposition (Graf, 1983, Gartner *et al*., 2015, Lea and Legleiter, 2016). Sediment transport is a key consideration for scientists, engineers, and managers wanting to determine which reaches along a river are prone to erosion or deposition (Gartner, 2016).

2.8.2 Manning's equation

The velocity of surface water flow is mathematically described using Manning's Equation:

$$V = \frac{R^{\frac{2}{3}} \times s^{\frac{1}{2}}}{n}$$

Where V is velocity, R is the hydraulic radius (cross-sectional area/wetted perimeter), s is slope, and n is Manning's roughness coefficient.

When all other variables are constant for a given discharge:

(a) for a given roughness and slope, wide, shallow channels have a lower velocity than deeper, narrower channels,

(b) for a given roughness and hydraulic radius, steep channels have a higher velocity than channels with a gentler gradient, and

(c) for a given slope and hydraulic radius, streams that are densely vegetated (high Manning's roughness value) have a lower velocity than unvegetated channels (Ellery *et al.,* 2009).

2.8.3 Manning's roughness coefficient

Hydraulic roughness is an essential variable in many hydrological calculations. As water flows over a land surface there is a certain amount of frictional resistance. The resistance to flow is a major factor that determines flow velocity. The higher the roughness coefficient, the lower the flow velocity. The resistance to flood flows in open channels and floodplains are represented by roughness coefficients. Manning's roughness coefficient, or n-value, is one roughness coefficient that is used extensively to predict the roughness in channels. Manning's n-value is what hydraulic modelling programs like HEC-RAS uses to represent roughness.

There are a range of factors that determine the Manning's roughness coefficient for channels and floodplains, like vegetation density, the type of sediment that compose the channel bed and banks,

channel sinuosity, and channel morphology (Schneider and Arcement, 1989). A number of researchers have published tables of suggested Manning's n-values for various types of natural channels based on channels and floodplains with verified roughness values (Chow, 1959, Henderson, 1966, Streeter, 1971). Assigning roughness values to different channel reaches for the purposes of hydraulic modelling can be challenging because of how variable Manning's n-value is. Values in natural channels differ significantly from values on vegetated floodplains because the physical shape, composition, and vegetation is quite different.

Schneider and Arcement (1989) published a guide for selecting Manning's roughness coefficients for natural channels and floodplains. This guide suggests that vegetation density of a floodplain should be evaluated to determine the roughness coefficient (Schneider and Arcement, 1989). Floodplains and channels should be divided into segments, and each segment should be assigned a base n-value. The base n-values should then be adjusted for factors such as irregularity of channel banks, variation in channel morphology, obstructions (boulders, stumps, logs, debris, bridges), vegetation, and the degree to which the channel meanders (Schneider and Arcement, 1989).

2.9 Modelling in fluvial geomorphology

Since the 1950s, modelling has become an increasingly significant tool in research activities, given the need to study environmental systems in an integrated manner (Wainwright and Mulligan, 2013). Modelling provides researchers with a virtual laboratory, or a low-risk, low-cost way to test hypotheses and predict the outcomes of processes (Wainwright and Mulligan, 2013). A model is simply an abstraction of a natural system. If maps and drawings are considered an abstraction of the form of a natural system, models can be viewed as an abstraction of the processes in a natural system. However, natural systems are extremely complex, and it is impossible to build a model that represents a system exactly as it is in reality (Wainwright and Mulligan, 2013).

Fluvial geomorphologists use models to investigate how landscapes are shaped by water – the mechanisms that drive fluvial processes, and the feedbacks and dynamics that exist (Coulthard and van de Wiel, 2013, Wainwright and Mulligan, 2013, Grenfell, 2015). Modelling allows geomorphologists to experiment with all the variables and parameters that characterize a system (Coulthard and van de Wiel, 2013, Grenfell, 2015). A geomorphic model is a computerised simulation of a geomorphic system (a reach of a river or a river catchment) that represents the most important parts of the system and how they interact based on physical laws (Coulthard and van de Wiel, 2013). Which parts and how they are represented within the model, depends on the question that the modeller seeks to answer (Coulthard and van de Wiel, 2013).

Fluvial geomorphic systems are particularly challenging to model due to their complexity and the non-linear nature of geomorphic responses (Coulthard and Van De Wiel, 2013). Modelling in fluvial geomorphology requires the modeler to break a complex system up into simple, manageable subsystems that are connected by flows of matter, energy, or causality (Wainwright and Mulligan, 2013). For example, instead of trying to model the movement of water from the head of a wetland to the toe, the wetland area can be divided into discrete units (squares in a raster grid), and the movement of water between squares can be modelled.

Numerical models allow researchers to predict the future and consider geomorphic changes over various time scales (Wainwright and Mulligan, 2013). Running repeated model simulations or iterations that have small differences in their variables and parameters leads researchers to answer questions and develop novel insights about the system (Coulthard and van de Wiel, 2013). This makes modelling an effective and widely used tool for environmental management planning (Grenfell, 2015, Schlegel, 2017).

Environmental policy makers often seek qualitative and quantitative predictions of how a certain management activity will affect a landscape, and modelling allows these forecasts to be made (Schlegel, 2017). Grenfell (2015) regards numerical modelling software as an essential tool for wetland geomorphologists, as it allows one complete control over the definition of physical laws and boundary conditions, making it possible to test conflicting hypotheses, explain and clarify key processes and assess what conditions are necessary to elicit a certain response from a system. Modelling allows researchers to gain insights that are beyond the scope of field observations and laboratory experiments (Grenfell, 2015).

Numerical models all vary in their level of complexity, computational cost, and realism (Coulthard and van de Wiel, 2013). Each model has a unique purpose for which it was designed (Wainwright and Mulligan, 2013), as well as strengths and weaknesses or limitations (Coulthard and van de Wiel, 2013). It is important to bear in mind that all models are simplified representations of reality and that it is impossible to create a model that represents all biological and physical processes, their feedback effects, and how they control the movement of water across a landscape (McCartney and Acreman, 2009, Wainwright and Mulligan, 2013).

The body of research on modelling approaches and applications has grown rapidly in recent years, and so has the number of fluvial modelling codes. They are available commercially and non-commercially (Grenfell, 2015). This wide variety presents a challenge when selecting a code that is appropriate for the purpose of the research. It is important to understand how key elements of the

code work and consider the spatial and temporal scale of the system to be modelled (Coulthard and van de Wiel, 2013).

Computational Fluid Dynamics (CFD) models are used in fluvial geomorphology to simulate the flow of water over a landscape based on basic physical laws like the conservation of mass (no water is created or destroyed as it flows) and the conservation of energy (water obeys Newton's second law of motion – when a force acts upon the flow there will be a change in flow velocity, Coulthard and van de Wiel, 2013). The equations describing a system are then solved using a numerical algorithm over a regular grid of cells that spatially represents the land surface (Coulthard and van de Wiel, 2013).

CFD models are coupled with sediment transport algorithms, allowing the model to change the topography over which flow is being modelled in response to the flow. This makes these models particularly useful for fluvial geomorphologists who want to investigate the entrainment, erosion, transport, and deposition of sediment (i.e., how a landscape changes due to flow) (Coulthard and van de Wiel, 2013). These coupled CFD models are more complex and have very high computational demands, meaning that they are best applied at a localised reach scale (Coulthard and van de Wiel, 2013).

2.10 Wetland degradation in South Africa

Wetlands in South Africa have experienced significant degradation and many wetland ecosystems have been completely lost through anthropogenic activities (Dini and Bahadur, 2016). The South African government has recognized the importance of wetlands to society, both in terms of biodiversity and the useful ecosystem services they provide. Therefore, in 2000, Working for Wetlands (WfW), a national wetland rehabilitation programme, was launched. Since it's establishment, WfW has worked on rehabilitating an average of 79 wetland ecosystems per year (Dini and Bahadur, 2016). However, despite the concerted effort to rehabilitate wetlands, the 2011 National Biodiversity Assessment revealed that wetlands are still the most threatened ecosystem type in South Africa (Driver *et al*., 2012).

2.10.1 Gully erosion in wetlands

Soil erosion is a global phenomenon that is recognized as central to land and water resource degradation (Wasson *et al.,* 2002, de Vente *et al.,* 2005, Valentin *et al.,* 2005). Globally, gully erosion is a serious issue because it destroys fertile land and generates large quantities of sediment, which increases the siltation rates of dams and affects the water quality. Gully erosion in wetlands is considered a major contributor to wetland degradation and collapse. It is viewed as central to destroying these ecologically and economically valuable ecosystems (Ellery *et al.,* 2009).

Gully erosion is considered a major cause of wetland loss and degradation in South Africa (Ellery *et al*., 2009, Russell *et al*., 2009, De Haan, 2016), especially in palmiet wetlands (Rebelo, 2018, Nieuwoudt *et al*., 2018). When gullies form, large quantities of sediment is generated, which can negatively affect water quality and the capacity of dams and reservoirs (Schlegel, 2017). Because gully development increases runoff and sediment connectivity in the landscape, gully erosion can lead to increased sedimentation rates in dams and reservoirs (De Haan, 2016).

Gullies are generally defined as deep, erosional, channel-like features that form when flowing water incises into a land surface (Kirkby and Bracken, 2009). If small erosional channels are present, surface runoff flows during a rainfall event will be concentrated in the narrow channels, and this will cause rapid soil loss, causing the gullies to grow in size (Tebebu *et al*., 2010, De Haan, 2016). Gully erosion does not occur consistently (De Haan, 2016). Research on gully development in the Ethiopian Highlands found that gully formation and proliferation is initiated when discharge increases suddenly, such as during the start of the rainy season (Carnicelli *et al*., 2009). Gullies tend to stabilize and fill up with sediment during drier periods where there is much lesss discharge (Carnicelli *et al*., 2009).

Gullly erosion has been identified as a key factor contributing to desertification (Avni, 2005). The erosion of fertile topsoil in narrow valleys exposes more bare rock, which increases the surface runoff during large flood events. This creates a positive feedback loop, leading to accelerated desertification (Avni, 2005). Gully erosion affects hydrology, and hydrology affects gully erosion (Tebedu *et al*., 2010). Gully erosion can, therefore, significantly impact the hydrology of wetlands. When gully erosion is initiated in a wetland, the elevation of the groundwater may drop because the drainage pathways to the outlet for the same elevation difference are shortened (Hagberg, 1995, Poesen *et al*., 2003).

A study by Riddell *et al*. (2013) examined the water table dynamics of the Sand River's severely eroded wetlands and found that the water table elevation around actively eroding gullies was significantly lower. However, it is not always the case that gully erosion in a wetland causes a localized drop in the water table and drainage of the wetland. A study by Rebelo *et al*. (2018) investigated the effect of gully erosion in palmiet wetlands in the Eastern and Western Cape and found no significant difference in the relative groundwater depth between degraded and intact sites. Research by Tanner *et al*. (2019) investigated the hydrological effect of erosion gullies in the upper Kromme River wetlands and found that they do not seem to have a significant negative hydrological impact. While there is a localized drop in the water table around erosion gullies, this is unlikely to result in excessive drainage of water from the wetland (Tanner *et al*., 2019).

2.10.2 Causes of gully erosion in wetlands

The factors that cause gully erosion in a particular wetland must be considered to plan effective, sustainable wetland rehabilitation projects. There is significant debate as to what causes gully erosion in wetlands. Most studies attribute wetland gully erosion to anthropogenic factors (Eitel *et al.,* 2002, Bork, 2003, Avni, 2005, Mieth and Bork, 2005, Valentin *et al.,* 2005, Nyssen *et al.,* 2006). Poor land management, incorrect farming practices, over-grazing of livestock, deforestation, invasive alien plant species, the building of roads, culverts and bridges, and wetland drainage to feed artificial dams are all believed to contribute significantly to gully erosion in wetlands (Bocco, 1991, Poesen *et al*., 2003, Valentin *et al*., 2005, Ellery *et al.,* 2009). Studies from all over the world, like in China (Liu *et al.,* 2004), Northern Ireland (Cooper *et al.,* 1991), South Africa (McCarthy *et al.,* 2007), the United Kingdom (Lane, 2001), and Zimbabwe (Lizias and Felix, 2013) have illustrated that changes in land use are expected to have an important impact on gully erosion in wetlands (Valentin *et al.,* 2005).

While it is certainly the case that human activities in and around wetlands can lead to gully erosion and wetland degradation a growing body of research is showing there are also natural factors that drive the initiation and propagation of gully erosion (Patton and Schumm, 1975, Job, 2014, Nelson and Rittenour, 2014). Gully erosion in wetlands is not only something that is seen in landscapes where land cover and land use have been heavily modified. It is also observed in wetland environments that are near-pristine (Ellery *et al*., 2009). Research suggests that gully erosion in wetlands may be a natural process that occurs due to climatic variation and intrinsic geomorphic thresholds in a landscape being transgressed (Schumm and Hadley, 1961, Patton and Schumm, 1975, Schumm, 1979, Ellery *et al*., 2009, Ngetar, 2011, Pulley *et al*., 2018). Non-anthropogenically driven gully erosion in wetlands is supported by evidence of gullies that pre-date human settlement and farming activities in some areas (McCabe and Dardis, 1989, Fryirs and Brierley, 1998, Lyons *et al.,* 2013, Tooth *et al.,* 2013). For example, four infilled gullies that dated to between 470 and 7060 BP were discovered in the Kromme wetlands (Pulley *et al.,* 2018, Lagesse, 2017). They clearly formed long before any commercial agricultural practices in the area, meaning that the formation of these gullies is driven by factors inherent to the system.

The initiation of gully erosion has both extrinsic controls, like climate, vegetation cover, and anthropogenic activity (Antevs, 1952, Balling and Wells, 1990, Brierley and Fryirs, 1999), and intrinsic controls, like the transgression of natural thresholds (Patton and Schumm, 1975, Womack and Schumm, 1977, Schumm, 1979, Botha *et al*., 1994). Geomorphic thresholds, highly erodible soil types, climatic variability, and vegetation degradation are some of the natural factors that research has identified (Patton and Schumm, 1975, Patton and Schumm, 1981, Prosser and Slade, 1994, Fryirs and Brierly, 1998, Lagesse, 2017).

Natural thresholds exist in many aspects of fluvial systems (Schlegel, 2017). One of the most well-known examples of a natural threshold is the threshold velocity needed to entrain and transport sediment of various sizes (Hjulström, 1935). As velocity increases on Hjulström's curve, the threshold velocities for smaller particles of sediment are crossed, and the particles are entrained and transported (Figure 2). Conversely, as velocity decreases the threshold velocities for larger particles of sediment are crossed, and the particles are deposited (Figure 2).

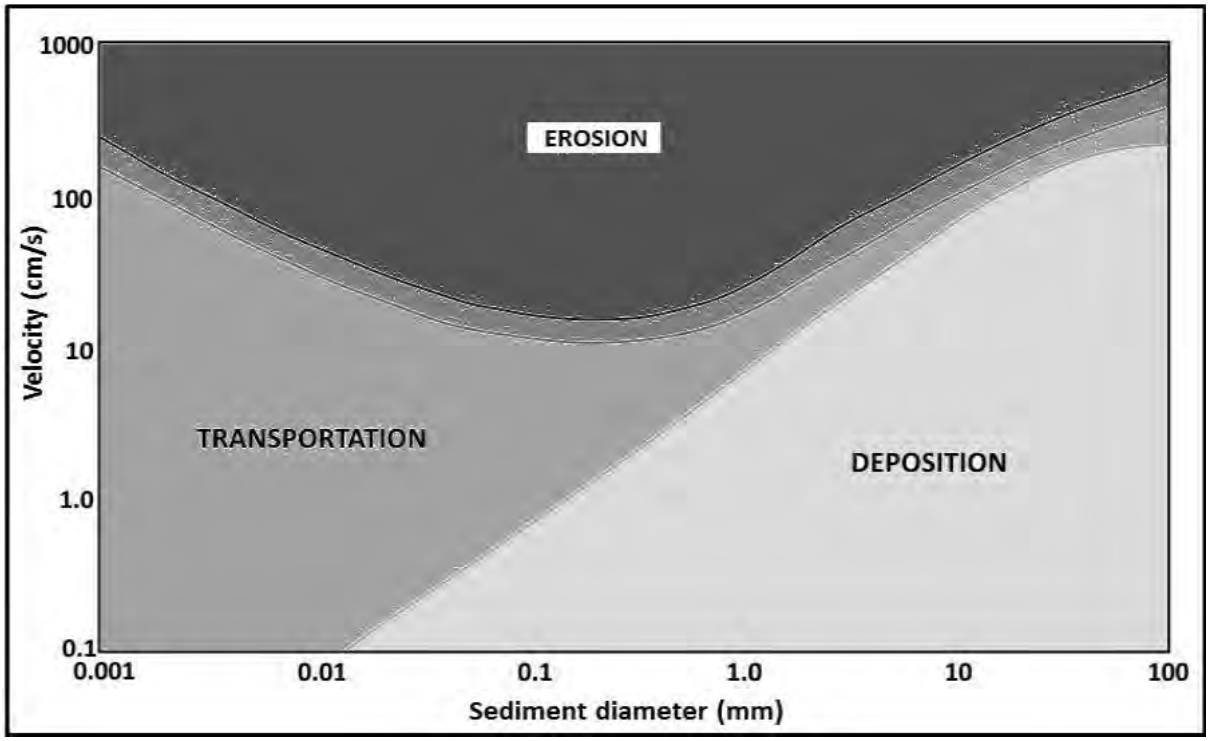

Figure 2: Hjulström's curve diagram that illustrates the relationship between flow velocity, sediment size, and erosion, transportation and deposition (Hjulström, 1935).

Geomorphic thresholds are a type of intrinsic threshold. When there is progressive, accumulative change within a system, but the external control factors remain constant, an intrinsic threshold can be encountered, which can cause the system to become unstable and can cause the system to fail (Schumm, 1973). For example, there is a cumulative increase in the valley's longitudinal slope as sediment is gradually deposited. Eventually a threshold slope will be transgressed, which can initiate incision (Fryirs and Brierly, 2012). The slope is a factor that is intrinsic to the system, therefore the threshold is termed intrinsic. A change in external factors is not always necessary to reach a threshold for a geomorphic change to occur. A study by Schumm and Hadley (1961) found that localised over-steepening of a valley surface can lead to the development of gullies concentrated along the valley floor. Field observations indicated that gully erosion was initiated at steeper, convex reaches of the valley floor, suggesting that there is an inherent instability in the system where the valley floor is steepest.

The concept of geomorphic thresholds has been used to develop a conceptual model describing the relationship between the longitudinal slope and size of a wetland, and how likely it is for incision to occur within a wetland (Ellery *et al*., 2009) (Figure 3). Generally, smaller wetlands have a steeper slope and larger wetlands are more gently sloping (Ellery *et al*., 2009). Valley bottom wetlands with a steep slope for their size are usually incised, whereas those with a gentle slope for their size are generally not incised (Figure 3). Wetland slope and wetland size are, therefore, two key factors to consider in order to understand whether a wetland is inherently vulnerable to erosion (Figure 4).

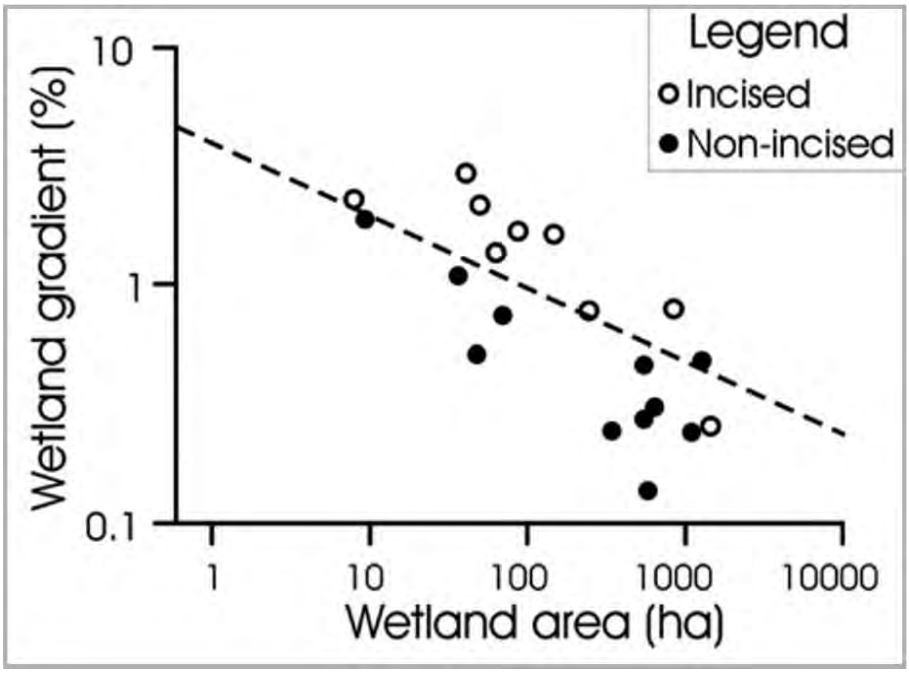

Figure 3: Graph showing the relationship between a valley-bottom wetland's longitudinal slope and its area. Wetlands with a high slope for their size are generally incised and wetlands with a low slope for their size are geneally non-incised. The threshold slope, above which wetlands are likely to incise, is represented by the dashed line (Ellery *et al*., 2009).

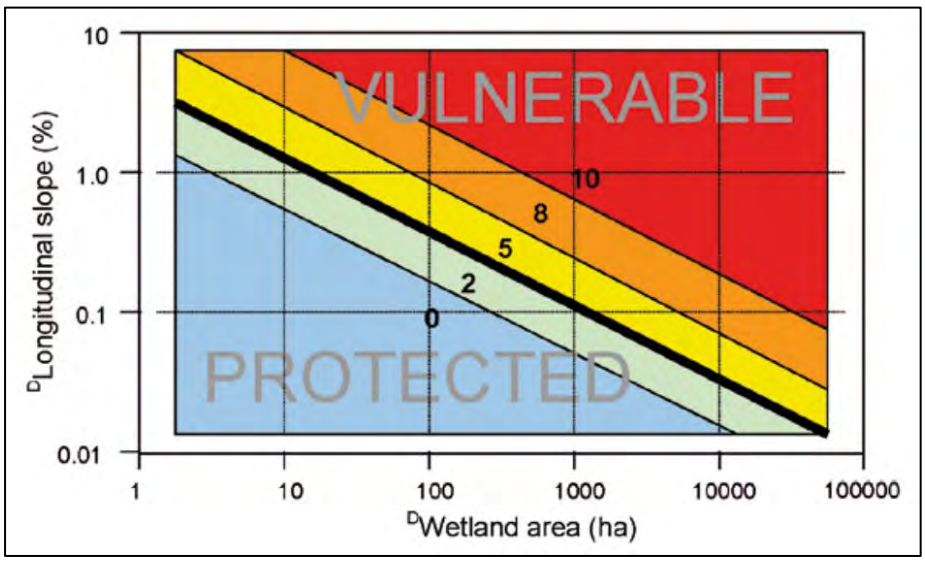

Figure 4: The relationship between a valley bottom wetland's longitudinal slope and area, indicating the wetland's vulnerability to incision (Ellery *et al*., 2009).

2.11 Wetland 'rehabilitation' versus 'restoration'

The terms 'rehabilitation' and 'restoration' are often used interchangeably by environmental scientists when referring to landscape degradation and ecosystem repair interventions (Mitsch and Gosselink, 1993, Streever, 1999, Cooke and Johnson, 2002). While there is only a very minor etymological difference between the two words, and the words generally share the same core meaning, it is important to distinguish between them when referring to efforts to address wetland degradation (Grenfell *et al*., 2007). How these words are used has direct implications for the objectives of ecosystem repair interventions, as well as for the way in which performance standards are set and monitored, and how the overall success or failure of an intervention is judged (Grenfell *et al*., 2007). It is difficult to determine the ecological starting point and the desired endpoint of a strategy if 'restoration' and 'rehabilitation' are used interchangeably. Because this study focuses on a new approach to wetland repair interventions in the Kromme River valley, it is important that the correct terminology be used.

Grenfell *et al*. (2007) did a critical review of wetland ecosystem repair terminology from local South African and international literature and developed more meaningful definitions for the terms 'restoration' and 'rehabilitation'. In this paper, wetland restoration is defined as "the process of reinstating natural ecological driving forces within part or the whole of a completely and permanently altered wetland to recover former or desired ecosystem structure, function, biotic composition and ecosystem services" (Grenfell *et al*., 2007). Wetland rehabilitation is defined as "the process of reinstating natural ecological driving forces within part or the whole of a degraded wetland to recover former or desired ecosystem structure, function, biotic composition and ecosystem services" (Grenfell *et al*., 2007). The key difference between these definitions is the ecological starting point. If a wetland ecosystem has degraded to the point where it is completely and permanently (but not irreparably) altered or replaced, restoration is required to repair the functionality of an ecosystem. If a wetland ecosystem is in a degraded state but is still an observable feature of the landscape, rehabilitation is required to repair its functionality.

The specific goal endpoint of an ecological repair intervention is also critical to define. There is a difference between historical restoration/rehabilitation and functional restoration/rehabilitation. Historical restoration/rehabilitation interventions aim to reinstate a wetland ecosystem's structure, function, biotic composition, and ecosystem services to what they were before anthropogenic disturbance (Grenfell *et al*., 2007). In contrast, functional restoration/rehabilitation interventions aim to reinstate a wetland ecosystem's desired structure, function, and biotic composition, so that it may again provide the desired ecosystem services (Grenfell *et al*., 2007). It is difficult to define a wetland ecosystem's state and functioning prior to anthropogenic disturbance. How far back in

history should one go? It is much simpler to define the types of ecosystem services a wetland needs to provide, like flood attenuation or water purification, and repair the wetland ecosystem to an acceptable, useful state.

The wetlands in the Kromme River valley have not yet degraded to a point where they have been entirely removed from the landscape. They are still visible features in the valley and parts of the wetlands are still functional, providing ecosystem services. Therefore, when referring to ecosystem repair interventions in the Kromme valley wetlands, rehabilitation is the word that should be used. Functional rehabilitation interventions are required in these wetlands, therefore the word ‘rehabilitation' is used throughout this study.

2.12 Current approaches to wetland rehabilitation in South Africa

Wetland ecosystem repair interventions in South Africa are guided by a series of publications by the Water Research Commission (WRC), entitled the *WET-Management Series*. The series was developed from a 9-year-long WRC wetlands research programme that aimed to create tools for people wanting to rehabilitate wetlands effectively in an informed manner. The series is intended as a roadmap to planning, designing, implementing, and managing wetland rehabilitation projects, and includes methods of monitoring to assess the success of interventions. *WET-RehabMethods* by Russell *et al.* (2009) was written as a guide for wetland practitioners to aid in the selection and implementation of rehabilitation methods. It recognizes that all wetland ecosystems are unique in their origin, form, functioning and dynamics, and therefore, guides wetland practitioners to choose rehabilitation methods that are appropriate for a particular problem being addressed, given the wetland and its context. All the methods and techniques described in *WET-RehabMethods* (Russell *et al*., 2009) are designed to halt erosion. Overall, this is the predominant approach to wetland rehabilitation in South Africa.

Traditionally, large concrete or gabion structures are used to arrest erosional gullies in wetlands (Nieuwoudt *et al*., 2018). These “hard” structures are intended to drown an erosional nick-point, halt gully propagation and, thereby, protect the intact wetland that lies upstream of the nick-point (Russell *et al.*, 2009). These structures are costly and time-consuming to construct, and they have large construction footprints because of the amount of soil that is disturbed (Nieuwoudt *et al*., 2018). In many cases, the disturbance is an opportunity for alien plants to invade the wetland (Nieuwoudt *et al*., 2018). These types of structures also require a substantial amount of maintenance, adding to their overall cost.

The methods for wetland rehabilitation described in *WET-RehabMethods* by Russell *et al.* (2009) mainly involve the use of concrete or gabion weirs, chutes, and diversions. The book is about 300

pages in length, and only 40 of those pages are about using vegetation in wetland rehabilitation. The chapter describing rehabilitation methods that involve vegetation generally focuses on how biological interventions can enhance the impact of “hard” structures.

More modern wetland rehabilitation projects, such as the Working for Wetlands project in the Pietersielieskloof wetland system, use innovative “soft” structures, like chute-drop inlets, to address erosional headcuts (Nieuwoudt *et al*., 2018). “Soft” structural interventions are much less costly to install and maintain. Presently, Working for Wetlands is focused on developing more wetland rehabilitation projects that use these types of structures.

2.13 The use of erosion control structures in the Kromme wetlands

The Kromme River valley wetlands are significantly degraded due to gully erosion driven by a combination of anthropogenic and natural factors. Working for Wetlands installed eleven large concrete and gabion erosion control structures in the Kromme River valley wetlands between 2002 and 2013 (De Haan, 2016). Since they were installed, the structures have successfully halted the erosional headcuts and prevented them from propagating in an upstream direction (De Haan, 2016). The structures have elevated the water table upstream of them, thereby increasing the saturation of the wetland (Tanner *et al*., 2019). However, despite these impacts, the overall success of this rehabilitation project remains disputed. The size of the palmiet wetland upstream of the structures decreased between 2002 and 2013, and downstream of the structures erosional gullies have grown in width and depth (De Haan, 2016).

The structures trap the majority of the sediment flowing from upstream, and this appears to have destabilized the gully beds downstream of the structures (De Haan, 2016, McNamara, 2017, Tanner *et al*., 2019). The reaches downstream of erosion control structures are starved of sediment, causing the reaches to erode to an extent that has never been experienced in the geomorphic history of the valley. This has been shown to be the case in the Kromme River as well as in the Karoo (Pulley *et al.,* 2018). The structures in the Kromme River disrupt the natural geomorphic dynamics of the system, which rely on the transportation of sediment eroding from the head of a gully to be deposited at the toe (McNamara, 2017, Pulley *et al.,* 2018).

CHAPTER 3: STUDY AREA

3.1 Location

The Kromme River Wetland (approximately 33°S, 24°E) is located in the southern part of the Eastern Cape, South Africa. The river is approximately 100km long with its headwaters at an altitude of about 550 m.a.s.l. The study area is about 30km west of the town of Kareedouw (Figure 5). The Kromme River mouth is near the small town of St Francis Bay, where it enters the Indian Ocean (Figure 5). The Kromme River flows through five quaternary catchments (K90A, B, C, D, and E). Together these catchments have a drainage area of 1022km^2 (Schlegel, 2017). The Kromme River is an important water resource for the Nelson Mandela Bay Metropole because it has two large dams along its length – the Churchill Dam (34°0'4"S 24°29'1"E) and the Impofu Dam (34°5'45"S 24°41'1"E) (Figure 5). The Kromme River lies in an inter-montain valley in the Cape Fold Mountain Belt. This mountain range, which is over 1000km long, is intensely folded with synclines and anticlines that are oriented in an east-west direction. The Kromme River is bounded by two mountain ranges that run from east to west: the Tsitsikamma Mountains (max. elevation 1251 m.a.s.l.) to the south and the Suuranys and Kouga Mountains (max. elevation 1073 m.a.s.l.) to the north (Figure 6; Dennis and Pretorius, 2006, Rebelo, 2012, Jansen and van Veen, 2014, Rebelo *et al.*, 2015, Lagesse, 2017, Schlegel, 2017). The valley has steep slopes of between 20% and 30% on the north-facing mountains and between 25% and 60% on the south-facing mountains (Kotze and Ellery, 2009). In reaches of the valley that have experienced erosion, the Kromme River exists as an open channel, but in intact reaches it exists as unchanneled valley bottom wetlands with diffuse flow across the width of the valley floor (Figure 7).

The Kromme wetlands are situated in the upper reaches of the Kromme River (quaternary catchment K90A). The study sites for this research are the Krugersland, Kompanjiesdrift and Jagersbos wetlands (Figure 6). The Krugersland and Kompanjiesdrift wetlands are largely intact, whereas the Jagersbos wetland has experienced major disturbance following a large flood event in 2012 (McNamara, 2017). These sites were selected to illustrate the contrast between intact and disturbed reaches of wetland.

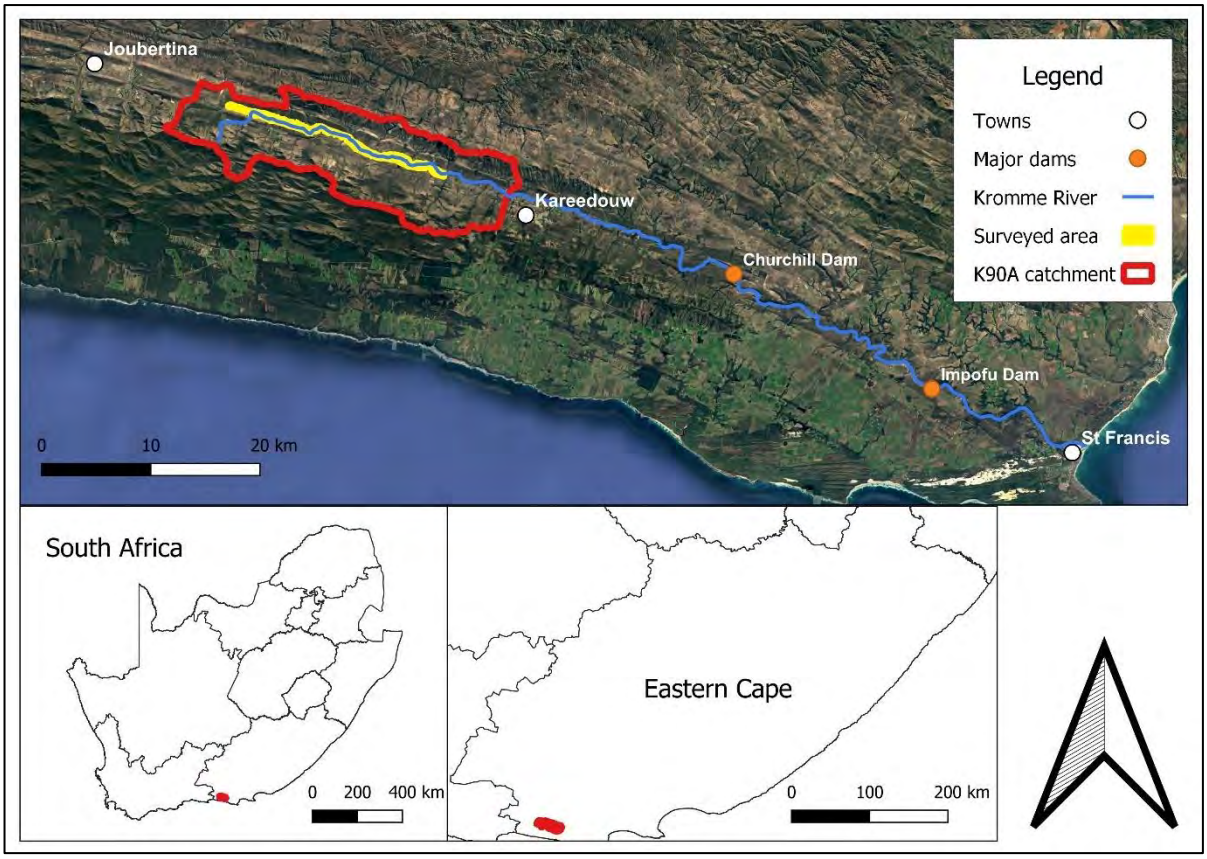

Figure 5: Map showing the location of the Kromme River and the K90A catchment in the Eastern Cape, South Africa.

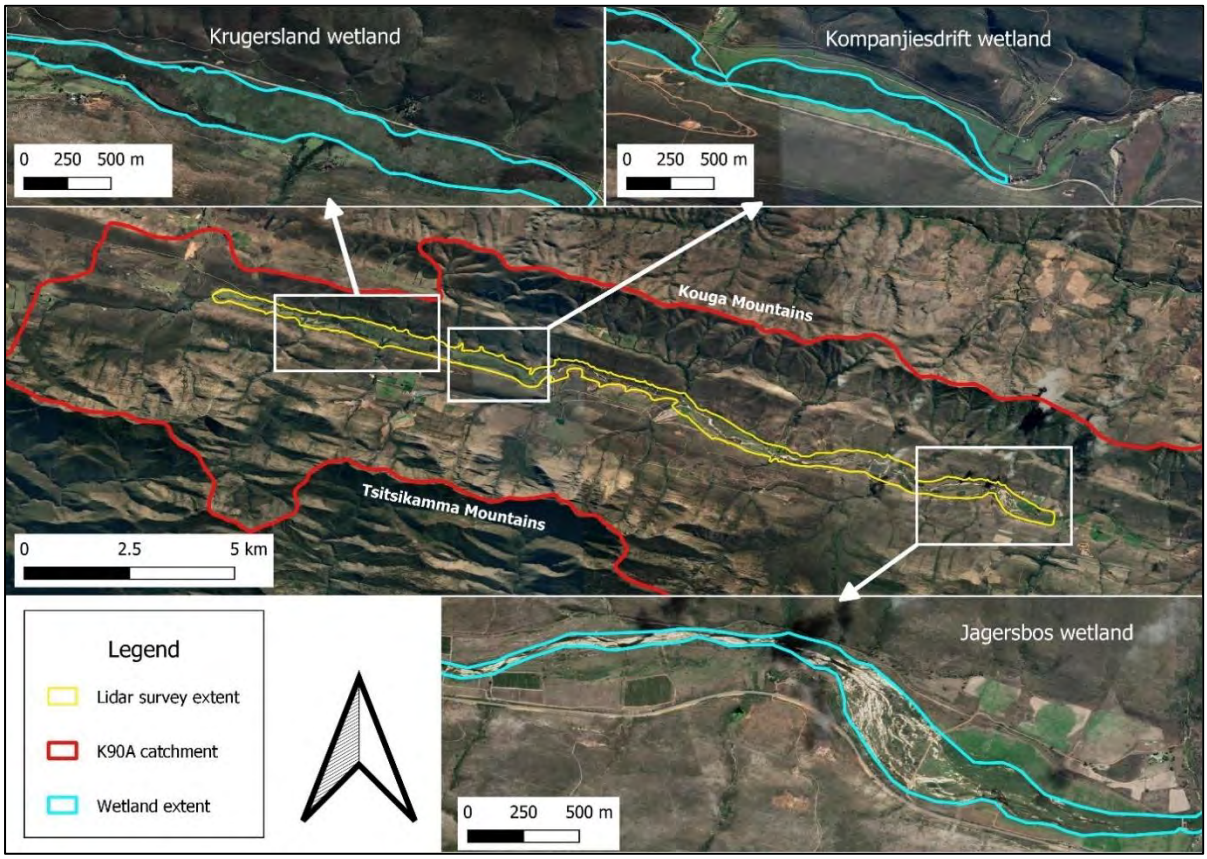

Figure 6: A map of the Krugersland, Kompanjiesdrift, and Jagersbos wetlands, showing their location within the study area, the extent of the wetlands, and the adjacent mountain ranges.

.

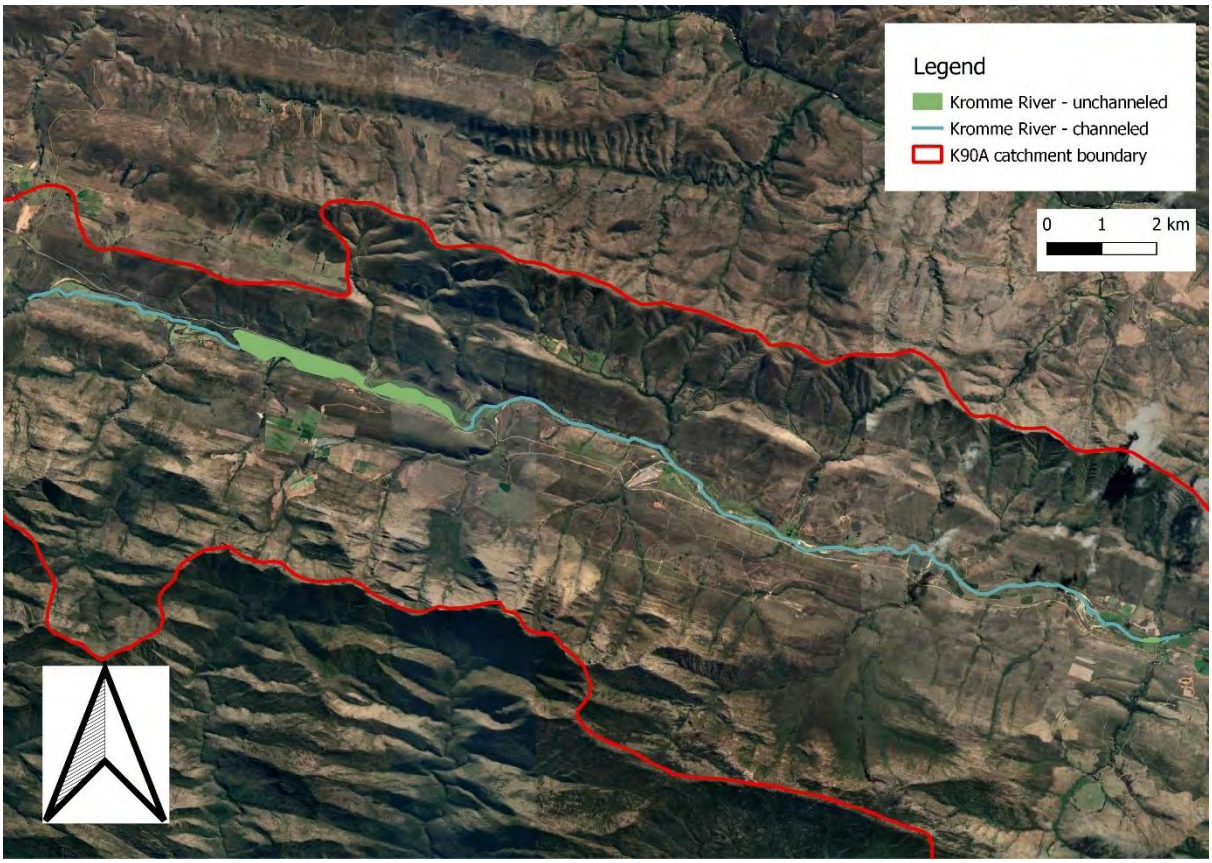

Figure 7: A map of the surveyed length of the Kromme River, showing where the stream exists as an open channel and as an unchanneled valley-bottom wetland.

3.2 Geology

The Kromme River catchment's geology comprises sedimentary rocks of the Table Mountain and Bokkeveld Groups at the base of the Cape Supergroup (Lagesse, 2017, Tanner *et al.,* 2019, Ellery *et al*., 2022). The stratigraphy of these lithologies of the Cape Supergroup that occur in the study area are shown in Table 1, comprising a generally upward-fining sequence of sediments, with the coarse-grained quartzites of the Peninsula Formation at the base. . The Cedarberg and Goudini Formations are shale and sandstone respectively, which are overlain by quarzitic sandstone of the Skurweberg Formation. The youngest rocks of the Table Mountain Group that are exposed in the study area are felspathic sandstones of the Baviaanskloof Formation, which are overlain by shales of the Gydo Formation (Bokkeveld Group).

Table 1: Stratigraphy of the Kromme valley (Toerien, 1986).

	Group	Subgroup	Formation	Lithology
	Bokkeveld	Ceres	Gydo	Black shale and minor siltstone, fossiliferous.
	Table Mountain	Nardouw	Baviaanskloof	Impure feldspathic sandstone, minor shale, fossiliferous.
			Skurweberg	White-weathering quarzitic sandstone, feldspathic towards the top, cross-bedded.
			Goudini	Brownish-weathering quarzitic sandstone, minor siltstone and shale.
			Cederberg	Black shale, arenaceous towards to the top and can be fossiliferous.
			Peninsula	Whitish-weathering quarzitic sandstone.

Over a distance of over 1 000 km, rocks of the Cape Supergroup have experienced folding and have metamorphosed, making the quarzitic sandstones of the Peninsula and Skurweberg Formations highly resistant to weathering and erosion, while the remaining rocks of the sediments of the Cape Supergroup weather more easily. The Kromme River Wetlands occupy the trough of a folded syncline, with the oldest, highly resistant quartzites of the Peninsula Formation forming the mountain peaks and ridges of the Tsitsikamma and Kouga Mountains on the southern and northern margins of the K90A catchment respectively (Figure 8). In contrast, the youngest, easily weathered rocks of the Baviaaanskloof and Gydo Formations, occupy the centre of the syncline, on which the wetlands themselves are situated. (Mucina and Rutherford, 2006).

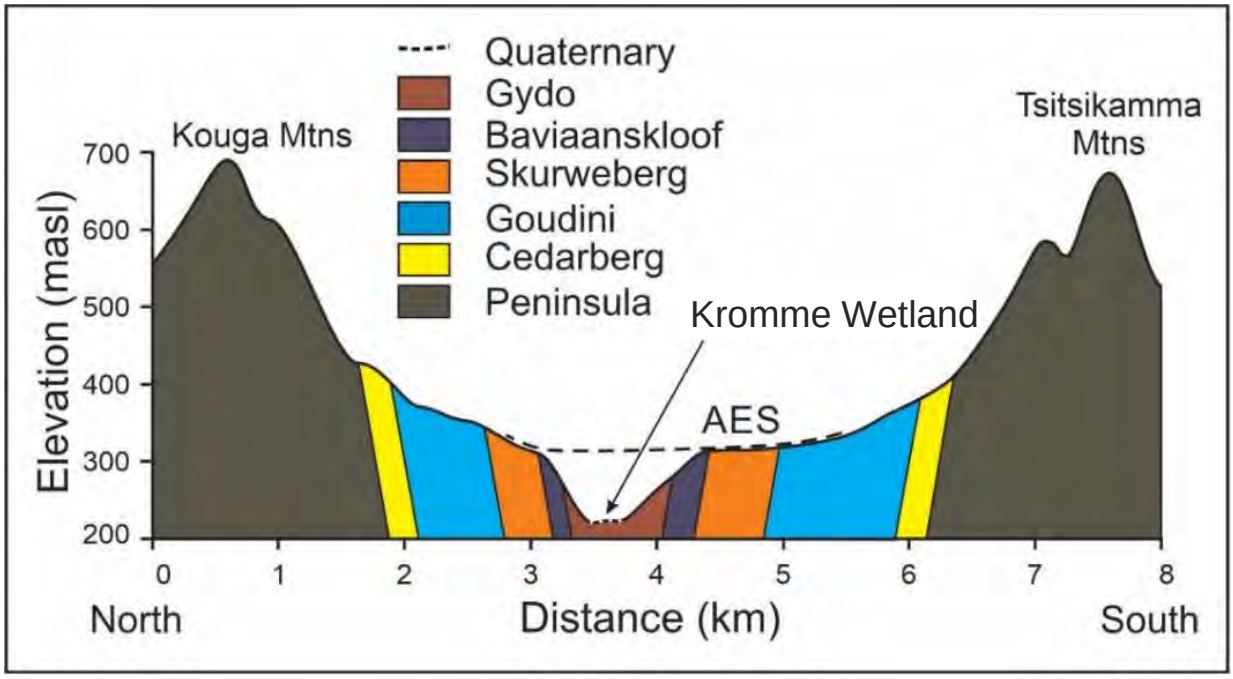

Figure 8: A generalized north-south transect across the valley in the Kompanjiesdrift wetland, showing the topography, the position of the wetland relative to the AES, and the geology of the valley based on the 1:250 000 geological map by Toerien (1986) (adapted from Ellery *et al*., 2022). The full stratigraphy and a more detailed description of the lithologies are presented in Table 1.

The African Erosion Surface (AES), which formed during the Cretaceous ending about 60 million years ago, is located at an altitude of 320 to 350 m.a.s.l. in Figure 8 (McCarthy and Rubidge, 2005, Lagesse, 2017, Tanner *et al*., 2019). It is likely that the wetland occupies the Post Africa I surface, which formed between 5 and 20 million years ago (Lagesse, 2017, Tanner *et al*., 2019, Ellery *et al*., 2022). Because the wetland occurs below the AES, it suggests that the valley has eroded over the last 20 million years after the isostatic uplift event that took place around 20 million years ago (McCarthy and Rubidge, 2005).

3.3 Wetland morphology

Many non-perennial tributaries flow into the Kromme valley from their sources in the adjacent mountain ranges (Rebelo, 2012). Where these tributary streams enter the trunk valley, alluvial fans are present (Rebelo, 2012, McNamara, 2017, Schlegel, 2017), varying in size in relation to the size of the catchments (Figure 10). The alluvial fans generally cause a reduction in the width of the trunk valley and also influence the local longitudinal slope of the trunk valley.

The Krugersland wetland is densely vegetated with palmiet. The wetland occupies almost the entire valley bottom. Tributaries, shown as black arrows in Figure 10, enter the trunk valley at a very high angle close to 90 degrees. Tributaries entering the trunk valley are generally associated with alluvial

fans that cause a reduction in trunk valley width. In the Krugersland basin there are three small tributaries that enter the valley from the south (A, B and C in Figure 9).

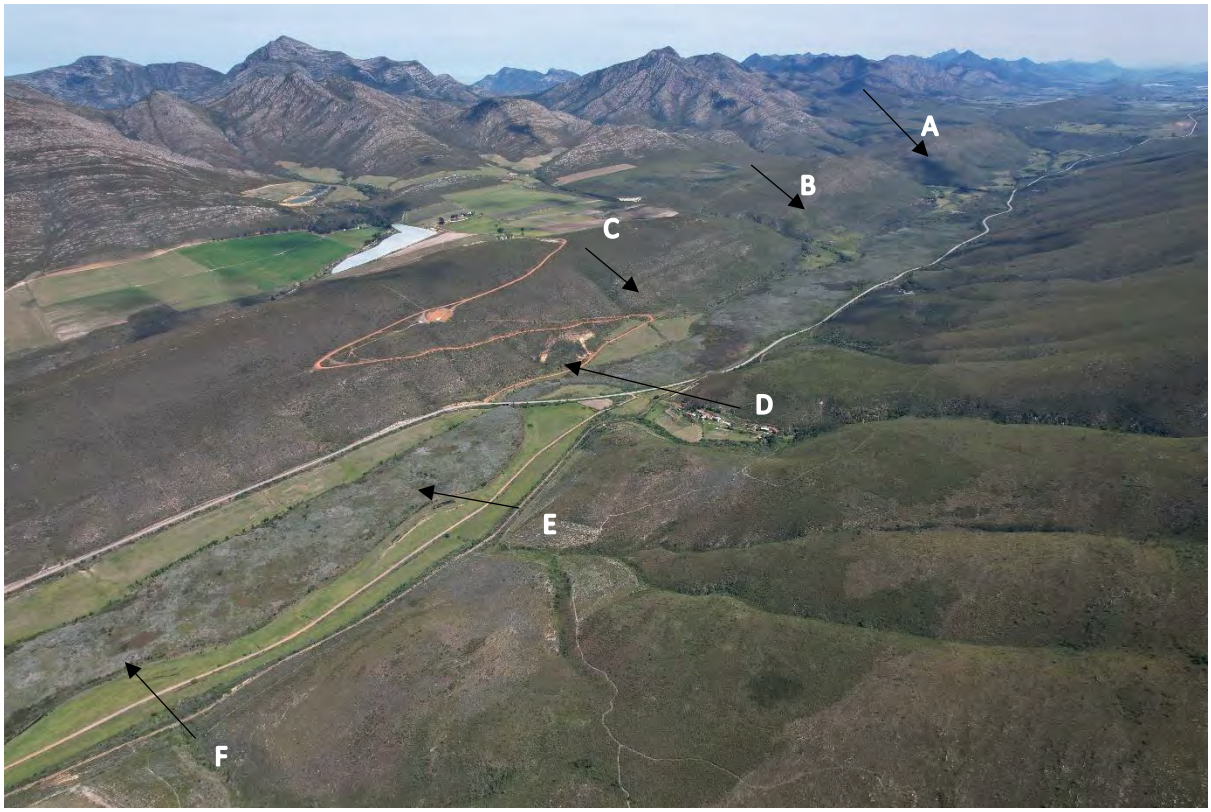

Figure 9: A drone image of the intact portions of the Krugersland and Kompanjiesdrift wetlands, taken from the north-east, looking south-west up the valley. The Krugersland wetland is on the right, above where the road crosses the wetland, and the Kompanjiesdrift wetland is below the road crossing. Alluvial fans are indicated by black arrows.

The Kompanjiesdrift Basin, which is directly downstream of the Krugersland Basin, is also densely vegetated with palmiet. At the head of the basin there is a large tributary alluvial fan that enters the valley from the north (D in Figure 9). It drastically reduces the width of the wetland valley-bottom . The R62 road crosses the valley on this alluvial fan (Figure 10). Where the road crosses, there is a small bridge across the wetland . Downstream of the large alluvial fan, the valley is broad and flat, and the wetland occupies almost the entire valley bottom. In the middle of the basin are two small alluvial fans that enter the valley from the north (A and F in Figure 9). At the lower end of the Kompanjiesdrift wetland a large alluvial fan enters the valley from the north, which again drastically reduces the width of the valley and the wetland.

Figure 10: A photograph captured with a drone from the head of the Kompanjiesdrift wetland, looking downstream. It shows the R62 road crossing the wetland at its narrowest point on a large alluvial fan. The palmiet wetland is blue-grey in colour, whereas the dryland pasture adjacent to the wetland is green.

The Jagersbos basin is approximately 9 km downstream from the Kompanjiesdriftbasin. This wetland has experienced major erosion in the last decade. There is a large alluvial fan that enters the valley from the south. Upstream of the alluvial fan, the wetland has eroded as a distinct gully with steep-sided walls (Figure 11). The gully is the main channel of the Kromme River in this particular reach. Downstream of the alluvial fan, where the valley loses confinement, there is a large depositional feature, or floodout, that spans almost the entire valley bottom. The floodout is about 1.5 km in length. On the floodout, the Kromme River exists as multiple distributary channels (Figure 11). The depositional reach is vegetated with palmiet, especially along the channels. Large amounts of alluvial sediment about 1 m thick but thinning downstream are present on the floodout.

The two uppermost basins, the Krugersland and Kompanjiesdrift, have not experienced major erosion for over a century. Four infilled gullies in the Kompanjiesdrift wetland were dated at 470 to 7060 BP, suggesting that the last major erosional event in the wetland occurred about 400 years ago (Pulley *et al*., 2018).

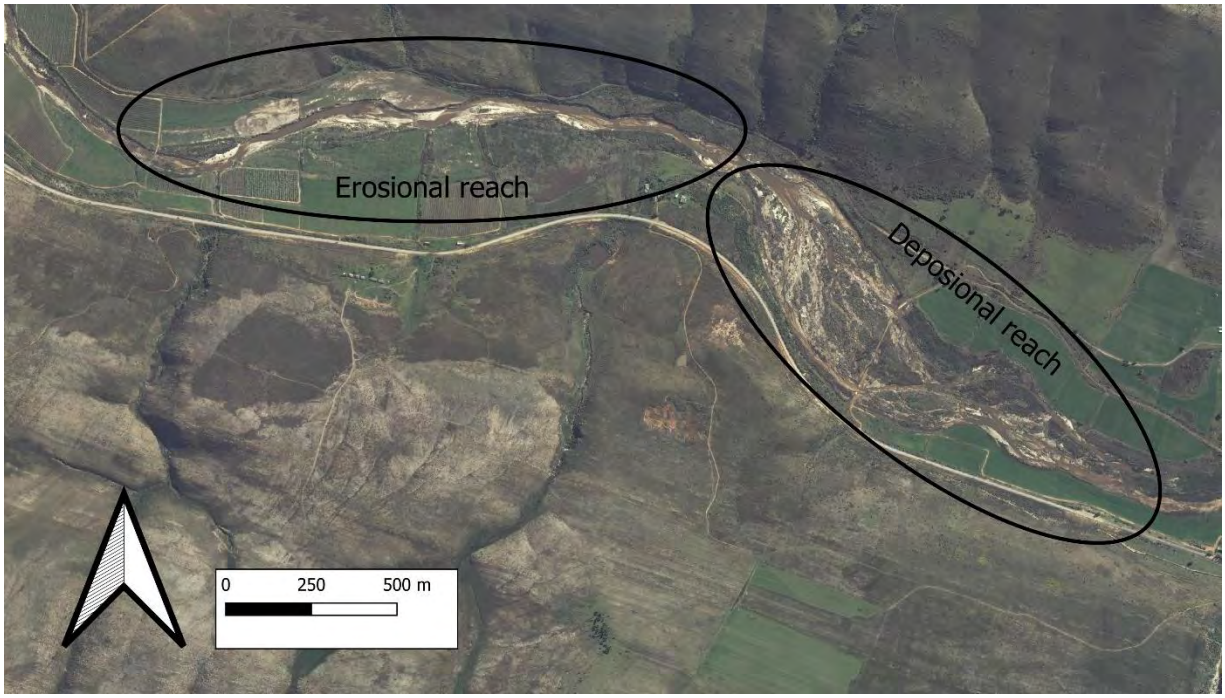

Figure 11: Aerial image of the Jagersbos wetland indicating the upper erosional reach and the lower depositional reach.

3.4 Rainfall and hydrology

The Kareedouw weather station is the closest source of rainfall data for the upper Kromme River wetlands. This weather station is located about 20km from the study sites. Data for this weather station to the end of 2020 was obtained from the South African Weather Service.

The Kromme River catchment (quaternary catchments K90A, B, C, D, and E) falls is in a transition zone between the coastal zone of the Eastern Cape, which is characterized by year-round rainfall, and the Western Cape winter rainfall zone (Schlegel, 2017). While rain occurs throughout the year, the catchment experiences a bimodal rainfall pattern, with most of the rainfall occurring during autumn (February to April) and spring (August to October; (Figure 12). The mean annual rainfall at the Kareedouw weather station is 688mm per annum (standard deviation of 200.5mm). The mean annual precipitation for the whole Kromme River catchment from 1950 to 2000 is 614mm (Rebelo *et al*., 2015).

Rainfall is highly variable interannually and seasonally. The coefficient of variation was calculated for the range of record for the Kareedouw weather stationwith a value of 29.1%, indicating moderate interannual rainfall variability (Tanner *et al*., 2019). The rainfall seasonality index was calculated to be 0.18, indicating that the rainfall is non-seasonal, as the seasonality index is ≤0.19 (Walsh and Lawler (1981).

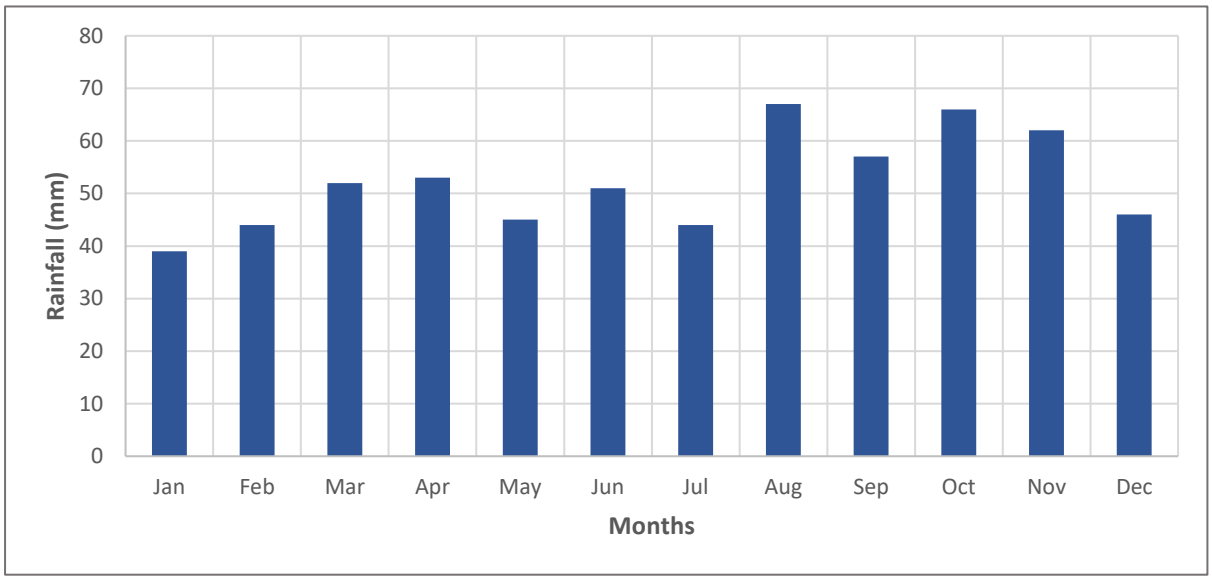

Figure 12: Mean monthly rainfall at the Kareedouw weather station from 1978 to 2020 (South African Weather Service).

There is significant spatial variation in rainfall within the study area, given a strong rainfall gradient that declines across the catchment from south to north by a factor of 2 (Kotze and Ellery, 2009, McNamara, 2017, Schlegel, 2017). The south and south-west parts of the K90A catchment, closest to the Tsitsikamma Mountains, experience far more rainfall than the north and north-west parts, closest to the Suuranys and Kouga Mountain ranges (Haigh *et al*., 2009, Bailey and Pitman, 2016). The southern parts of the K90A catchment have an average annual rainfall of 800mm, whereas the northernmost parts have an average annual rainfall of only 400mm (McNamara, 2017).

According to the Water Resources 2012 database (Bailey and Pitman, 2016), the mean annual runoff for the K90A catchment is 27 million m^3. The mean annual runoff for the entire Kromme River catchment (all five quaternary catchments) is about 75 mm, which amounts to about 10% of the rainfall (Middleton and Bailey, 2008). The mean annual evaporation for the K90A catchment is 1400mm (Tanner *et al*., 2019).

Most of the catchment runoff occurs over short periods of time, leading to flood events (Rebelo, 2018). Due to the steep, mountainous landscape, floods are common in the Kromme valley. Major flood events occurred in 1931, 1965, 1981, 1996, 2001, 2006, 2007 and 2012 (McNamara, 2017). The flood return intervals and their accompanying discharges for the Kromme River downstream of Churchill Dam are given in Table 2, but the discharge for given return intervals for wetlands on the Upper Kromme will be much lower because catchment size declines progressively upstream

Table 2: Flood return intervals and their associated discharges for floods in the Kromme River downstream of Churchill Dam for the period from 1955 to 2006 (Adapted from Haigh *at al*., 2008).

Flood return interval (years)	**Discharge (cumecs)**
2	2.26
5	25.17
10	93.18
25	389.73
50	999.06
100	2366
200	5264.15

3.5 Valley sedimentary fill

Lagesse (2017), McNamara (2017), Schlegel (2017), and Pulley *et al*. (2018), carried out systematic coring in the Jagersbos and Kompanjiesdrift wetlands to characterize the upper Kromme River valleys sedimentary fill. It was found to be made up mainly of layers of fine to medium-grained sand and organic-rich sediment. Medium sand, fine sand, very fine sand and silt are the most abundant particle size classes in the valley. Organic content is generally much lower than 10 %.

Many of the cores from the Kompanjiesdrift wetland indicate several layers of coarse sand interrupted by layers of finer, more organic sediments. One of the coarser sand layers (made up mainly of fine and medium sand) is present buried at a depth of about 3 m, extends across the entire Kompanjiesdrift basin (Lagesse, 2017). The sandy layer in Kompanjiesdrift was dated at around 7000 BP (Lagesse, 2017). It is evidence of a large flood event that deposited sediment over the whole Kompanjiesdrift wetland at that time.

The cores from the lower depositional reach of the Jagersbos wetland showing the stratigraphy of the deposit, which is a large floodout (McNamara, 2017). The upper layers of the cores had fine sediments (mainly fine sand, very fine sand, and silt), while the deeper layers had coarser sediments (mainly medium sand). There is thus a general upward fining pattern across the whole floodout (McNamara, 2017). Over the length of the floodout there is also a pattern of fining, as the percentage of fine and medium sand increased with distance downstream from the top of the floodout (McNamara, 2017).

3.6 Vegetation

The upper Kromme River catchment (K90A) is situated within the fynbos biome. Sandstone fynbos, shale renosterveld, and shale band vegetation characterise the vegetation in the area (Rebelo *et al.*,

2006). Almost 50% of the vegetation in the catchment is fynbos, 12.5% is grassland, while thicket, renosterveld, and forest each comprise less than 10% of the catchment vegetation (Mucina and Rutherford, 2006).

In accessible parts of the catchment with relatively gentle slopes, there is widespread cultivation of fruit trees and timber-producing trees. Eroded reaches are generally flanked by agricultural pastures and orchards. Grasses dominate eroded reaches that have not been cultivated.

In pristine reaches, the entire core of the wetland is dominated by dense stands of palmiet (*Prionium serratum*; Barclay, 2017). Alien trees such as black wattle (*Acacia mearnsii*) have invaded parts of the catchment and encroached on the wetland, contributing to degradation.

3.7 Land use

Historically, the Kromme River valley has been an important agricultural area. The valley has been farmed since the mid-1700s. The majority of the land adjacent to the Kromme wetlands has been transformed through agricultural activities. A detailed history of land use and land cover change in the catchment is given in Haigh et al. (2009), Rebelo (2012), and Nsor and Gambiza (2013).

Today, the economic activity in the area is still predominantly agricultural. The land is used for growing deciduous fruit (mainly apples and pears), producing timber, and pasture production for livestock (cattle and sheep). Most of the land adjacent to the Kromme wetlands is used for orchards, irrigated farming, and dryland farming (Rebelo, 2012, Tanner *et al*., 2019). In the past, the farms in the Kromme River valley were smaller, family-owned enterprises. More recently, large commercial agriculture companies such as the DuToit group have bought up almost all the farms in the area. The agricultural land adjacent to the Krugersland and Kompanjiesdrift wetlands is used for dryland pasture (Figure 13), and the land adjacent to the Jagersbos wetland is used for irrigated and dryland pasture.

Figure 13: A photograph captured with a drone, taken looking east to west up the Kromme River valley. The image shows the Kompanjiesdrift wetland in the foreground and the Krugersland wetland in the background. Adjacent to the wetland, dryland pastures are visible and are distinct from the darker-coloured wetland vegetation.

CHAPTER 4: METHODS

The aim of this study was to use hydraulic modelling techniques to determine locations most likely to be favourable for testing wetland rehabilitation strategies that involve palmiet. Desktop analysis and hydraulic modelling techniques were the main methods used to achieve the aim of this study. In this chapter, the methods that were used are subdivided into three sections, one for each of the three objectives. An overview of the methods employed to achieve each objective is given in Table 3.

Table 3: An overview of the objectives of this project and a summary of the methods employed to achieve each objective.

Objective	Method
1. Analyse the valley morphology in relation to geomorphic features and processes.	An aerial LiDAR survey of a 23km-long reach of the valley provided a high-resolution topographic dataset and orthophotographs. The data was used to create a digital terrain model (DTM). The DTM and orthophotographs were used to identify and map geomorphic features. Longitudinal profiles and cross-sections of the valley and the wetlands were created.
2. Apply the model and analyse hydraulic modelling outputs to determine the effect of valley morphology on stream hydraulics.	HEC-RAS was used to build a hydraulic model to simulate how water flows down the length of the valley after a large rainfall event. A raster dataset of flow velocity, stream power, and depth were the modelling outputs. The spatial distribution of the stream hydraulics were examined in relation to valley morphology.
3. Select sites for trialling new wetland rehabilitation strategies that employ palmiet.	A classical GIS overlay technique using the model outputs at identified sites with low flow velocity and stream power, and sufficient depth of flooding for palmiet to establish and regenerate.

4.1 Modelling software

The software used for the hydraulic modelling in this study was originally developed at the Hydrologic Engineering Centre, a division of the Institute for Water Resources at the United States Army Corps of Engineers by Mr Gary Brunner (Brunner, 2016). The software is called HEC-RAS (Hydraulic Engineering Centre – River Analysis System). It is available for free and is suitable for use

by hydraulic engineers. HEC-RAS is one of the most well-known, analysed and used models for flood mapping in the scientific literature and in practice (Costabile *et al*., 2020).

HEC-RAS is a spatially fully-distributed event-based river hydraulic model designed to simulate steady flows, unsteady flows, sediment transport, water temperature, and water quality (Brunner, 2016). The HEC-RAS model was designed to use momentum and energy equations to calculate hydraulics at riverine cross-sections.

HEC-RAS can model water in a river system in 1, 2, or 3 dimensions. Depending on the objectives of a study, the model can provide increasingly sophisticated outputs. 1D models are the most simplistic, requiring less terrain data and computational power. However, 1D models are not very accurate for wide, flat floodplains because it assumes all the water flows in one direction (Brunner *et al*., 2020). 2D models account for the lateral movement of water, so they can more accurately represent systems with multiple flow paths and varying water surface elevations and velocities, such as unchanneled valley-bottom wetlands (Brunner *et al*., 2020). 3D models are far more data-intensive and require vastly more computing power. They can simulate the vertical variation in flow velocity, so they are useful for modelling differences between flow along the bottom on the water columb and the surface, and stratification of the water columb due to temperature or salinity gradients (Brunner *et al*., 2020).

For this study, 2D flow characteristics were modelled so that depth of flooding, flow velocity, and stream power could be displayed spatially. 3D modelling requires bathymetric data, so would not have been possible for this study (Brunner *et al*., 2020). The 2D model outputs provided sufficient insight to achieve the aim of this study.

4.1.1 Topographic inputs for HEC-RAS

Hydraulic models like HEC-RAS require topographic data as the basic input, generally in the form of a digital elevation model (DEM). A DEM is a grid (raster) that is made up of cells. Using a physical spatial coordinate system, each cell is assigned a location and cell properties such as elevation and roughness. The resolution of the DEM used in modelling is extremely important. According to Grenfell (2015), the value of a highly accurate survey that captures a high density of elevation points cannot be overstated when the aim of the research is to examine complex flow in two dimensions.

High-resolution topographic data can be obtained from an airborne LiDAR (laser imaging, detection, and ranging) survey. LiDAR sensors emit pulses of light waves from a laser onto the ground. The light bounces off objects on the ground and back to the sensor. The sensor measures the time it takes for the light to reflect off the ground and back to the sensor. This time is used to calculate the distance the light travelled, in other words, the ground's elevation. The backscattering of light that is

detected by the LiDAR sensor and the different types of backscattering can be used to deduce the nature of objects on the ground. Vegetation can be distinguished from the soil, making it possible to determine the elevation of the top of the vegetation canopy and the land surface. The uppermost surface that scatters light is the vegetation canopy. This signal can be used to create a digital surface model (DSM). The lowest surface to scatter the light is bare earth, reflecting the topography of the land surface, which is mapped as a digital elevation model (DEM). The differences between a DSM and DEM for a small reach of the Kromme wetland are shown in Figure 14. The DSM is based on the first signal to return to the sensor, so every pixel represents the maximum elevation in the pixel. The DEM, on the other hand, is based on the average of all reflectance values for each pixel.

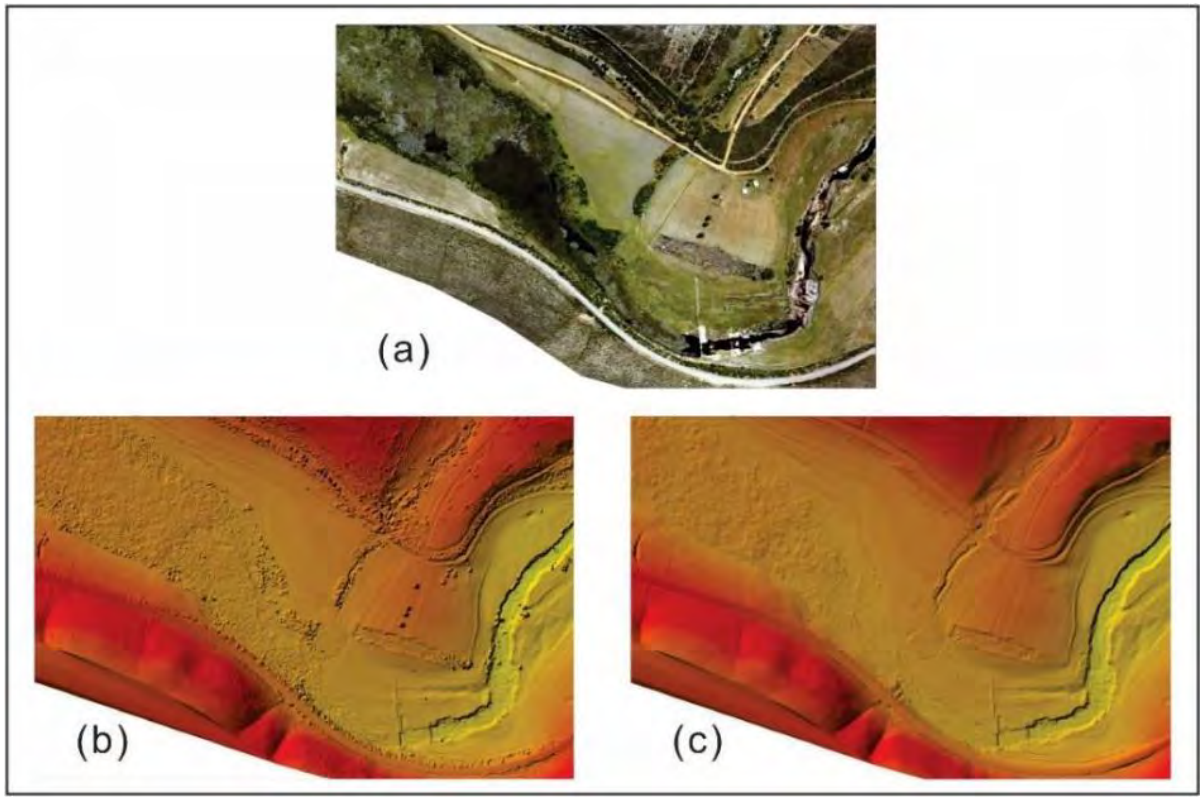

Figure 14: Comparison of the difference between a high-resolution orthophotograph (a), DSM (b), and DEM (c). All three of the images are of a reach in the Kompanjiesdrift wetland in the upper Kromme River valley and show the wetland upstream of a Working for Wetlands erosion control structure.

4.1.2 Flow data as an input for HEC-RAS

Hydraulic models require flow data as an input. Flow can either be entered as stage height (the height of the water surface above the bed) or discharge (flow in cubic meters per second (cumec)). Discharge is the key hydrological input required by HEC-RAS. Input to hydraulic models requires those factors that affect flow velocity to be mapped for the whole valley bottom. The factors that affect the flow of water are captured by understanding Manning's equation:

$$V = (R^{2/3} \times S^{2/3}) / n$$

V refers to velocity, R is the hydraulic radius (the cross-sectional area divided by the wetted perimeter), and n represents Manning's roughness value.

The equation reveals that flow velocity is affected by factors that:

1. Promote water flow, like slope. When all other variables are constant, water flows faster down a steep slope than on a gentle slope.
2. Resist the flow of water, like friction associated with the hydraulic radius and bed roughness. Water flows faster down a valley with a semi-circular cross-section than in a broad, shallow valley. Water flows more slowly the rougher the valley bed.

4.2 Model calibration

Parameters, in the context of numerical models, are properties or conditions that are defined for each simulation and remain constant while a simulation is run (Coulthard and van de Wiel, 2013). Some parameters pertain to algorithms and numerical aspects of the model (e.g., the maximum number of iterations), while others represent physical conditions within the model (e.g., flow, topography, vegetation roughness, Coulthard and van de Wiel, 2013). Parameters are usually set to a restricted range of values but can be assigned any value. The values assigned to parameters influence the results of the simulation. The process of changing the parameter values, so that simulation results reflect known empirical data is called calibration (Coulthard and van de Wiel, 2013). Calibration is one of the most crucial steps in the process of developing a hydraulic model because it allows the modeler to understand whether the model is capable of simulating past and present flows (Brunner *et al*., 2020). An uncalibrated hydraulic model may or may not reproduce realistic flows and should thus never be used to make important decisions (Wainwright and Mulligan, 2013).

Calibrating a 2D hydraulic model can be difficult and time consuming. The calibration of 2D models requires the following general data (Brunner *et al*., 2020):

- Observed land cover and roughness
- Observed water surface elevations at stream gauges
- Computed flows at stream guages
- Rainfall records
- Inundation extents or boundaries from aerial photography and field observations
- Photos or videos captured during flood events
- Anecdotal accounts of water surface elevations during flood events

The calibration process for 2D models starts with the hydrology. A useful hydraulic model requires the modeler to provide accurate flow boundary conditions (Brunner *et al*., 2020). The modeler must check that modelled inundation boundaries and water surface elevations are sufficiently similar to

observed inundation extents and water surface elevations. Roughness coefficients should be adjusted up and down to reproduce realistic flow velocity (Brunner *et al*., 2020).

4.3 Non-linearity and model uncertainty

Field data from river systems have shown their geomorphological responses to be non-linear in general (Coulthard and van de Wiel, 2013). This adds an additional level of complexity to modelling. Coulthard and van de Wiel (2013) recommend that in highly non-linear and therefore unpredictable sections of a river, conventional modelling approaches are futile. There are ways to incorporate the variability of model outputs into the final modelled results, such as reporting a range of predicted values rather than exact values (Coulthard and van de Wiel, 2013).

Uncertainty is inherent in any model due to the nature of a model being a simplified representation of reality. Uncertainty analysis is done to determine the accuracy of model outputs (Coulthard and van de Wiel, 2013). In numerical models, there are many sources of uncertainty: the input data, structure of algorithms, simplifications of the model, the calibration process itself, the data used for calibration and validation, as well as equifinality (Coulthard and van de Wiel, 2013). Equifinality in models is where two different sets of parameters give the same modelled results.

Assessing model uncertainty is easy in simple models, with a small number of inputs, a simple structure, and a system that responds linearly. However, uncertainty analysis is very challenging in more complex, physical-based models that have many parameters and represent fluvial systems that respond nonlinearly (Coulthard and van de Wiel, 2013). Geomorphological modelers need to engage with uncertainty analysis if they are to create models that are relevant for any practical or theoretical application (Coulthard and van de Wiel, 2013).

4.4 Analysis of valley morphology in relation to geomorphic features and processes

In terms of topographic data collection, an aerial LiDAR survey was the primary method used. The survey was undertaken by GeoSense, a company that specializes in providing aerial photography, LiDAR, mobile mapping and ground surveys across sub-Saharan Africa. A high-resolution topographic dataset was key to achieving objectives 1 and 2.

The aerial LiDAR survey was performed using a fixed-wing aircraft. A 23km length of the Kromme River valley was surveyed. The aircraft flew at the height of 700 meters over the study area, at a flying speed of 110 knots (Appendix 1). The sensors' scan rate was 300KHz, and the point density of the LiDAR data was approximately 5.5 points per square meter. The SAG2010 geoid model was used to convert ellipsoidal heights to orthometric heights.

Using the open-source software QGIS, LiDAR data in LAS format were converted into a DTM point cloud with a 5 points per square meter resolution. The ground surface was approximated by using the minimum elevation of the backscattered LAS data. The DTM used for modelling of water flow made use of LiDAR data with a resolution of 5m as it effectively removed structures like bridges and roads across the wetland. This simplified the simulation significantly as it meant that computational efficiency was acceptable for available computer hardware.

Geomorphic features associated with the Kromme River wetlands and tributaries flowing into the trunk valley were interpreted from high resolution orthophotography that came with the LiDAR dataset, Google Earth imagery, published information (Lagesse, 2017, McNamara, 2017, Schlegel, 2017, Ellery *et al*., 2022, In Prep) and the high resolution DTM data obtained from the LiDAR survey. The geomorphic features that were most important for this study were unchannelled valley-bottom wetlands (imagery and DTM longitudinal sections), gullies (imagery and DTM valley cross- and longitudinal sections), floodouts (McNamara, 2017, imagery) and tributary alluvial fans (DTM data obtained from the LiDAR survey, remotely sensed imagery and Lagesse, 2017, Schlegel, 2017, and Ellery *et al*., 2022, In Prep). Shapefiles of these features were created through heads-up digitization in QGIS.

The Profile tool in QGIS was used to examine the longitudinal slope of the valley. A longitudinal profile of the entire surveyed length of the Kromme River valley was plotted. This was intended to investigate the overall longitudinal profile of the river valley in order to understand the slope changes along the entire section and the effect of tributary alluvial fans on trunk valley morphology. The focus of analysis was the Krugersland, Kompanjiesdrift, and Jagersbos basins.

Cross-sectional profiles across the width of the valley in each wetland were created using the DTM. Longitudinal profiles of each wetland were created using the DTM. The data were exported to Excel for statistical analysis. In Excel, the average longitudinal slopes for each wetland were calculated using linear trendlines ($y=mx + c$). From these trendlines, the slope (m) and the R^2 values were obtained.

Changes in the average longitudinal slope and width of the valley near geomorphic features like tributary alluvial fans, gullies and floodouts were analysed in order to determine the effect af tributaries on trunk valley morphology.

4.5 Application of the model and analysis of hydraulic modelling outputs

4.5.1 Building and applying the model

HEC-RAS requires several input parameters to perform a hydraulic analysis of the geometry of the river valley and wetlands and the flow of water through them. RASMapper, a GIS application within HEC-RAS, was used to digitize all the necessary geometries for building the model. These included:

- The perimeter of the valley margin
- The computational grid
- Computational points within the grid
- Breaklines representing the river centre line
- Boundary conditions
- Breaklines for each boundary condition

The DTM and orthophotography were used to define the perimeter of the valley floor margin (light blue polygon figure 14). The valley floor perimeter was used to create a 10m resolution computational grid. A 10m grid seems appropriate for numerical stability and computational efficiency, given the very long reach of the wetland being investigated (MC Grenfell Personal Communication, Institute for Water Studies, Department of Earth Sciences, University of the Western Cape).

Topographic information in the DTM and orthophotos were used to determine the most likely flow path. A breakline representing the most likely flow path (the river centre line), was added to the computational grid.

A boundary condition for the inlet to the computational grid was specified (Figure 15). Inflow information for the boundary condition was provided for the duration of the model run. An outlet boundary condition at the foot of the computational grid was added (Figure 15). This allowed water to escape the grid.

At points where sub-catchment boundaries cross the valley, internal boundary conditions were specified (Figure 15). This allowed flows from tributary streams to be added. Flows coming from each sub-catchment were proportional to the size of the sub-catchment (Table 4). This allowed flows to increase downstream in proportion to the discharge leaving the computational grid.

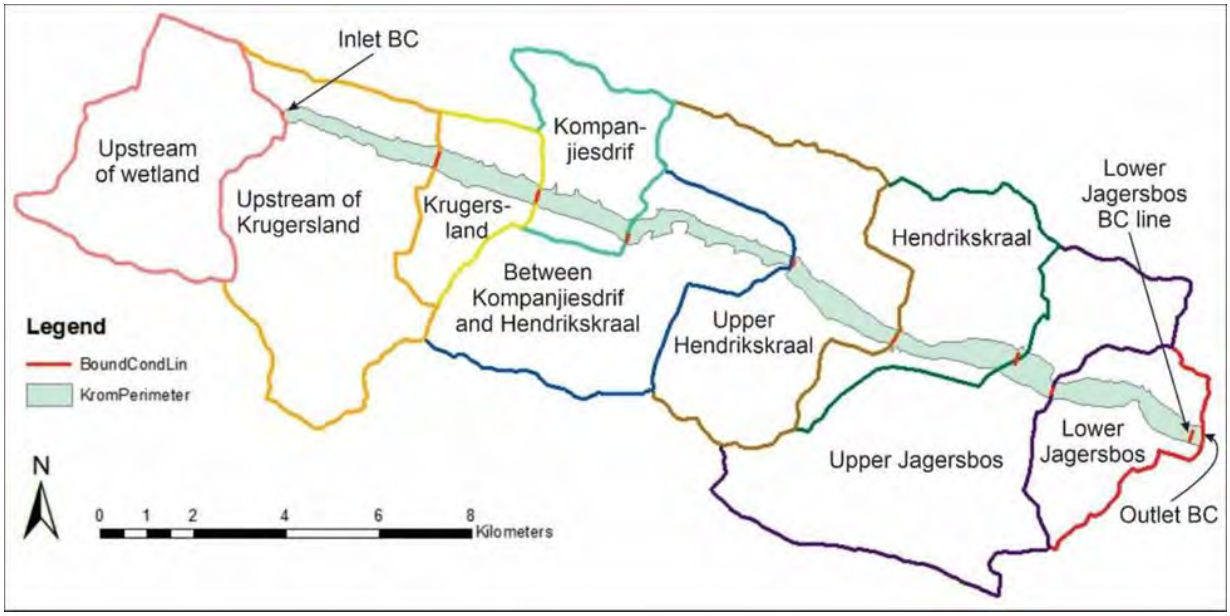

Figure 15: The sub-catchments and associated internal boundary conditions (BC). The reach between the Kompaniesdrif and Jagersbos wetland is known as Hendrikskraal. While this reach was not focused on in this study, the sub-catchments of the tributaries flowing into this reach of the valley were included.

A discharge of 45 cumecs at the outlet boundary of the computational grid was modelled. This discharge was decided upon because it is the approximate bankfull flow for the cross-section at the wetland outlet (assuming Manning's roughness = 0.045), and it represents the discharge following a 1:50 year flood in the upper Kromme River.

The flows were made more realistic based on the proportion of the catchment receiving runoff because the discharge increases systematically downstream as tributaries join the trunk stream. Furthermore, the discharge was not uniform over the duration of the model run. It varied systematically, increasing by flow 1 cumec for each boundary condition over the duration of the analysis (Table 4). The discharge values for each sub-catchment were scaled on an area-weighted basis so that the discharge at the outflow of the Jagersbos wetland was approximately 45 cumecs.

Table 4: The discharges added across each internal boundary condition that flow out of successive sub-catchments into the wetland downstream.

Sub-catchment	**Discharge (cumecs) added at internal boundary conditions**
Upstream of wetland	5 – 6
Upstream of Krugersland	7 – 8
Krugersland	2 – 3
Kompanjiesdrift	2 – 3
Between Kompanjiesdrift and Hendrikskraal	5 – 6
Upper Hendrikskraal	6 – 7
Hendrikskraal	4 – 5
Upper Jagersbos	8 – 9
Lower Jagersbos	5 – 6

Manning's roughness coefficients throughout the computational grid were required as another input to the model. High-resolution orthophotography that came with the LiDAR dataset and field observations of vegetation types along the Kromme valley bottom were used for digitizing the distribution of land cover classes. Each land cover class was assigned a roughness value, varying from 0.025 to 0.155 (Table 6). Manning's roughness values for natural streams described by Chow (1959) were used as a reference (Table 5), as well as the values used by Schlegel (2017) in her hydraulic modelling of the Krugersland and Kompanjiesdrift wetlands. The assigned values were based mainly on the degree to which wetland vegetation has colonized the bed and the typical plant height, density and stem thickness of emergent stems. The LiDAR data was useful for assessing roughness because it captured the height and density of the vegetation.

Table 5: Manning's roughness (n) values for natural channels (Chow, 1959).

Manning's roughness coefficient (n)			
Type of channel and description	Minimum	Normal	Maximum
Natural streams			
Main channels			
A. clean, straight, full stage, no rifts or deep pools	**0.025**	**0.03**	**0.033**
B. same as above, but more stones and weeds	**0.03**	**0.035**	**0.04**
C. clean, winding, some pools and shoals	**0.033**	**0.04**	**0.045**
D. same as above, but some weeds and stones	**0.035**	**0.045**	**0.05**
E. same as above, lower stages, more ineffective slope and sections	**0.04**	**0.048**	**0.055**
F. same as "d" with more stones	**0.045**	**0.05**	**0.06**
G. sluggish reaches, weedy, deep pools	**0.05**	**0.07**	**0.08**
H. very weedy reaches, deep pools, or floodway's with heavy stand of timber and underbrush	**0.075**	**0.1**	**0.15**

Table 6: Manning's roughness values for each land cover class mapped in the Kromme wetland.

Land cover class	**Manning's roughness (n)**
Dense wetland vegetation	0.155
Wetland vegetation	0.135
Grassy floodplain	0.115
Sandy, grassy floodplain	0.095
Sandy with some vegetation	0.075
Open water, bare rocks, stones	0.55
Dirt road	0.035
Concrete weir	0.025

The parameters that formed the basis of the HEC-RAS simulations were as follows:

- Computational interval of 20 seconds.
- Map output interval of 2 minutes.
- Hydrograph output interval of 2 minutes.
- Detailed output interval of 2 minutes.
- 2D unsteady diffusion wave equation.

Computed flows at stream gauges, such as the one downstream of Churchill Dam, were used to calibrate the model. Manning's n-values were adjusted to reproduce computed flows. Brunner *et al*. (2020) suggests that models should always be reviewed by an independent expert to ensure that the model was applied correctly, calibrated effectively, and reproduces reasonable results for the flood event being modelled. Professor M.C. Grenfell, an expert in hydraulic modelling at the University of the Western Cape, reviewed this model by comparing it to a model he developed using the same input data using the modelling software Delft3D . Results were also compared to Schlegel (2017), who used HEC-RAS to model flow in the Kompanjiesdrift basin.

4.5.2 Analysis of modelling outputs

The HEC-RAS model outputs are in the form of raster layers. Each cell has a value for velocity, stream power and depth. QGIS was used to display and analyse the model outputs.

The Profile tool in QGIS was used to determine the velocity, stream power, and depth values down the length of each wetland. The breakline representing the river centre line was used as the independent variable , while velocity, stream power, and depth were the dependent variables .

The Profile tool in QGIS was used to determine the average velocity, stream power, and depth in particular reaches within each of the three wetlands. Three cross-sections in each reach were created, and the data were exported into Excel. The average values of the hydraulic characteristics for each of the three cross-sections were calculated. Then the average of those three values was calculated to get the mean velocity, stream power, and depth values in a particular reach.

To analyse the effect of valley morphology on hydraulic characteristics, the longitudinal profiles of each of the three wetlands were compared to variation in flow velocity, stream power, and depth over the length of the wetlands. The model results were displayed on a map along with geomorphic features like gullies, alluvial fans, and floodouts. This allowed visualisation of the effect of these features on flow characteristics. The locations of erosion control structures in each of the three wetlands were mapped to show the effect of these structures on flow characteristics.

4.6 Selection of sites to trial new rehabilitation strategies

Schlegel (2017) conducted hydraulic modelling in the Kompanjiesdrift basin that involved sediment particle size, as well as factors like velocity, stream power, and depth. It was found that fine to

medium sand makes up the majority of the bedload in the Kromme and that it takes a minimum velocity of 0.3 m/s to entrain sediment with this particle size (Schlegel, 2017). Therefore, areas with a flow velocity of 0.3 m/s and less may be the optimal sites to test new rehabilitation methods.

A classical GIS overlay technique was used on the model outputs to identify sites that are depositional in nature and, therefore, appropriate to trial new rehabilitation strategies. In the modelled velocity layer, pixels with a value less than or equal to 0.3 m/s were isolated — these identified sites with a low enough velocity and stream power for palmiet to establish.

Palmiet's regeneration niche was considered in conjunction with hydraulic characteristics. According to Van Eck (2022, In Prep), palmiet colonizes exposed sediment on the beds of gullies and on depositional features like floodouts. Sites with exposed sediment and sufficiently low flow velocity were mapped as they were considered suitable for palmiet establishment. Furthermore, sites within 0.5 m of the elevation of a local thalweg were considered appropriate.

CHAPTER 5: RESULTS

5.1. Longitudinal slope of the Kromme River valley

The Kromme River valley has a broadly logarithmic longitudinal slope (Figure 16). The difference in elevation is 170 m over a distance of roughly 23 km. There is a consistent decline in slope from the top of the wetland in a downstream direction. The Krugersland wetland has a slope of -1.09%, the Kompanjiesdrift wetland has a slope of -0.92%, and the Jagersbos wetland has a slope of -0.33%.

Along the longitudinal profile, there are minor localized increases and decreases in slope (Figure 16). These irregularities are due to geomorphic processes associated with trunk-tributary stream interactions and erosional and depositional features on the trunk valley floor.

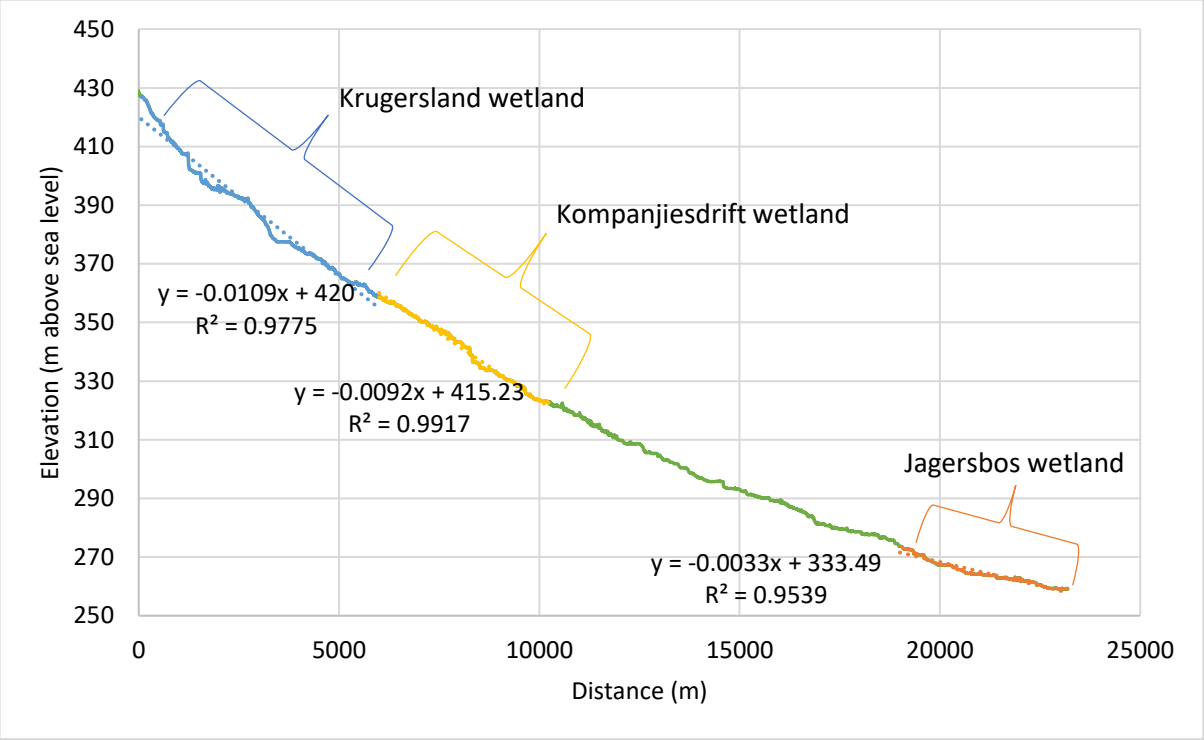

Figure 16: Graph of the longitudinal profile of the Kromme River valley with the three wetlands indicated in different colours – Krugersland in blue, Kompanjiesdrift in yellow, and Jagersbos in orange.

5.2. Krugersland wetland morphology

The map of the Krugersland wetland Figure 17, shows the extent of the intact portion of the wetland, the section of the wetland that is channelled, the tributary streams that flow into the trunk valley, the locations and extents of tributary alluvial fans (labelled A, B, and C) that impinge the trunk valley, the location of a depositional floodout, and the locations of four concrete erosion control structures. Upstream of the floodout, the Kromme River exists as a channeled wetland because it flows in an eroded gully. The river exists as an unchanneled valley-bottom wetland downstream of the gullied reach.

Alluvial fan B is a large depositional feature that enters the valley from a large tributary stream to the south of the valley. The fan crosses the trunk valley from a distance of about 2250 m to 3100 m along the trunk valley. Over this distance it causes narrowing of the trunk valley from about 180 m upstream of the feature to 80 m opposite the centre of the tributary fan at a distance of about 2700 m down the length of the trunk valley.

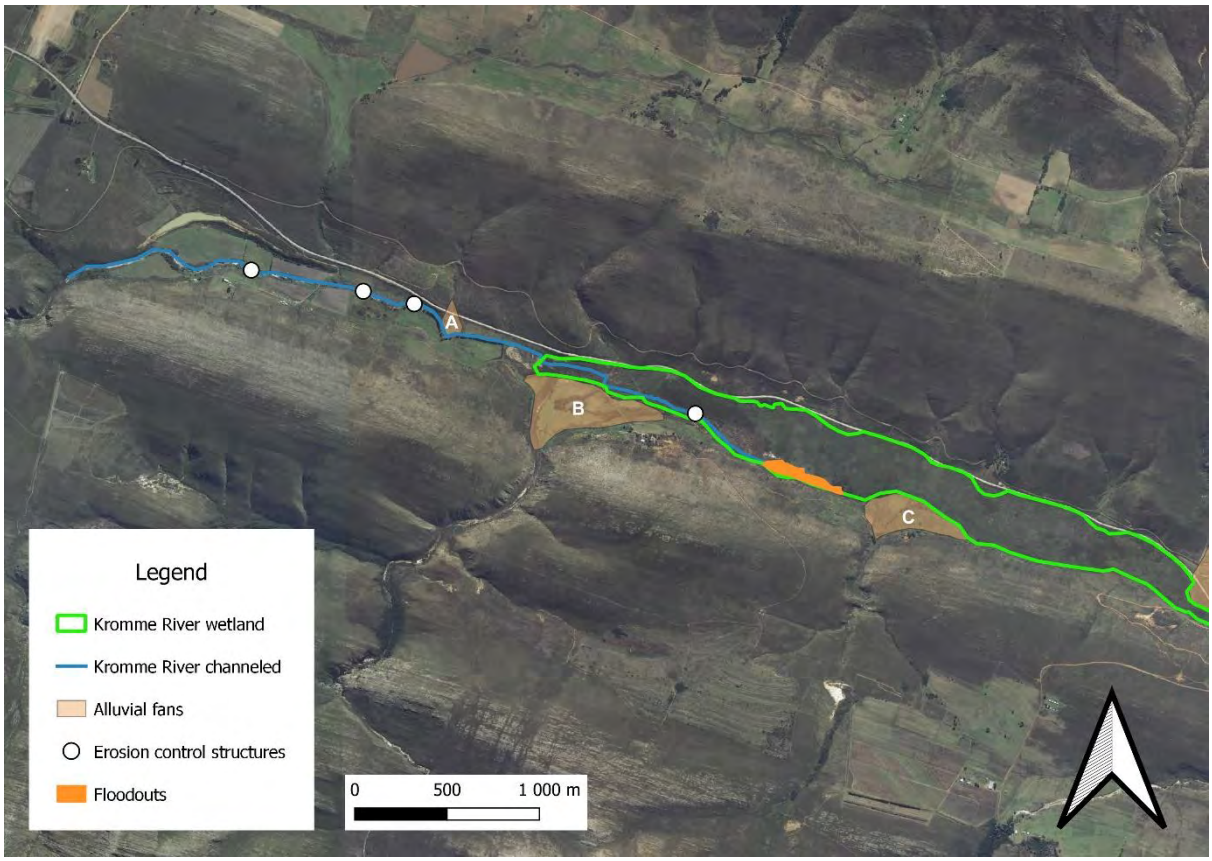

Figure 17: Map of the Krugersland wetland indicating the locations of erosion control structures, alluvial fans, and erosional gullies.

The first erosion control structure is about 600 m down the length of the eroded reach (Figure 18A). The second and third are 1250 m and 1550 m down the length of the eroded reach, respectively (Figure 18B and C). Downstream of alluvial fan B, about 3275 m down the valley's length, is the fourth erosion control structure (Figure 18D). Downstream of the gullied reach, below the fourth erosion control structure, is a depositional floodout feature (from about 3775 m to 4225 m down the length of the trunk valley).

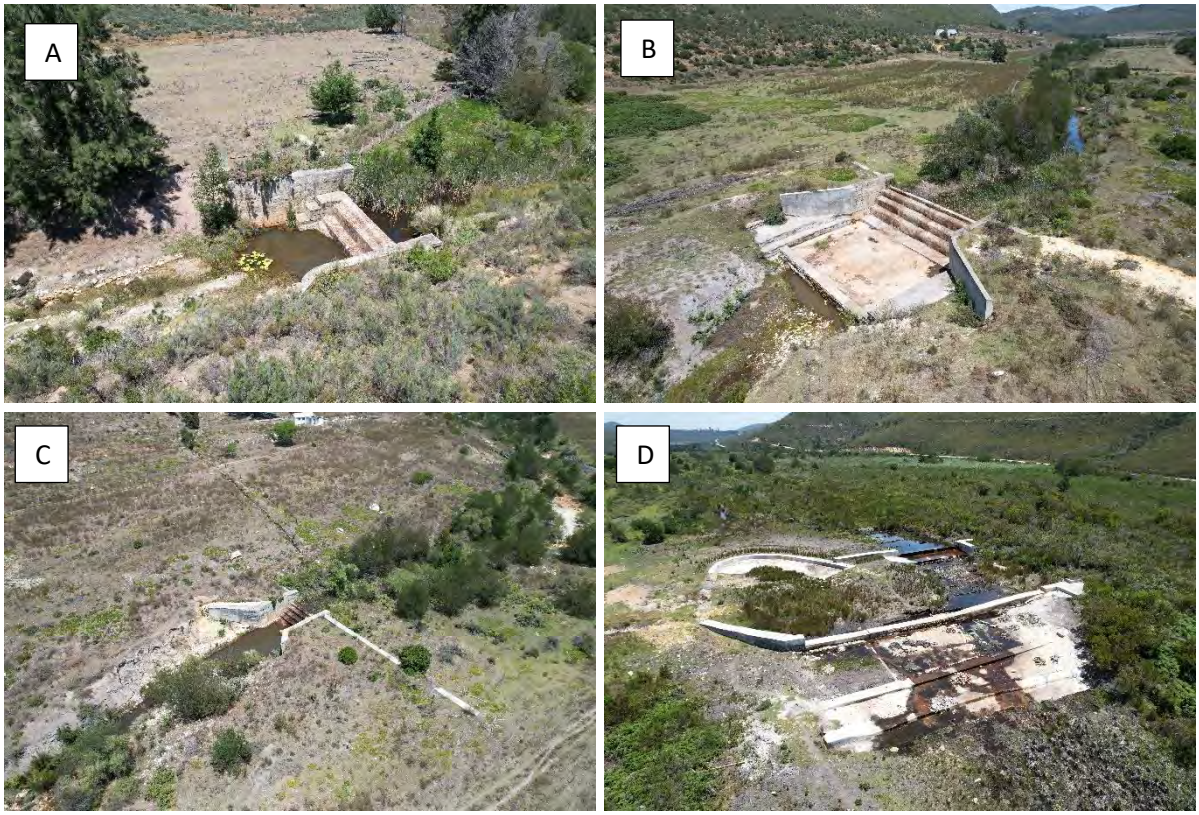

Figure 18: Photographs of the four erosion control structures in the Krugersland wetland, taken with a drone. Images A, B, and C were captured looking upstream, and image D was captured looking downstream.

5.2.1 Longitudinal characteristics of the Krugersland wetland

The longitudinal profile of the Krugersland wetland is shown in Figure 19, indicating about eight distinct reaches where there is a change in longitudinal slope, above and below which the slope is uniform. The locations of erosion control structures along the length of the profile are also shown.

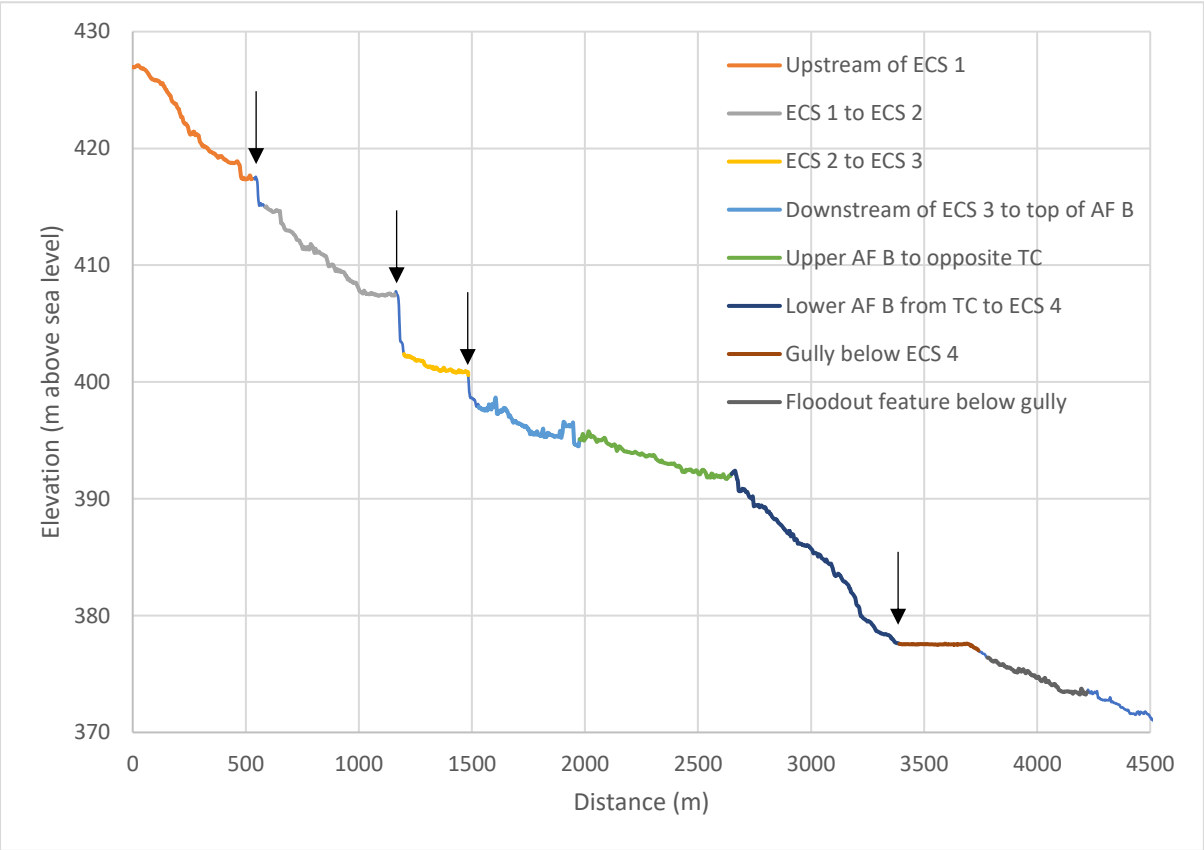

Figure 19: Longitudinal profile of the Krugersland wetland. Erosion control structures (abbreviated ECS in the figure legend) are indicated by black arrows. The reaches within the wetland with uniform slopes are indicated in different colours as indicated in the figure legend. Further abbreviations in the figure legend: alluvial fans = AF and tributary confluence with the trunk stream = TC.

Upstream from the first erosion control structure, the bed has a slope of -2.08 % (Table 7). This is higher than any other reach in the Krugersland wetland. The slope decreases to -1.45 % downstream of the first erosion control structure and decreases further to -0.55% downstream of the second structure.

Alluvial fan B is evident from about 2000 m to 3400m along the longitudinal profile. The upper half of this large alluvial fan has a slope of -0.59%. The bed downstream from where the tributary stream joins the trunk stream has a much steeper slope of -1.97%.

The erosional gully downstream of alluvial fan B and erosion control structure 4 has a shallow slope of -0.06%. The depositional floodout feature downstream of where the gully loses confinement has a steeper slope of -0.74 %.

Table 7: Mean slopes of eight different reaches in the Krugersland wetland.

Reach	Description	Start (m)	End (m)	Slope (%)	R^2
1	Upstream of ECS 1	0	526	-2.08	0.9742
2	ECS 1 to ECS 2	586	1159	-1.45	0.9632
3	ECS 2 to ECS 3	1200	1483	-0.55	0.8813
4	Downstream of ECS 3	1530	1977	-0.66	0.7229
5	Upper AF B to opposite TC	1978	2648	-0.59	0.973
6	Lower AF B from TC to ECS 4	2648	3389	-1.97	0.9873
7	Gully below ECS 4	3390	3740	-0.06	0.2825
8	Floodout feature below gully	3780	4220	-0.74	0.9726

5.2.2 Cross-sectional characteristics of the Krugersland wetland

The locations of cross-sections across the width of the Krugersland wetland (all oriented from south to north across the valley) are shown in figure 20. The cross-sections are ordered from 1 to 7 in a downstream direction. Cross-sections 1, 2, and 3 are taken upstream of alluvial fan B across the erosional gully. Cross-sections 4 and 5 are taken just upstream from and in the middle of alluvial fan B. Cross-section 6 is taken across the gully downstream of the fourth erosion control structure, and cross-section 7 is taken across the depositional floodout downstream of this gully.

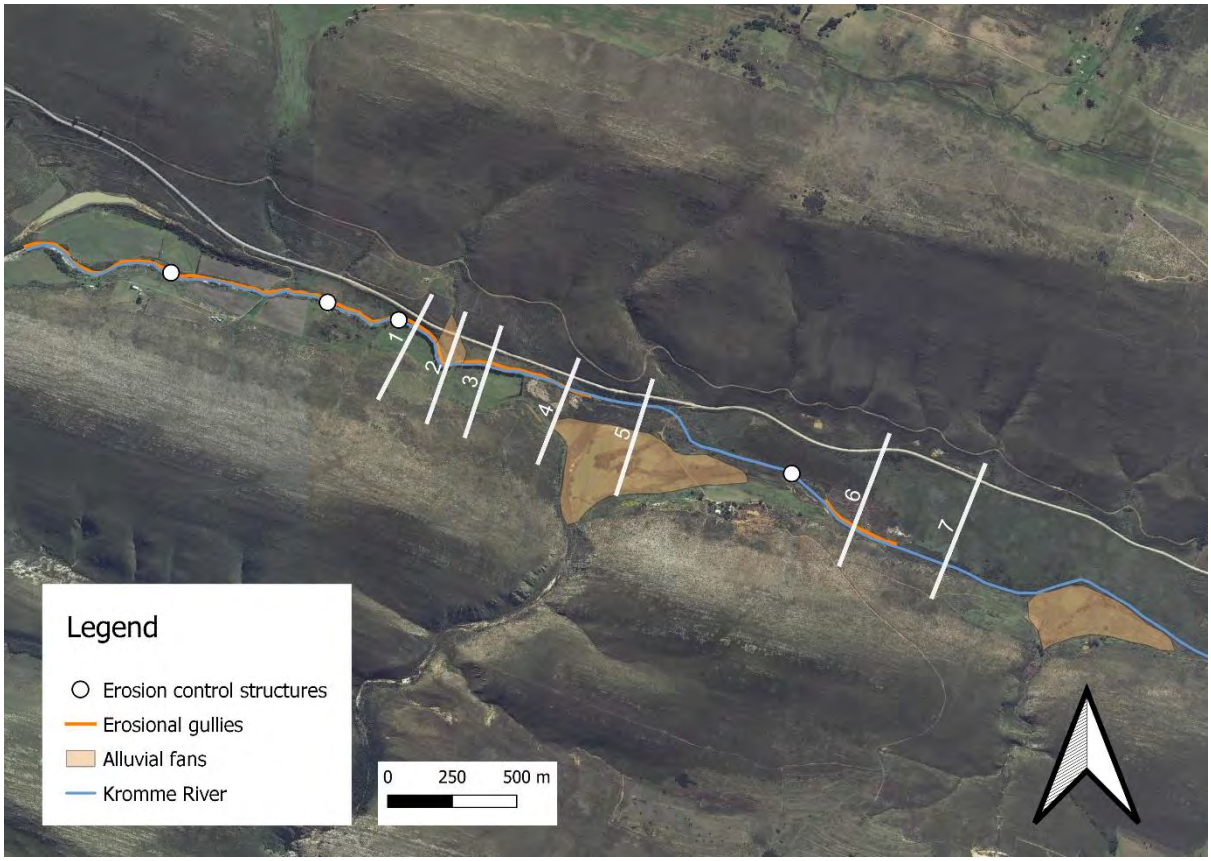

Figure 20: Map of the Krugersland wetland indicating the locations of cross-sections 1 to 7.

In cross-section 1 (Figure 21), the gully is evident on the northern side of the valley-bottom. The valley is otherwise near-horizontal in form. In cross-section 2, alluvial fan A impinges the valley from the north, narrowing the valley-bottom. In cross-sections 3 and 4, downstream from alluvial fan A, the valley widens again and has a broad, horizontal valley floor with steep sides. The gully is still seen on the northern side of the valley-bottom, but its depth and width decline systematically downstream such that it is no longer evident in section 4. The wetland in Section 4 is about 160 m.

Across the middle of alluvial fan B (cross-section 5), the wetland is confined to the northern side of the valley-bottom. While the valley appears wide in cross-section 5, much of the section has a gently sloping alluvial fan impinging the trunk valley from the south such that at the location of cross-section 5 the trunk valley wetland is only about 30 m wide. Alluvial fan B impinges the valley from about 80 m to 390 m along the cross-section. In cross-section 6, the erosional gully is evident on the southern side of the valley-bottom. The intact wetland to the north of this gully is broad and flat. In cross-section 7, to the north of the floodout the intact wetland is broad and flat.

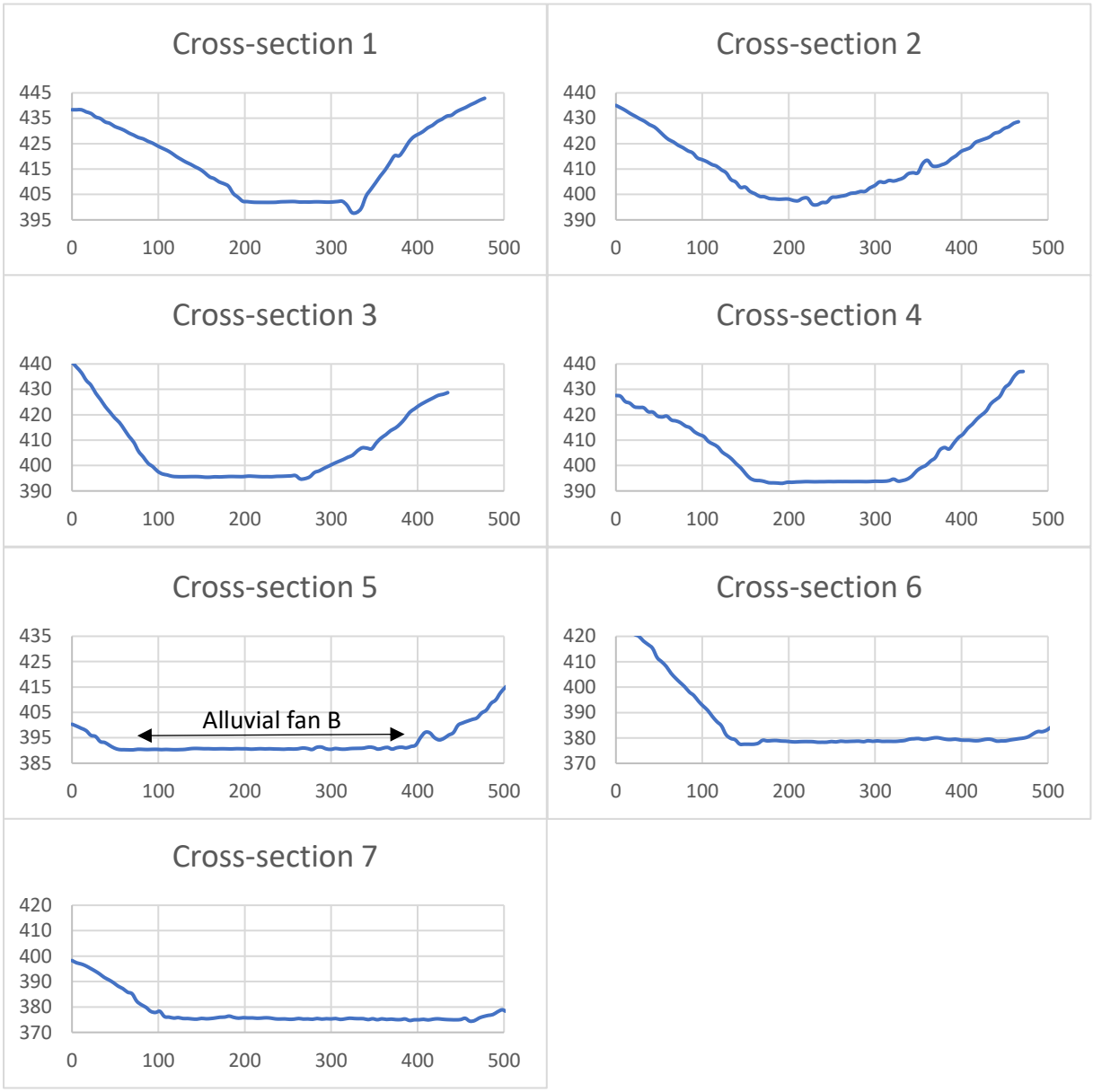

Figure 21: Cross-sectional profiles 1 to 7 of the Krugersland wetland. All are oriented south-to-north across the valley.

5.3 Krugersland wetland hydrogeomorphic characteristics

Figure 22 shows the longitudinal slope of the Krugersland wetland over the upper 4 300 m of the surveyed reach (a), and the associated stream power, velocity, and depth (b). For this reach, the modelled flow was 45 $m^3.s^{-1}$, which approximates a 1:50 year flood for this reach. It is evident that sudden breaks in slope associated with erosion control structures are linked to significant increases in stream power, velocity, and depth. Over the upper approximately 2 400 m (as far downstream as the south bank tributary confluence associated with alluvial fan B) flow characteristics are variable in response to variation in slope, roughness, and valley width. It is noteworthy that downstream of the tributary confluence of alluvial fan B, flow characteristics are relatively constant, largely reflecting variation in the width of flooding of the valley floor.

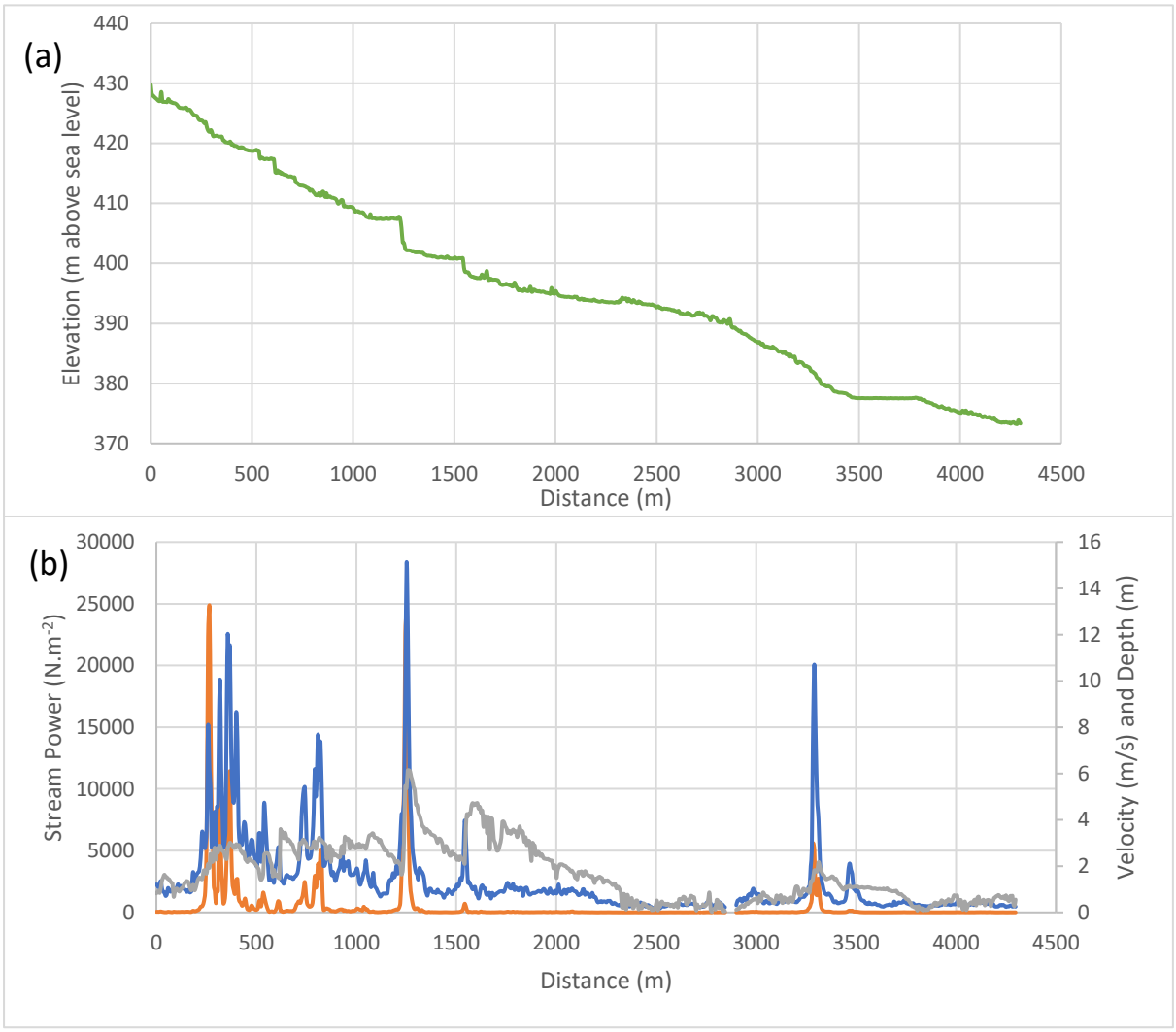

Figure 22: The longitudinal profile of the Krugersland wetland (a), and the velocity (blue), stream power (orange), and depth (grey) down the length of the wetland (b).

Along the main watercourse and flood as shown in Figure 22, and for this magnitude of flooding, the mean flow velocity for the entire Krugersland wetland is 1.046 m/s. The mean stream power is 60.747 $N.m.s^{-2}$, and the mean depth of flow is 1.354 m.

For the main watercourse and flood as shown in Figure 22, velocity, depth, and stream power values are all higher in the eroded reach of the wetland upstream of alluvial fan B than below it. The mean velocity upstream of alluvial fan B is 2.2 m/s (standard deviation = 2.09 m/s), whereas below the fan it is 0.57 m/s (standard deviation = 0.83 m/s). The mean stream power upstream of alluvial fan B is 1024.4 $N.m.s^{-2}$ (standard deviation = 3142.5 $N.m.s^{-2}$), whereas below the fan, it is only 68.6 $N.m.s^{-2}$ (standard deviation = 424.8 $N.m.s^{-2}$). The mean depth upstream of alluvial fan B is 2.79 m (standard deviation = 0.9 m), and below the fan, it is 0.56 m (standard deviation = 0.8 m).

5.3.1 Outputs from the HEC-RAS model

Figures 23, 24, and 25 are maps showing the outputs from the HEC-RAS model for the Krugersland wetland. These results clearly show that velocity, stream power, and depth values are at their highest upstream and, especially, downstream of erosion control structures and opposite alluvial fans, particularly along the valley margins.

In the widest portion of the wetland, downstream of alluvial fan B, where there are dense stands of palmiet, the velocity, stream power, and depth values are lowest. Upstream of alluvial fan B, where there is no palmiet and erosion has occurred, the velocity, stream power, and depth values are higher.

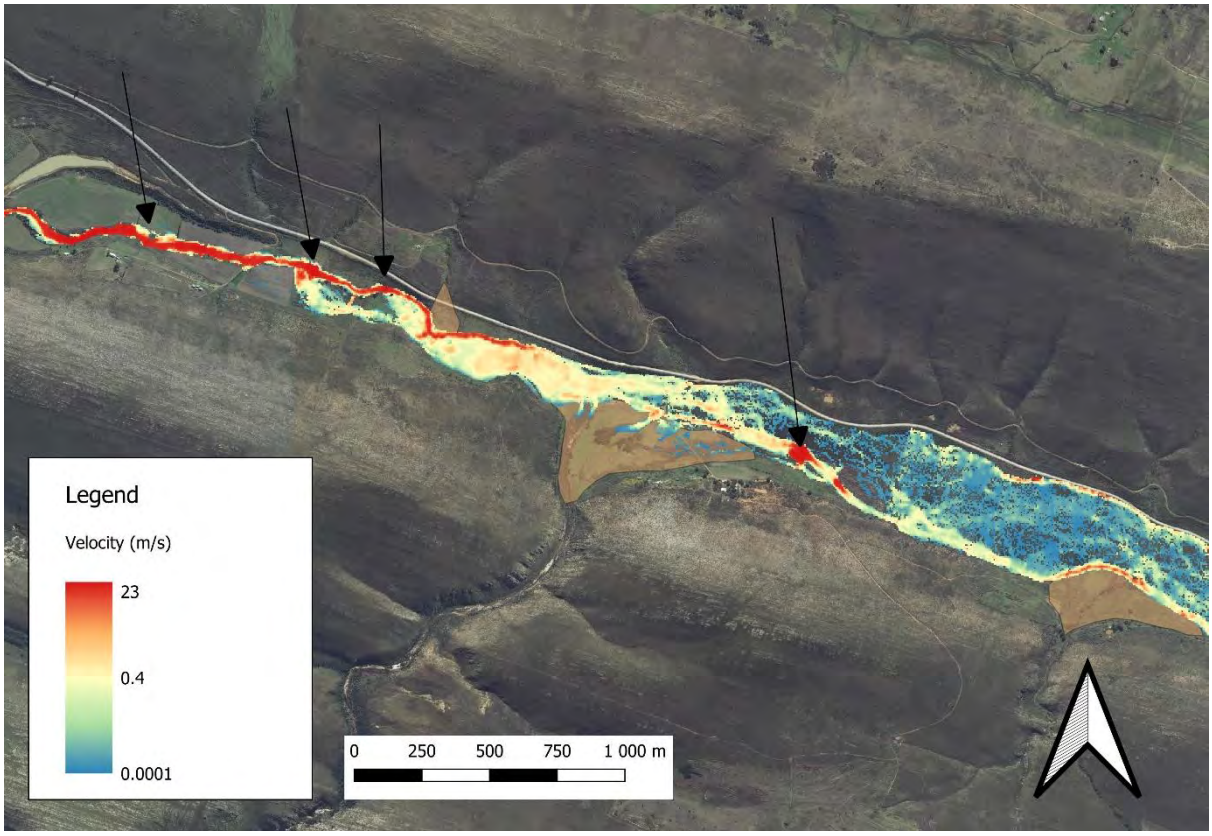

Figure 23: Modelled velocity down the length of the Krugersland wetland. Locations of erosion control structures are indicated by black arrows.

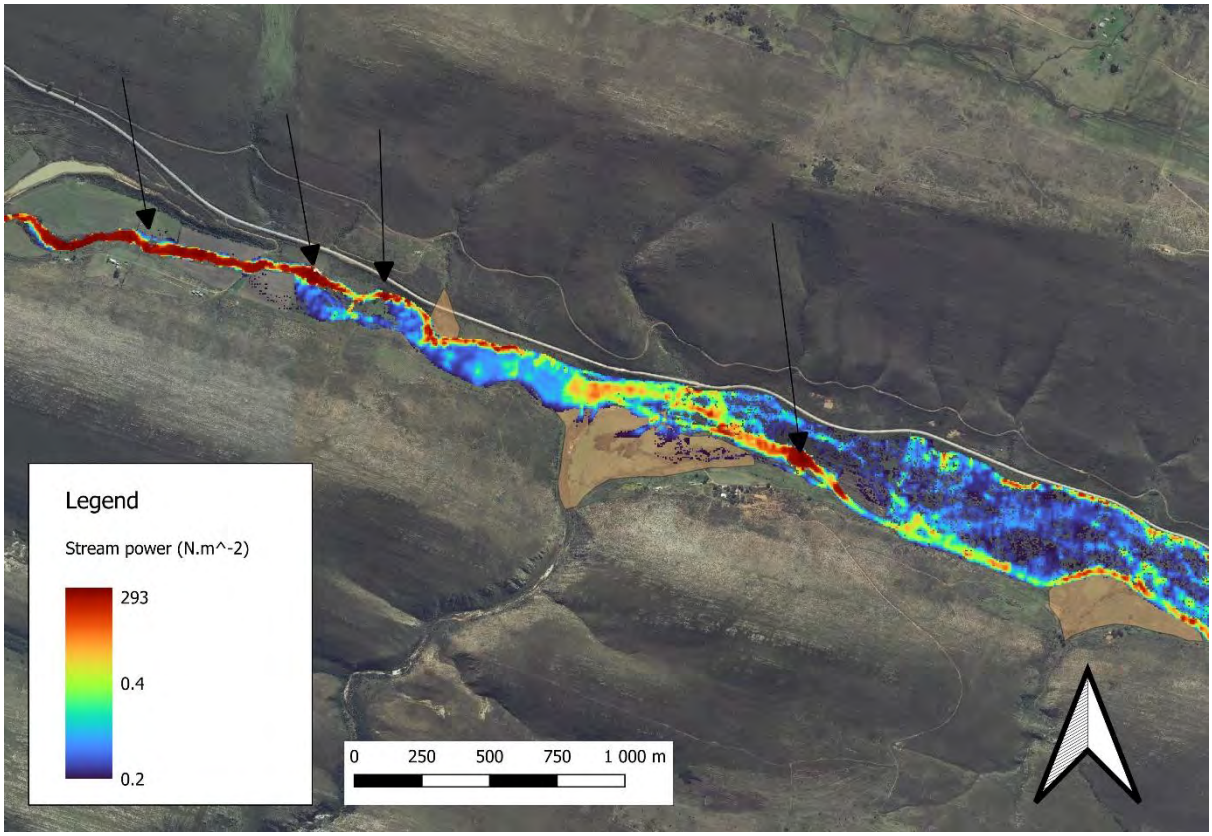

Figure 24: Modelled stream power down the length of the Krugersland wetland. Black arrows indicate the locations of erosion control structures.

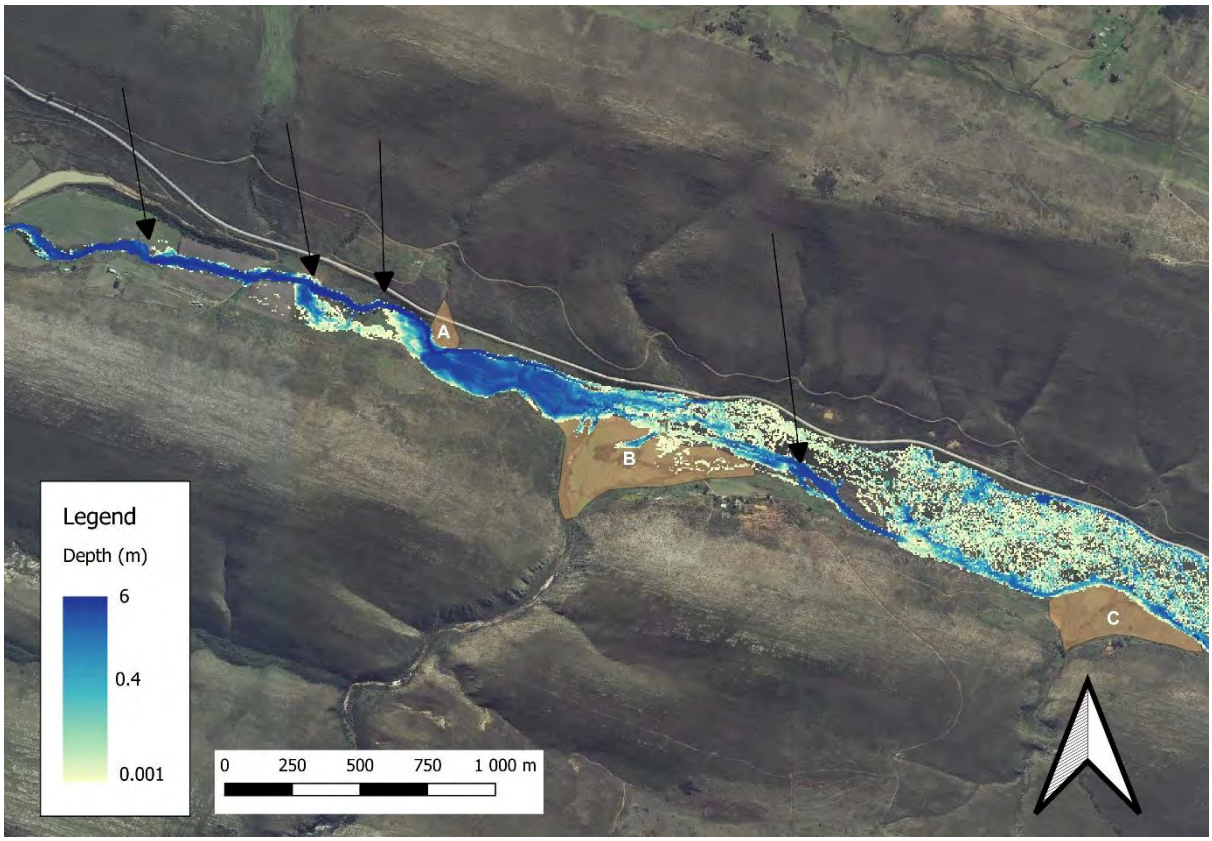

Figure 25: Modelled depth down the length of the Krugersland wetland. Black arrows indicate the locations of erosion control structures.

5.4 Kompanjiesdrift wetland morphology

The map of the Kompanjiesdrift wetland (Figure 26) shows the extent of the intact wetland, the tributary streams that enter the trunk stream, the locations and extents of alluvial fans D, E, F, G, and H, and the locations of two erosion control structures. Upstream of the erosion control structures, the Kromme River exists as an unchanneled valley-bottom wetland. Downstream of the structures, the river is channeled because it flows along an eroded gully.

Alluvial fan D is a large depositional feature that enters the valley from the north and reduces the valley width from about 200 m to just 60 m. At this narrow point in the valley, the R62 road crosses the wetland via a bridge. Alluvial fans E and F are much smaller alluvial fans arising from smaller tributary streams that enter the valley from the north. They reduce the valley width from about 250 m to about 160 m. The most significant alluvial fan in this wetland is alluvial fan G. It enters the valley from a large tributary stream to the north of the trunk valley. It reduces the width of the valley from about 200 m to a mere 50 m. In the middle of alluvial fan G, just downstream of where its tributary joins the trunk stream, there are two large concrete erosion control structures (Figure 27). Downstream of the structures is a large erosional gully that extends all the way down past the end of the Kompanjiesdrift reach.

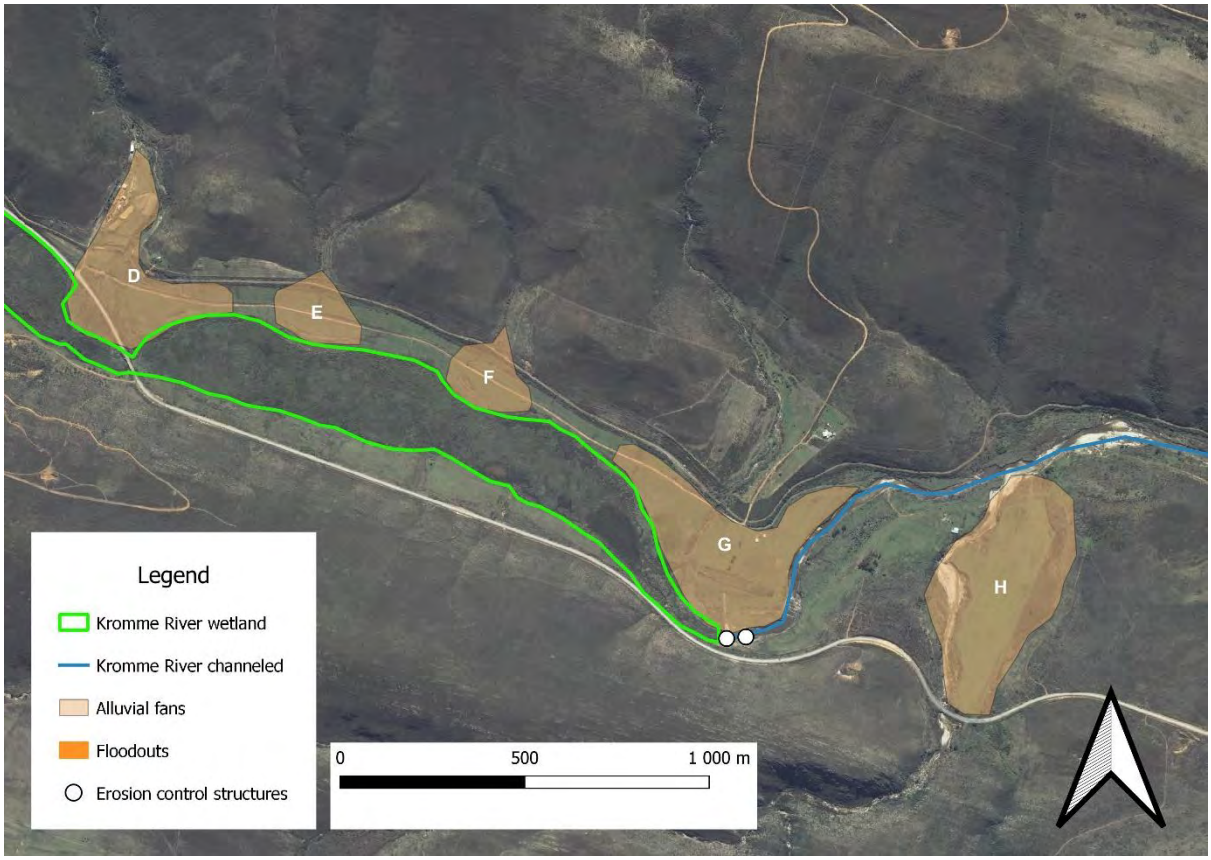

Figure 26: Map of the Kompanjiesdrift wetland indicating the locations of erosion control structures, alluvial fans, erosional gullies, and floodouts.

Figure 27: Photograph of the two large concrete erosion control structures downstream of the intact portion of the Kompanjiesdrift wetland. The gully erosion downstream of these structures is evident from the incised channel banks.

5.4.1 Longitudinal slope of the Kompanjiesdrift wetland

Figure 28 shows the longitudinal profile of the Kompanjiesdrift wetland and the difference in the slope of the bed upstream and downstream from the erosion control structures. The two erosion control structures are clearly visible in the profile as sudden breaks in the slope (shown in blue). Upstream of alluvial fan G, the average slope of the intact portion of the wetland is -0.91% (Table 8). Downstream of alluvial fan G and the erosion control structures, the average slope on the gully bed is -0.69%. This constitutes about a 25% reduction in slope.

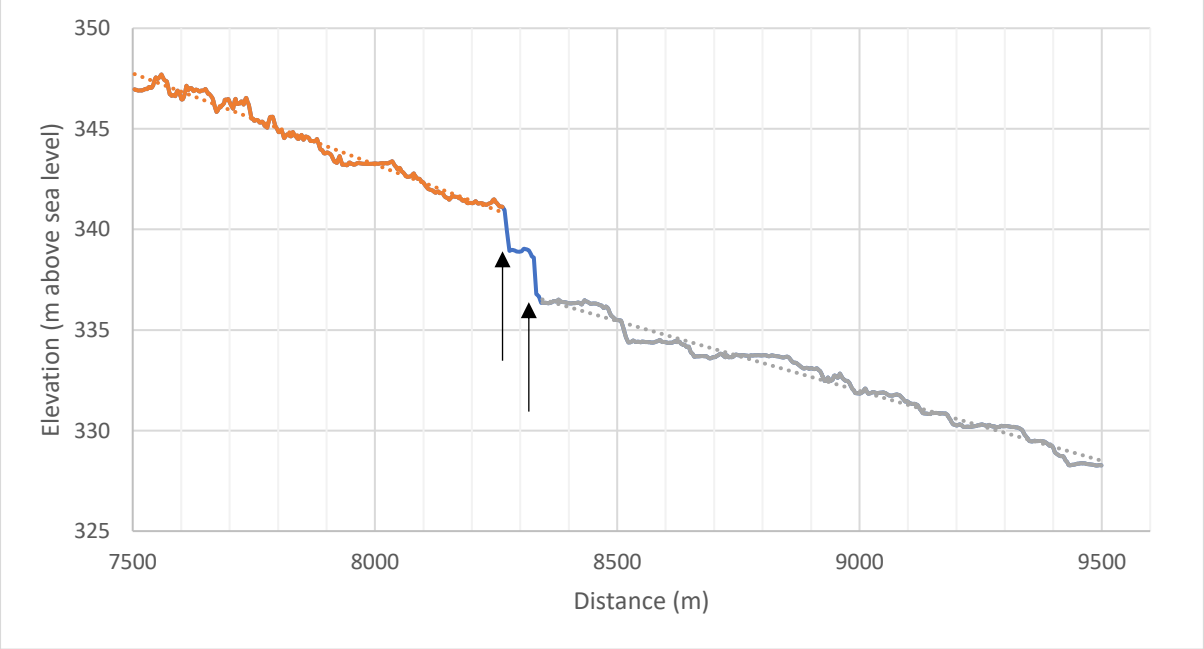

Figure 28: Longitudinal profile of the Kompanjiesdrift wetland. Erosion control structures are indicated by black arrows. The reach upstream from the two erosion control structures is indicated in orange and the reach downstream of the erosion control structures is indicated in grey.

Table 8: Mean slope in the Kompanjiesdrift wetland above and below erosion control structures.

Reach	Description	Start (m)	End (m)	Slope (%)	R^2
1	Upstream from erosion control structures	7500	8263	-0.91%	0.975
2	Downstream from erosion control structures	8345	9500	-0.69%	0.977

5.4.2 Cross-sectional characteristics of the Kompanjiesdrift wetland

The locations of cross-sections across the Kompanjiesdrift wetland are shown in Figure 29. The cross-sections are ordered from 1 to 9 in a downstream direction. Cross-section 1 is between alluvial fans D and E, cross-section 2 is across the middle of alluvial fan E, cross-section 3 is between alluvial fans E and F, and cross-section 4 is across the middle of alluvial fan F.

Cross-section 5 is upstream of alluvial fan G. Cross-sections 6 and 7 are across the upper half of alluvial fan G, upstream from the erosion control structures. Cross-sections 8 and 9 are across the lower half of alluvial fan G, downstream from the erosion control structures.

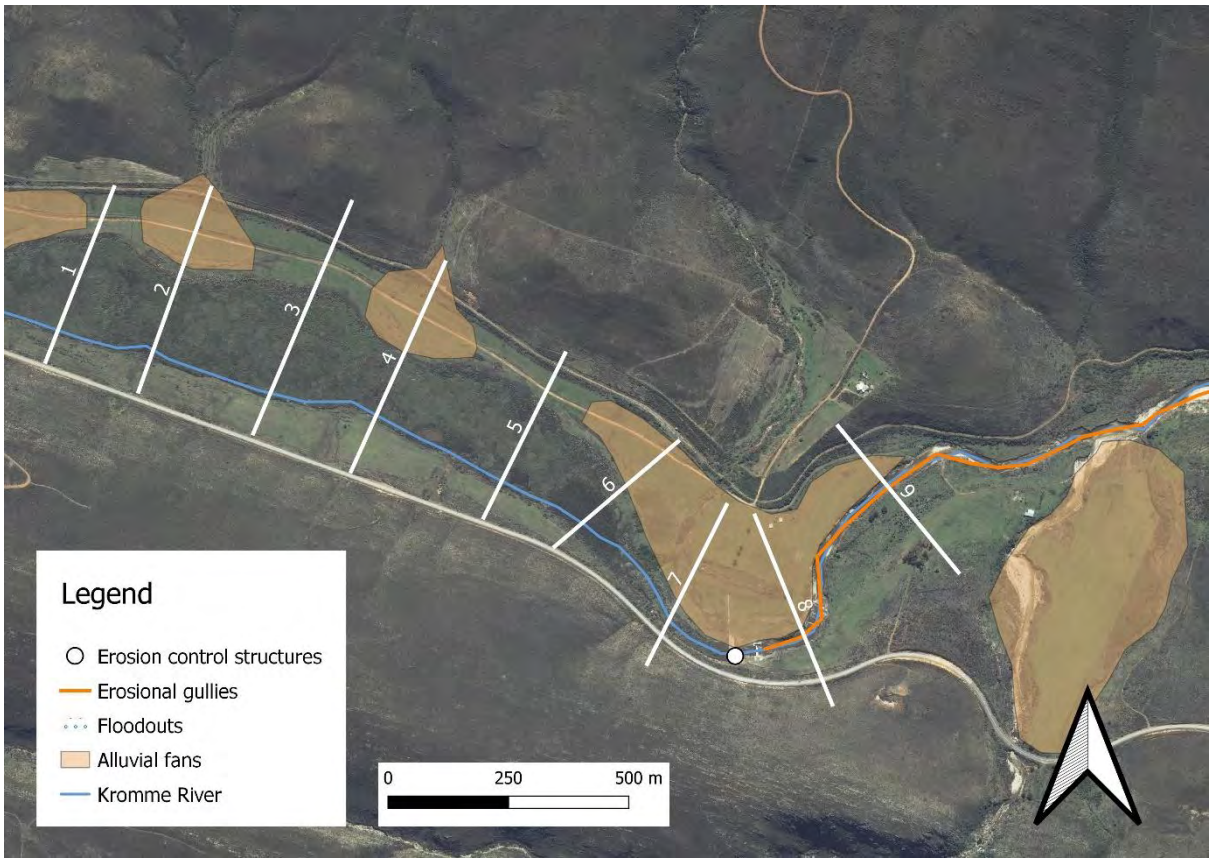

Figure 29: Map of the Kompanjiesdrift wetland indicating the locations of cross-sections 1 to 9.

Comparing cross-sections 1 and 3, which are taken downstream of small alluvial fans, to cross-sections 2 and 4, which are in the middle of small alluvial fans, it is clear these depositional features reduce the width of the trunk valley floor (Figure 30).

Cross-sections 5 and 6 illustrate the effect of alluvial fan G on valley width. In the unconfined reach, cross-section 5 shows the flat valley-bottom is almost 200 m wide. In the confined reach, cross-section 6 shows the valley width is reduced to about 50 m.

Cross-sections 7 and 8 are both in the middle of alluvial fan G, but one is above the erosion control structures, and the other is downstream of them. The valley width is very narrow in both these cross-sections, with flow confined to a valley floor that is less than 50 m wide.

In cross-section 8, there is a steep-sided gully in the middle of the eroded valley floor. In cross-section 9, the valley width increases downstream of alluvial fan G, but a 40 m wide, 6 m deep gully is evident in the middle of the trunk valley.

From high-resolution aerial imagery, outcrops of bedrock along the length of the eroded reach are visible. The gully downstream of the erosion control structures has, therefore, cut down to bedrock.

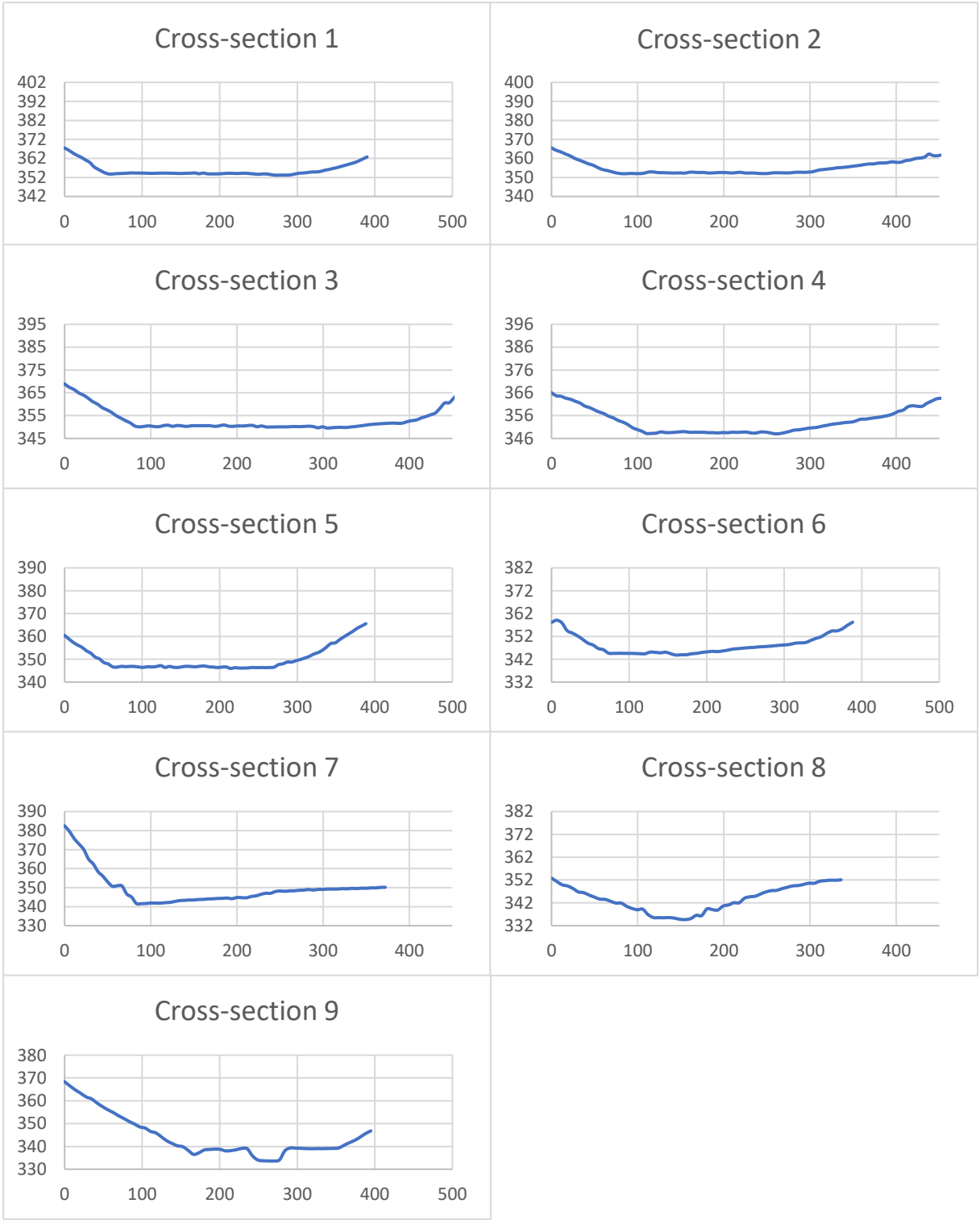

Figure 30: Cross-sections 1 to 9 in the Kompanjiesdrift wetland.

5.5 Kompanjiesdrift wetland hydrogeomorphic characteristics

Figure 31 shows the longitudinal slope of the Kompanjiesdrift wetland (a) and the associated stream power, velocity, and depth values down the length of the wetland (b) for a discharge of about 20 m3/s (approximately a 1:50 year flood). The sudden break in the slope is caused by the erosion

control structures. The mean flow velocity for the entire Kompanjiesdrift wetland is 0.748 m/s. The mean stream power is 48.108 N.m.s-2, and the mean depth of flow is 0.671 m.

Velocity, depth, and stream power values are much higher in the eroded reach, downstream of the erosion control structures, and alluvial fan G. The mean velocity upstream of alluvial fan G, in the intact reach of wetland is 0.34 m/s (standard deviation =0.12). In contrast, below the fan on the bed of the eroded gully, it is 1.13 m/s (standard deviation = 0.24). The mean stream power upstream of alluvial fan G is 15.64 $N.m^{-2}$ (standard deviation = 29.54), whereas below the fan it is 48.34 $N.m^{-2}$ (standard deviation = 29.93). The mean depth upstream of alluvial fan G is 0.49 m (standard deviation = 0.26), and below the fan, it is 0.80 m (standard deviation = 0.21).

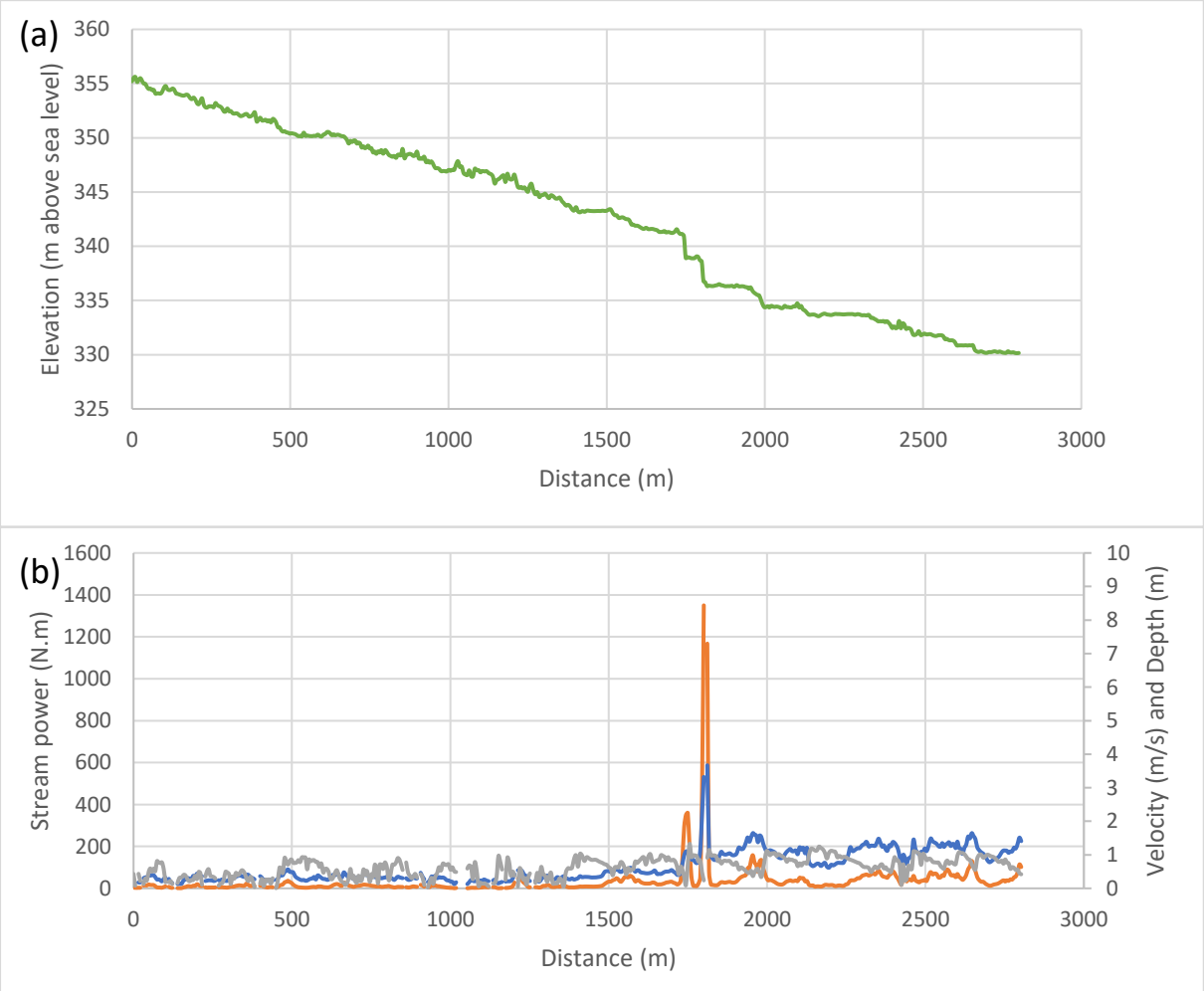

Figure 31: The longitudinal profile of the Kompanjiesdrift wetland (a), and the velocity (blue), stream power (orange), and depth (grey) down the length of the wetland (b).

5.5.1 Outputs from the HEC-RAS model

The mapped HEC-RAS model outputs (Figures 32, 33, and 34) show that velocity, stream power, and depth values are greatest downstream of alluvial fan G, below the erosion control structures, where

flow is confined to an erosional gully. The velocity, stream power, and depth also increase directly upstream of the structures.

In the extant palmiet wetland in the upper portion of Kompanjiesdrift, the velocity, stream power, and depth values are at their lowest in the entire valley. There is an increase in velocity, stream power, and depth along the margins of the wetland, most notably opposite where small alluvial fans impinge the valley.

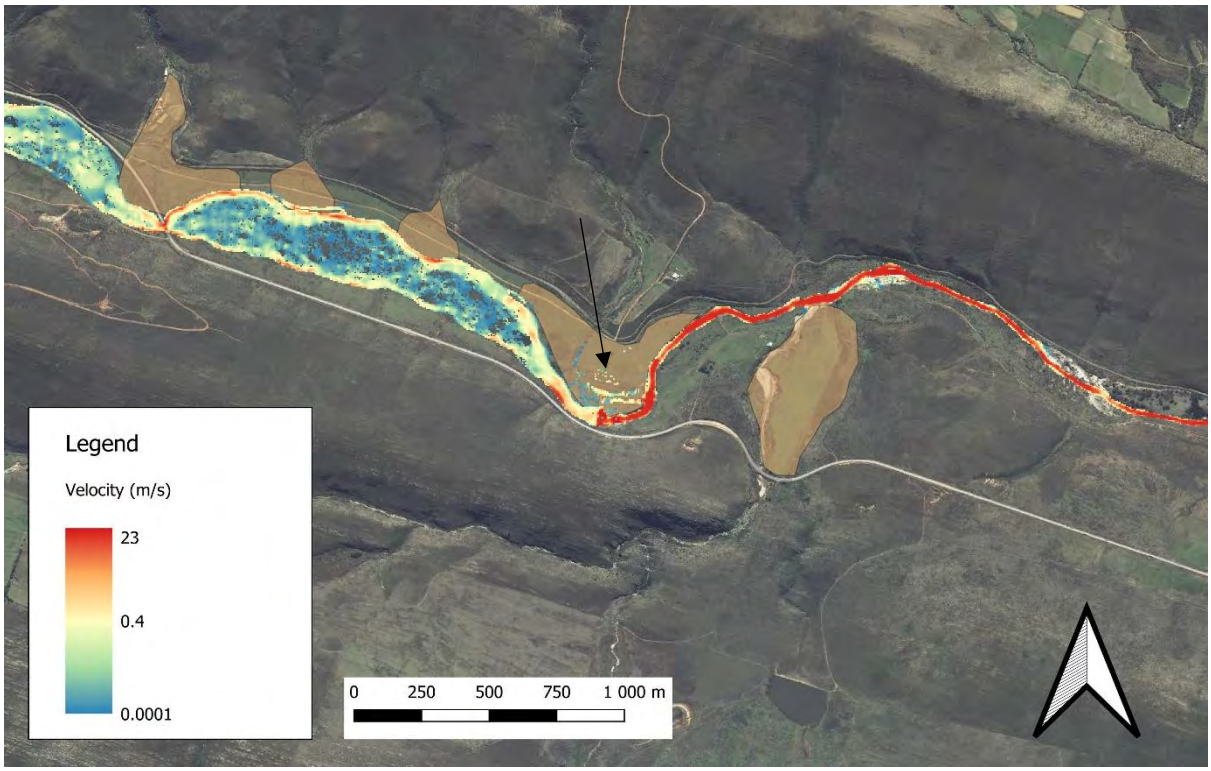

Figure 32: Spatial variation in modelled velocity (m/s) down the length of the Kompanjiesdrift wetland. The location of an erosion control structure is indicated by a black arrow.

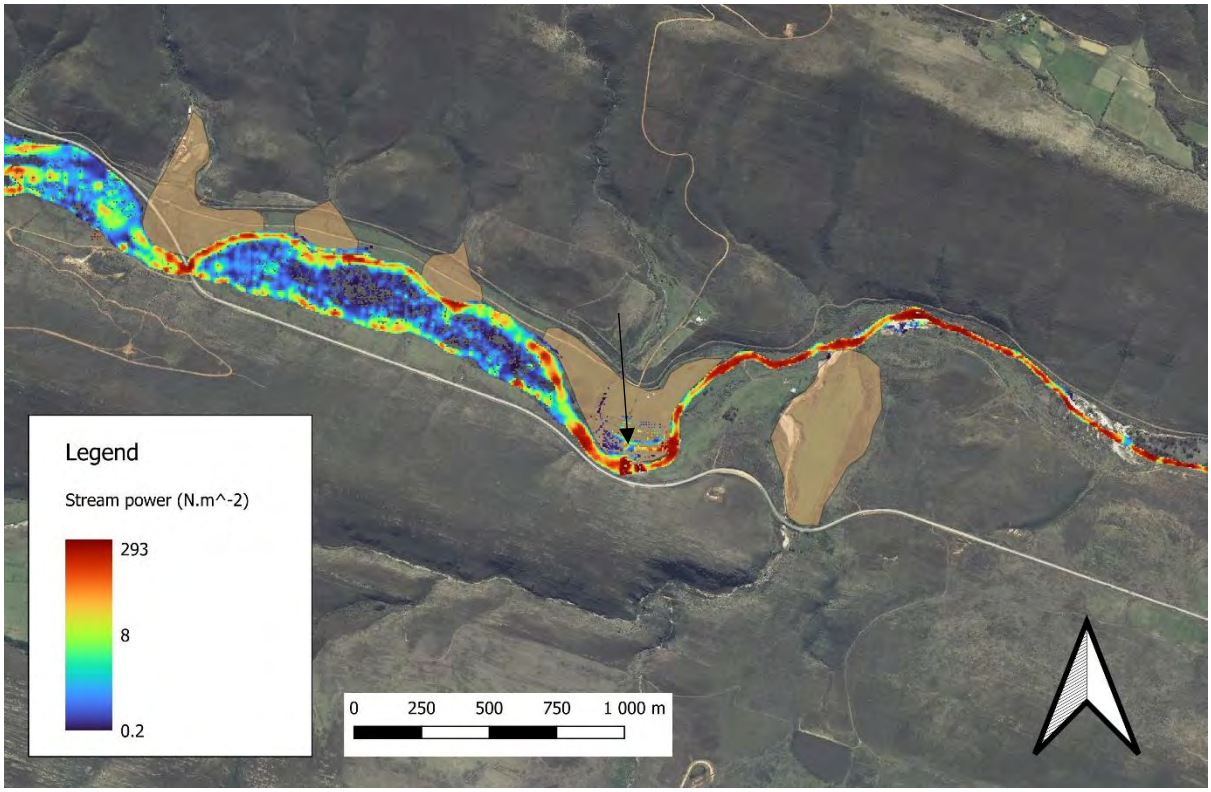

Figure 33: Spatial variation in modelled stream power ($N.m^{-2}$) down the length of the Kompanjiesdrift wetland. The location of an erosion control structure is indicated by a black arrow.

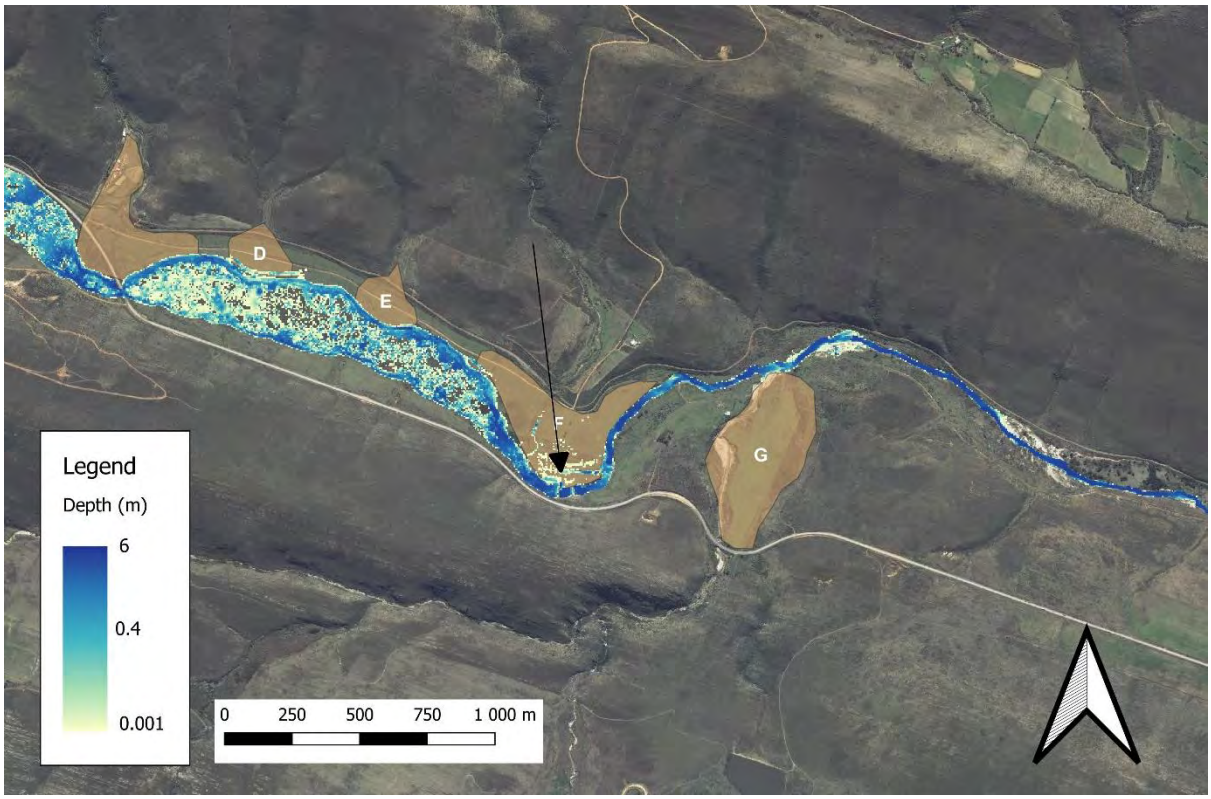

Figure 34: Spatial variation in modelled depth (m) down the length of the Kompanjiesdrift wetland. The location of an erosion control structure is indicated by a black arrow.

5.6 Jagersbos wetland valley morphology

The map of the Jagersbos wetland (Figure 35) shows the extent of the wetland, the tributary streams that join the trunk stream, and the locations and extents of tributary alluvial fans I, J, and K that impinge the valley.

The Jagersbos wetland consists of two reaches – an erosional upper reach and a depositional lower reach. The Kromme River exists as a channeled stream in both reaches. Upstream of alluvial fan K that enters the valley from the south is an erosional gully extending up the whole wetland. Downstream of alluvial fan K, where the valley loses confinement, there is a large depositional feature in the form of a floodout.

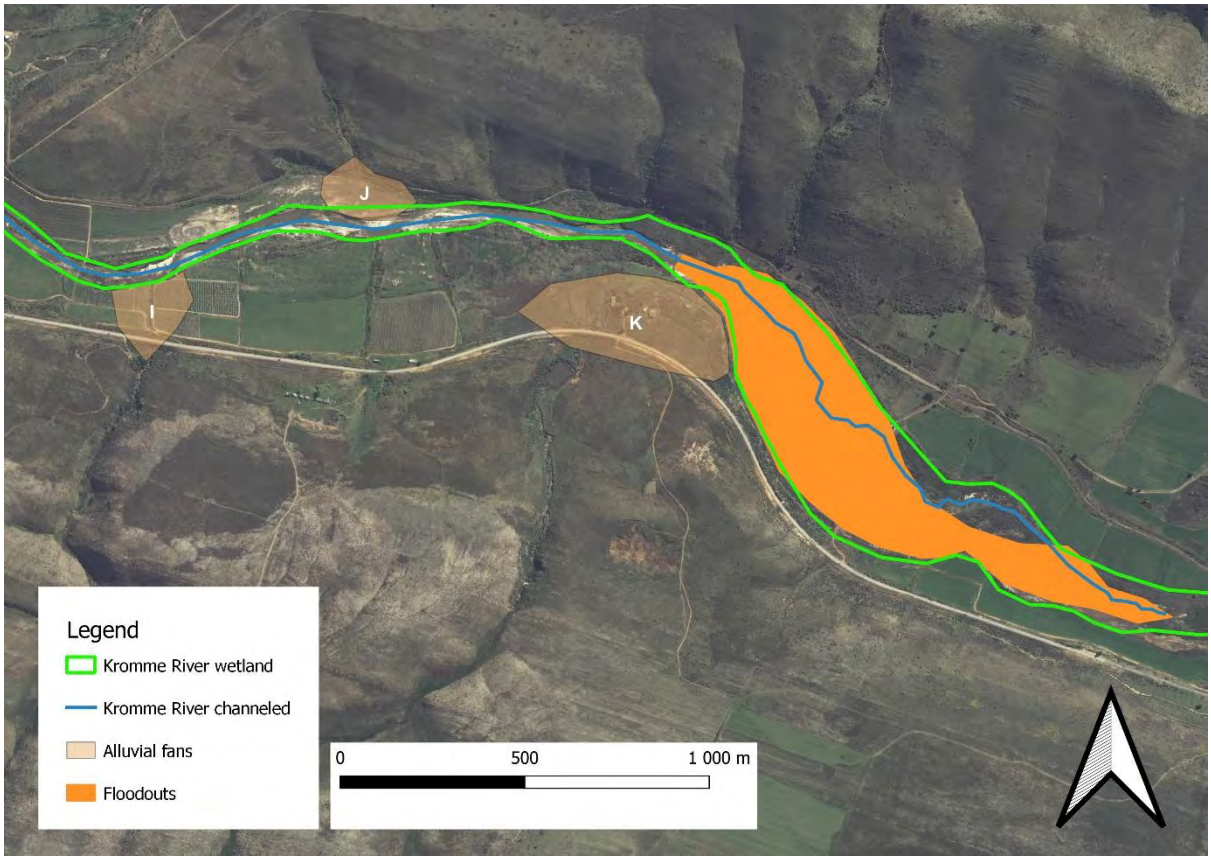

Figure 35: Map of the Jagersbos wetland indicating the locations of alluvial fans, the erosional gully, and the large floodout.

5.6.1 Longitudinal slope of the Jagersbos wetland

Figure 36 shows the longitudinal profile of the Jagersbos wetland. The orange line represents the slope of the eroded stream bed above the depositional floodout. The average slope upstream of the floodout is -0.22% (Table 9). The slope of the floodout downstream from where the valley loses confinement is shown in green. The average slope on the floodout is -0.46%. This is more than double the slope of the eroded reach. In the centre of the valley at the head of the floodout there is a slight mounding caused by deposition.

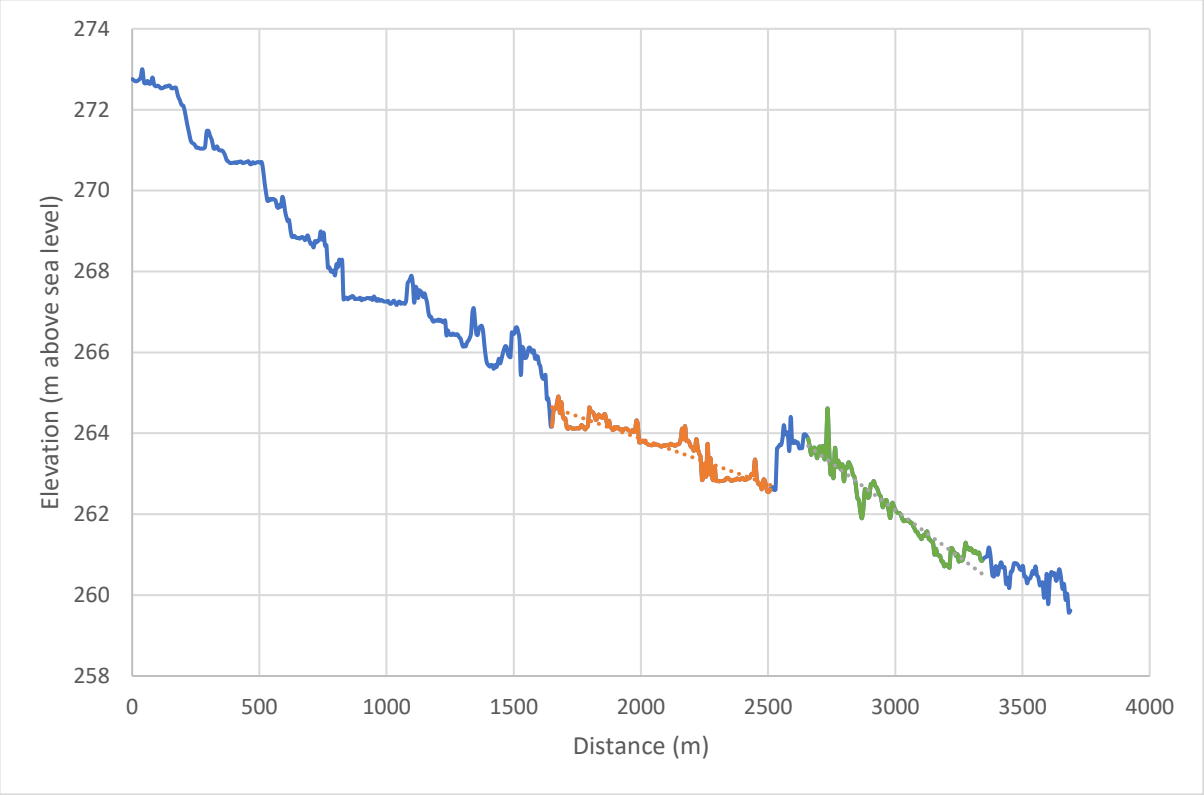

Figure 36: Longitudinal profile of the Jagersbos wetland (blue), indicating the bed upstream of the floodout (orange), and the floodout feature (green)

Table 9: Mean slopes of the erosional and depositional reaches of the Jagersbos wetland.

Reach	**Description**	**Start (m)**	**End (m)**	**Slope (%)**	**R^2**
1	Upstream of floodout in eroded reach	1650	2529	-0.22%	0.853
2	On the depositional floodout downstream of alluvial fan	2657	3340	-0.46%	0.916

5.6.2 Cross-sectional characteristics of the Jagersbos wetland

The locations of cross-sections across the Jagersbos wetland are shown in Figure 37. The cross-sections are ordered from 1 to 10 in a downstream direction.

Cross-section 1 is upstream of alluvial fan I, cross-section 2 is downstream of alluvial fan I, cross-section 3 is across alluvial fan J extending across the valley, and cross-sections 4, 5 and 6 are across alluvial fan K. Cross-sections 7, 8, 9 and 10 are progressively downstream across the depositional floodout.

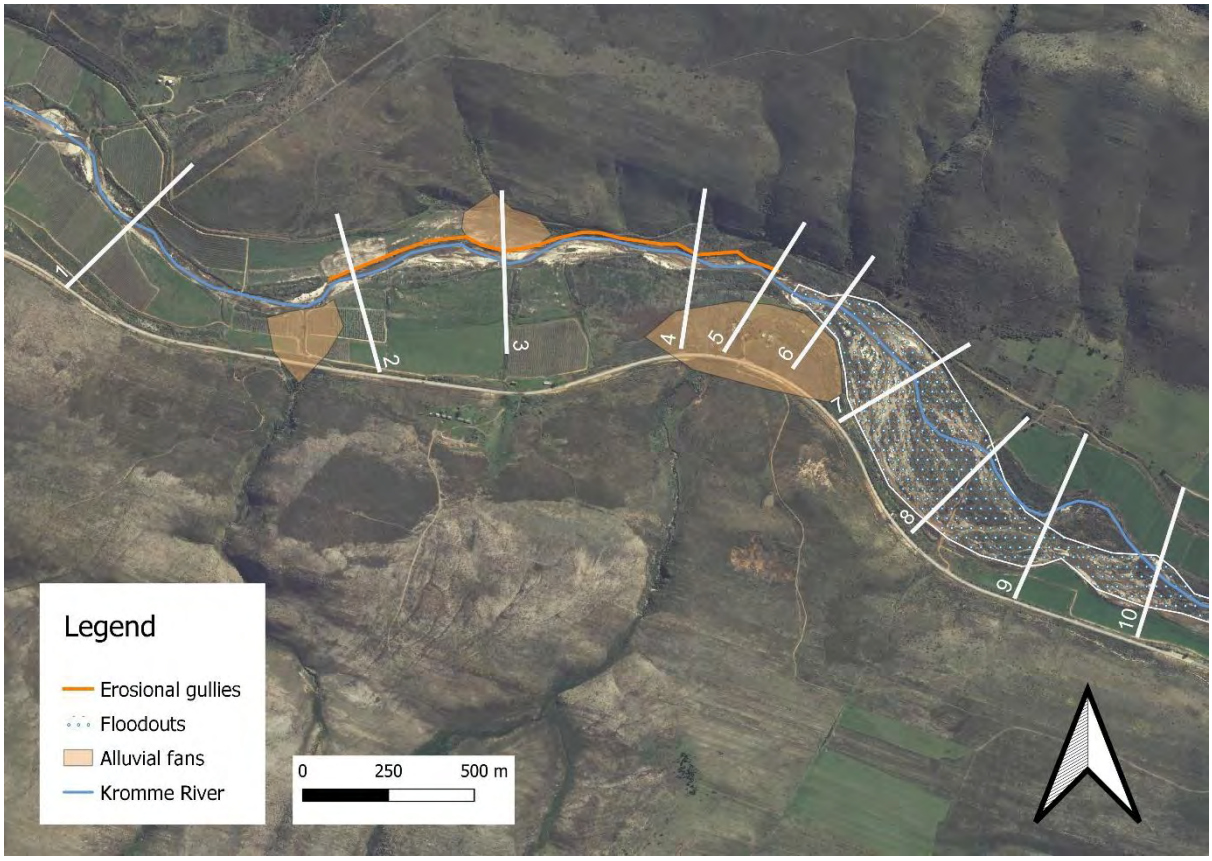

Figure 37: Map of the Jagersbos wetland indicating the locations of cross-sections 1 to 10.

Cross-section 1 shows a broad, relatively flat valley-bottom with a minor gully on the south side of the valley-bottom and a broader and slightly deeper gully between 200 and 300 m along the transect (Figure 38). Cross-section 2 indicates how the gully (between 250 and 300 m along the transect) increases in depth to about 4 m, downstream from where a tributary stream enters the trunk valley from the south. Cross-section 3 shows that the gully has deepened to about 6m and developed steep sides and a near-horizontal bed. as the confined flow incised where alluvial fan F enters the trunk valley from the north

Cross-section 4, opposite the large alluvial fan G, shows that the valley width is drastically reduced and the depth of the gully has decreased to about 3.5m. Cross-section 5, across the middle of alluvial fan G, where a tributary stream enters the trunk valley, further shows the effect of the alluvial fan on valley width. It also shows that the erosional gully has reduced in width and depth to about 3m. Cross-section 6 shows the valley floor confined by alluvial fan G and the toe of the gully that has reduced further in width and depth, such that it is about 1m deep. The gully no longer has steep vertical sides.

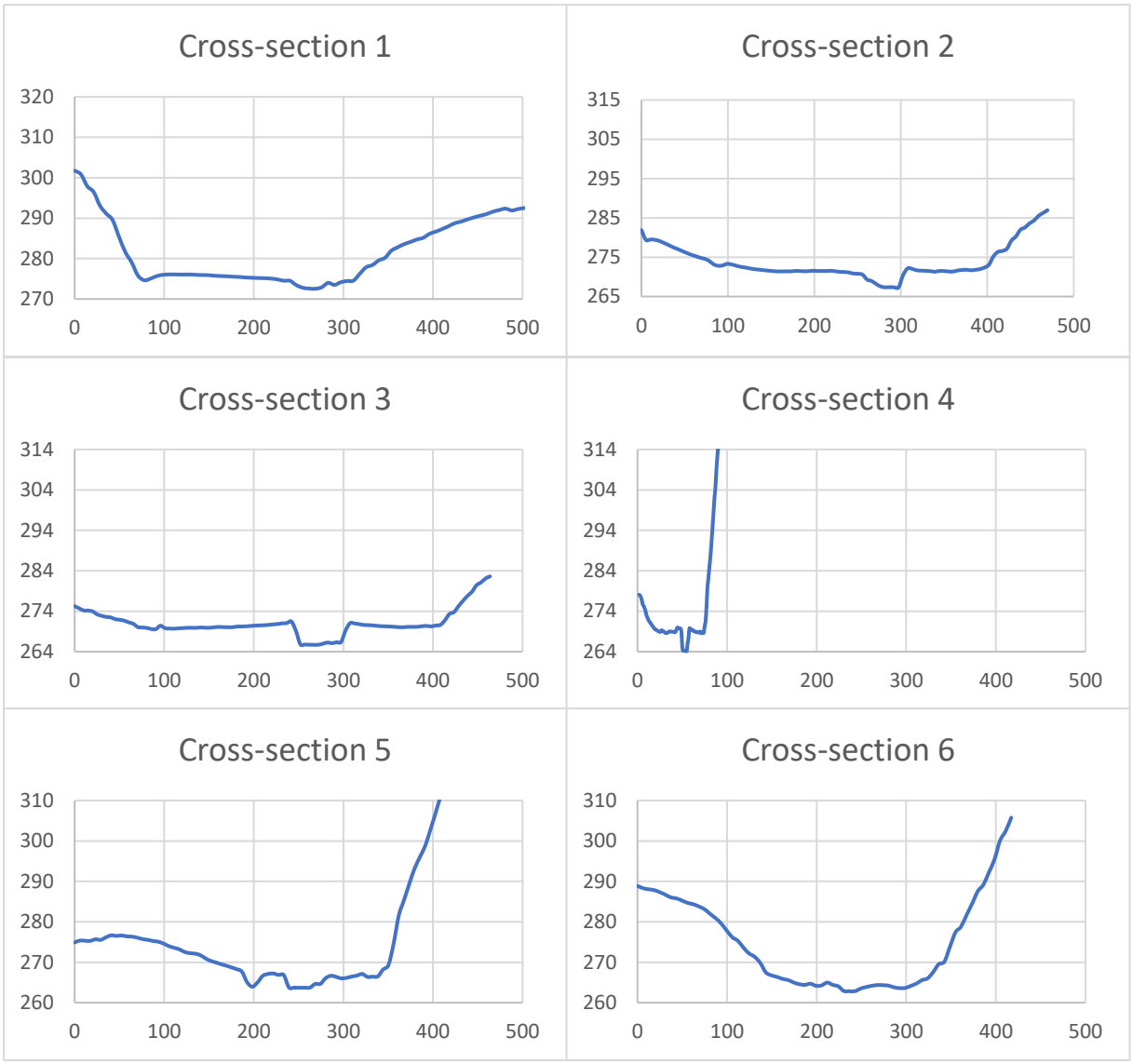

Figure 38: Cross-sections 1 to 6 in the erosional reach of the Jagersbos wetland.

Cross-section 7 (Figure 39) shows that the valley widens as it loses confinement downstream from alluvial fan G. The depositional floodout is visible across the valley floor. The margins of the valley are slightly lower than the centre of the valley floor. A small gully that has re-incised into the floodout is visible about 260 m along the transect.

Cross-sections 8 and 9 across the floodout feature show the broad valley bottom and how the floodout feature widens along its length. There is a slight mounding in the centre relative to the valley margins about 100 to 330 m along the transect. This demonstrates the effect of the depositional feature that seemingly has a broad conical shape. Cross-section 10, near the toe of the floodout, shows a reduction in the mounding effect in the centre of the valley.

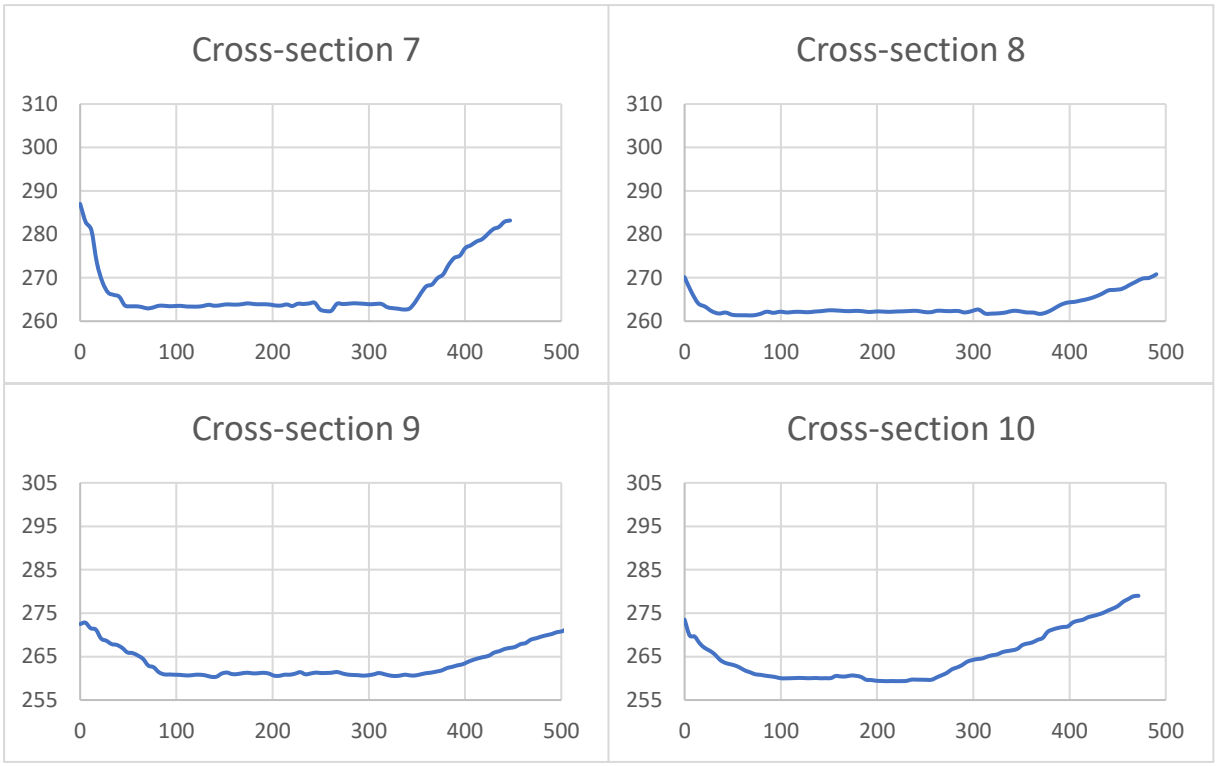

Figure 39: Cross-section 7 to 10 in the depositional reach of the Jagersbos wetland

5.7 Jagersbos wetland hydrogeomorphic characteristics

Figure 40 shows the longitudinal slope of the Jagersbos wetland and the associated stream power, velocity, and depth values down the length of this reach. Despite the increase in the slope of the floodout compared to the gully bed upstream of the floodout, there is a reduction in velocity, stream power, and depth on the floodout.

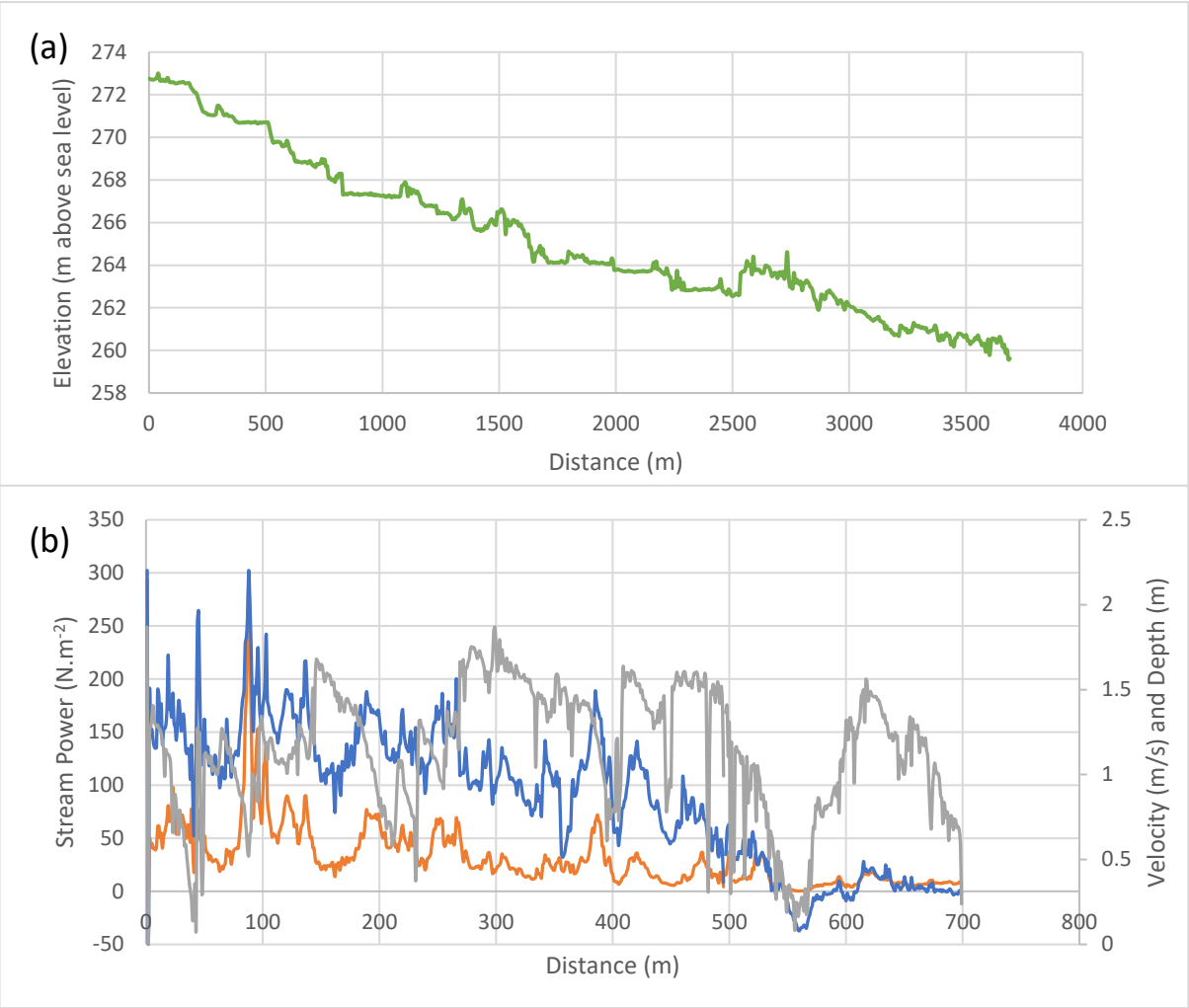

Figure 40: The longitudinal profile of the Jagersbos wetland (a), and the velocity (blue), stream power (orange), and depth (grey) down the length of the wetland (b).

The mean flow velocity for the entire Jagersbos wetland is 0.890 m/s. The mean stream power is 32.731 N.m.s^{-2}, and the mean depth of flow is 1.146 m. Velocity, depth, and stream power values are all higher in the eroded reach of the wetland upstream of the floodout feature than in the depositional reach. The mean velocity on the floodout (depositional reach) is 0.43 m/s (standard deviation = 0.19 m/s), whereas upstream of the floodout on the bed of the eroded gully it is 1.13 m/s (standard deviation = 0.24 m/s). The mean stream power on the floodout is 10.79 N.m.s^{-2} (standard deviation = 7.51 N.m.s ^{2}), whereas in the eroded reach upstream of the floodout it is 44.08 N.m.s^{-2} (standard deviation = 30.96 N.m.s^{-2}). The mean depth on the floodout is 1.03 m (standard deviation = 0.40), and in the eroded reach, it is 1.22 m (standard deviation = 0.33 m).

5.7.1 Outputs from the HEC-RAS model

The HEC-RAS model outputs (Figures 41, 42, and 43) clearly indicate the contrast in velocity, stream power, and depth values in the eroded reach and the depositional reach. Velocity, stream power, and depth are lowest on the floodout feature and greatest in the gully upstream from where the valley loses confinement.

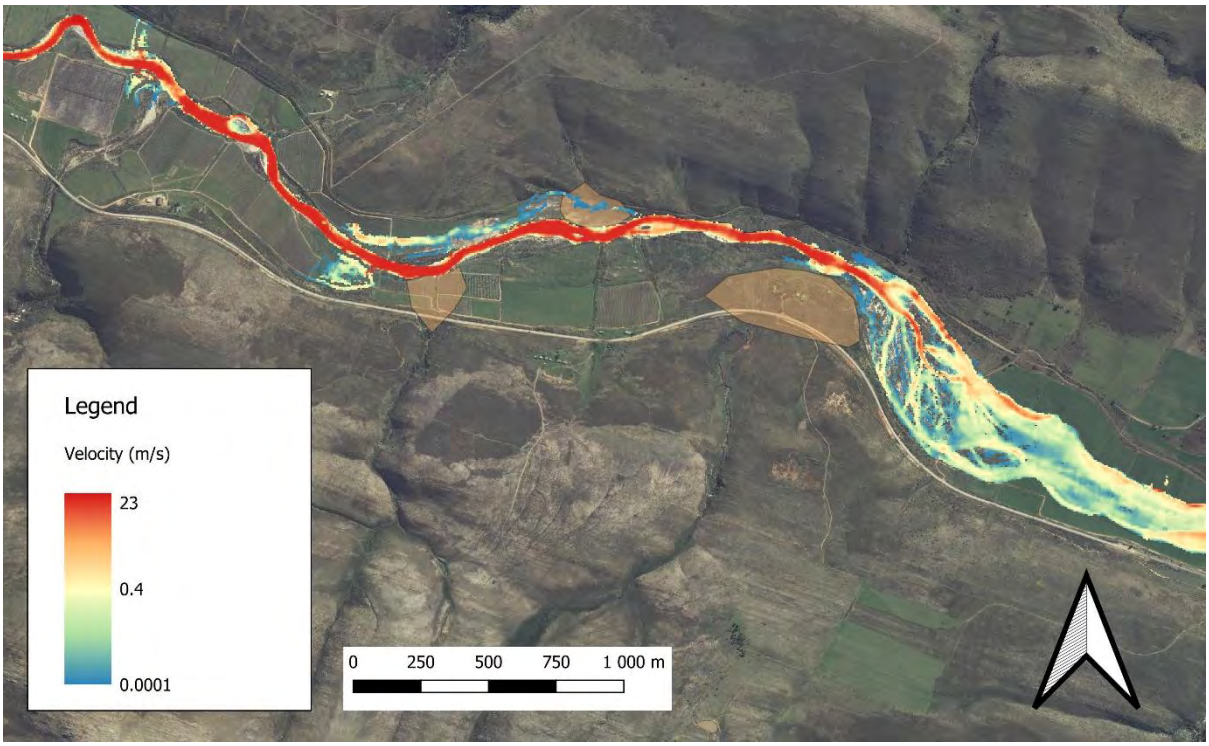

Figure 41: Spatial variation in modelled velocity (m/s) down the length of the Jagersbos wetland.

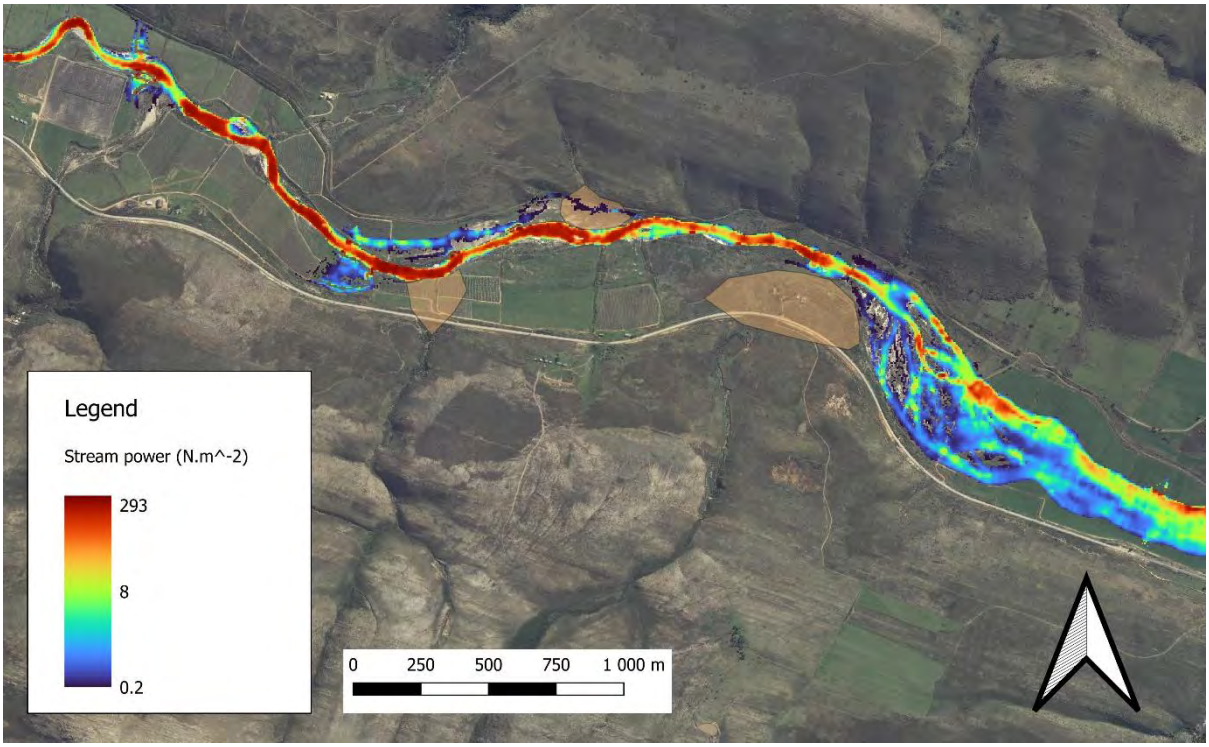

Figure 42: Spatial variation in modelled stream power ($N.m^{-2}$) down the length of the Jagersbos wetland.

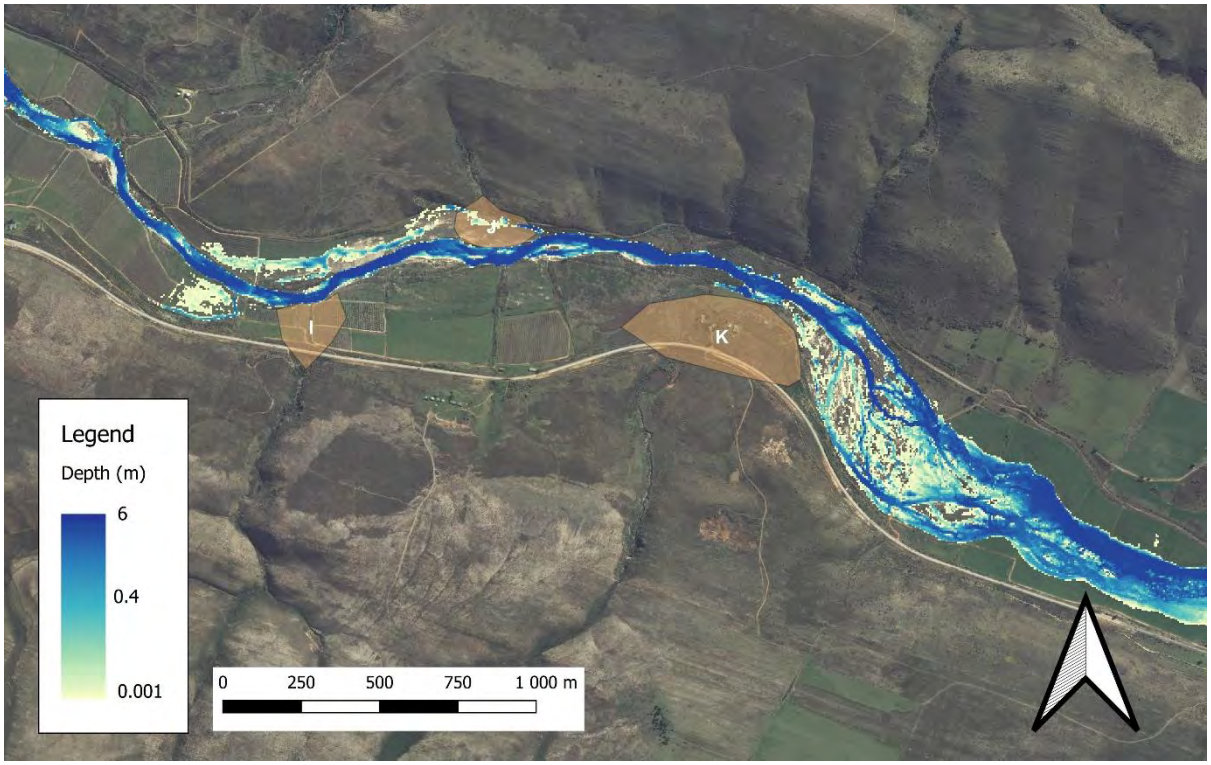

Figure 43: Spatial variation in modelled depth (m) down the length of the Jagersbos wetland.

5.8 Trends in hydrogeomorphic characteristics

5.8.1 Variation in hydraulic characteristics down the length of the Kromme River valley

Down the length of the Kromme River valley, there is a systematic decrease in the slope of the valley bottom, but hydraulic characteristics do not decrease down the length of the valley in the same way. Without placing an inordinate amount of emphasis on the mean values for the hydraulic data because of the high variability of the values for each wetland, it is useful to compare the values for each wetland to get an overall sense of downstream variation in hydraulic characteristics. The slope in the Jagersbos wetland is about 3 times lower than in the upper reaches, but we do not see this magnitude of decrease in velocity, stream power, or water depth down the length of the Kromme River valley (Table 10).

Table 10: Mean velocity, stream power, depth, and slope in the three wetlands.

	Krugersland	**Kompanjiesdrift**	**Jagersbos**
Mean velocity ($m.s^{-1}$)	1.046	0.748	0.890
Mean stream power ($N.m.s^{-2}$)	60.747	48.108	32.731
Mean depth (m)	1.354	0.671	1.146
Mean slope (%)	-1.09	-0.92	-0.33

To get better insights, it is useful to compare values for different geomorphic settings within wetlands and similar geomorphic settings between different wetlands.

5.8.1.1 Confined reaches vs unconfined reaches

The Krugersland, Kompanjiesdrift, and Jagersbos wetlands all have confined reaches and unconfined reaches as a result of tributary alluvial fans impinging on the valley floor from the adjacent sub-catchments.

The reduction in valley width affects velocity, stream power, and depth (Figures 44, 45 and 46). In all three wetlands, the flow velocity, stream power, and depth are greater in reaches that are confined by alluvial fans than in unconfined reaches (Tables 11, 12, and 13). Of the three variables considered, depth adjusts least (mean O / D = 0.895), followed by flow velocity (mean O / D = 0.787), while the difference in stream power shows the greatest response (mean O / D = 0.482) to variation in valley width.

It is also evident that there is no systematic variation within similar geomorphic settings in respect of flow velocity, stream power, or depth downstream in the wetland. Furthermore, within each of the sections of each wetland in which the valley bottom is not confined by an alluvial fan, the flow velocity, and stream power values are higher at the edges of the wetland than in the centre. It seems

that this is due to lower friction by palmiet along the wetland margins because there is no evidence of longitudinal depressions along the edges of the wetland.

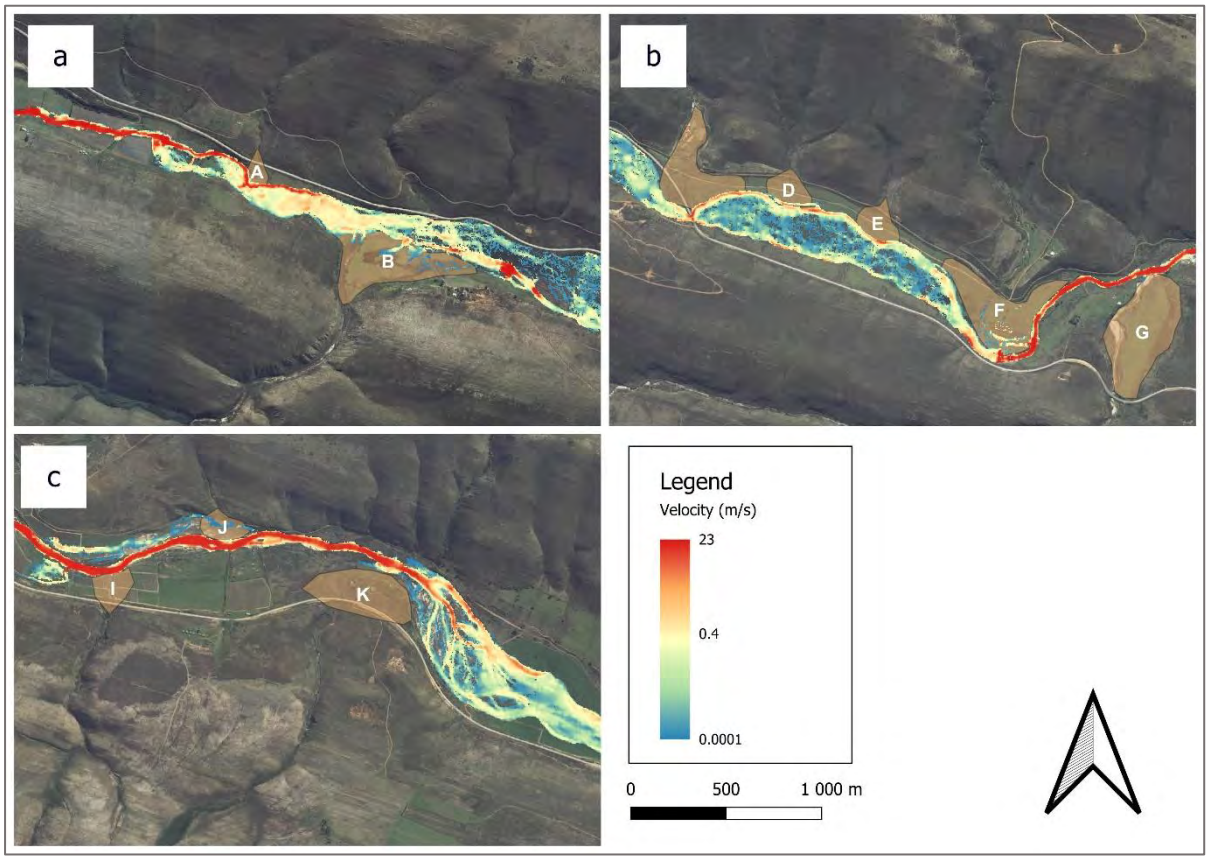

Figure 44: Spatial variation in modelled velocity in confined and unconfined reaches of the valley in the Krugersland (a), Kompanjiesdrift (b), and Jagersbos wetlands (c).

Table 11: Mean velocity in confined reaches opposite alluvial fans (O) and in unconfined reaches downstream from alluvial fans (D) in the three wetlands.

Reach	**Mean**	**O / D**	**Mean O / D**
Krugersland – opposite alluvial fan A	0.531		
Krugersland – downstream alluvial fan A	0.432	0.814	
Kompanjiesdrift – opposite alluvial fan D	0.256		
Kompanjiesdrift – downstream alluvial fan D	0.223	0.871	
Kompanjiesdrift – opposite alluvial fan E	0.316		
Kompanjiesdrift – downstream alluvial fan E	0.203	0.642	
Jagersbos – opposite alluvial fan J	0.841		
Jagersbos – downstream alluvial fan J	0.689	0.819	0.787

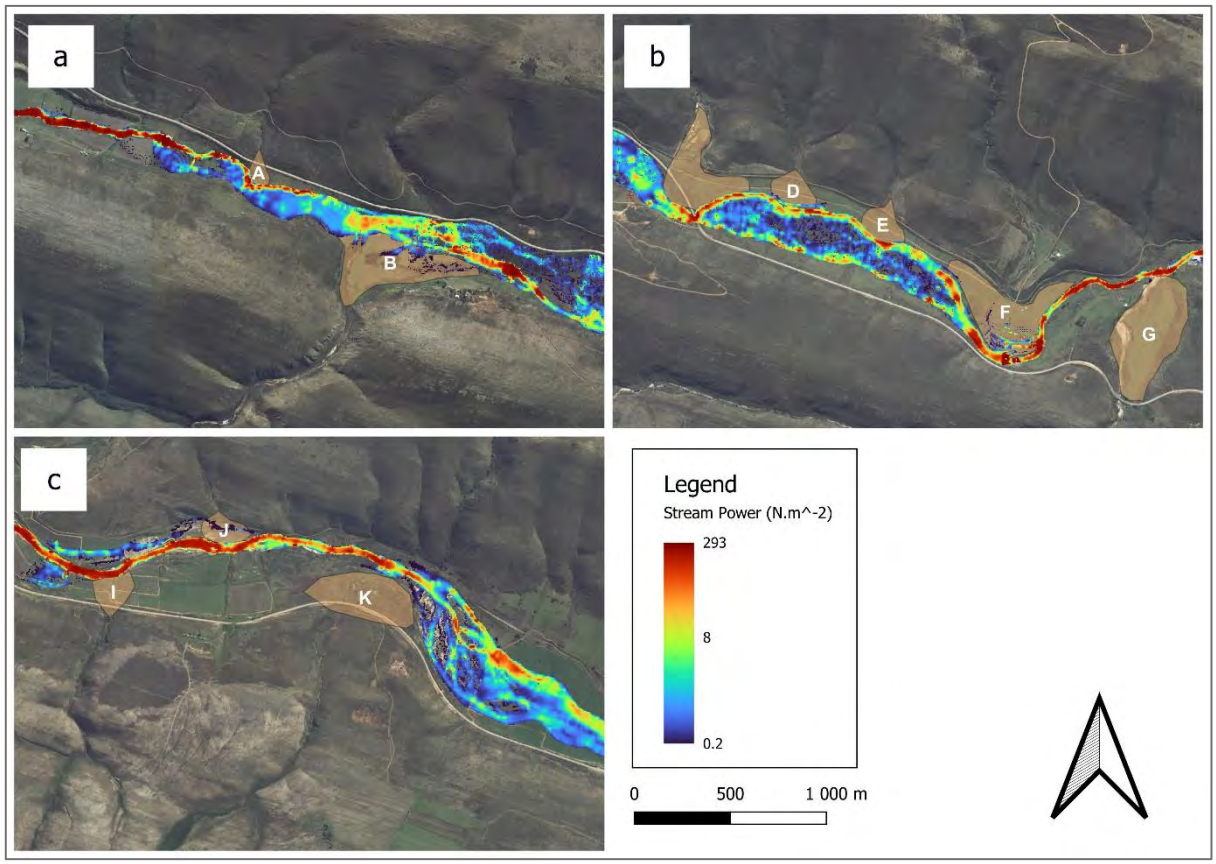

Figure 45: Spatial variation in modelled stream power in confined and unconfined reaches of the valley in the Krugersland (a), Kompanjiesdrift (b), and Jagersbos wetlands (c).

Table 12: Mean stream power in confined reaches opposite alluvial fans (O) and in unconfined reaches downstream from alluvial fans (D).

Reach	**Mean**	**O / D**	**Mean O / D**
Krugersland – opposite alluvial fan A	16.234		
Krugersland – downstream alluvial fan A	5.566	0.343	
Kompanjiesdrift – opposite alluvial fan D	6.751		
Kompanjiesdrift – downstream alluvial fan D	4.534	0.672	
Kompanjiesdrift – opposite alluvial fan E	9.670		
Kompanjiesdrift – downstream alluvial fan E	3.900	0.403	
Jagersbos – opposite alluvial fan J	37.065		
Jagersbos – downstream alluvial fan J	18.915	0.510	0.482

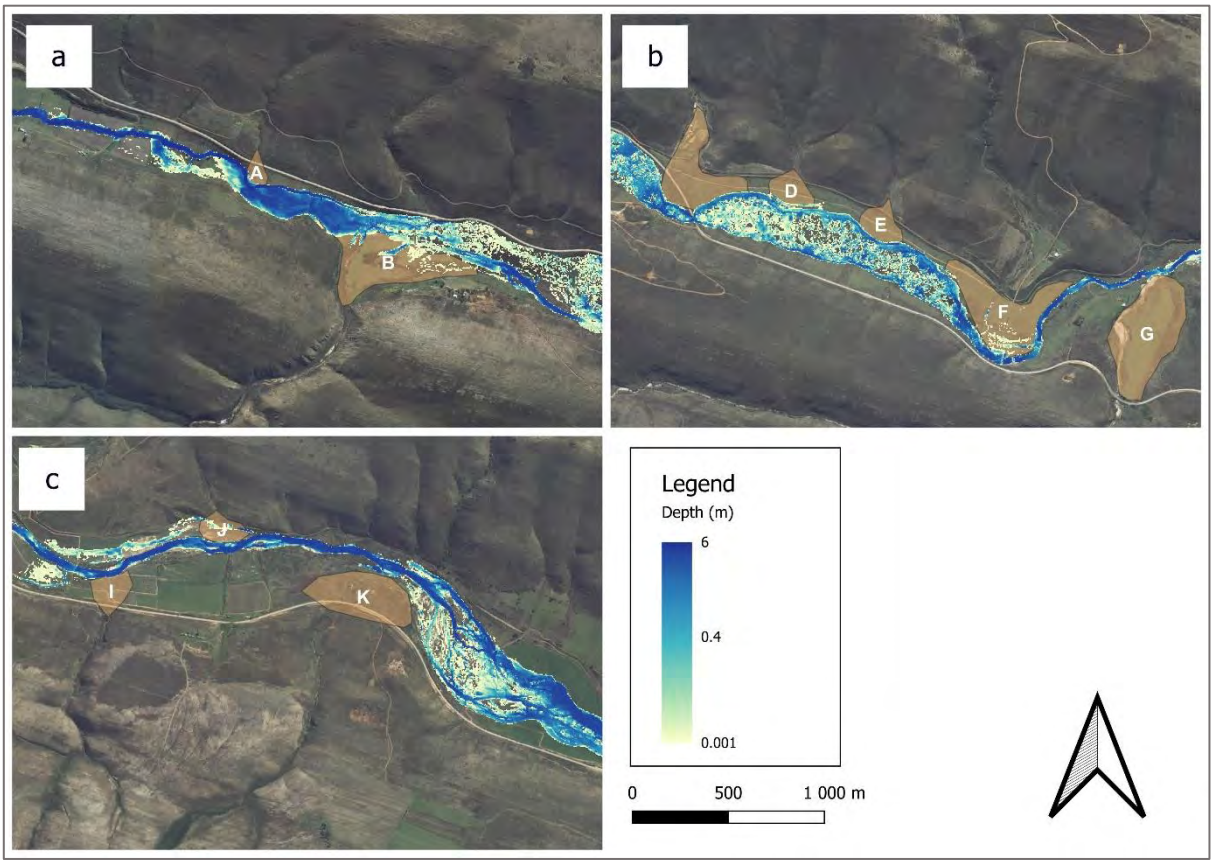

Figure 46: Spatial variation in modelled depth in confined and unconfined reaches of the valley in the Krugersland (a), Kompanjiesdrift (b), and Jagersbos wetlands (c).

Table 13: Mean depth in confined reaches opposite alluvial fans (O) and in unconfined reaches downstream from alluvial fans (D) in the three wetlands.

Reach	**Mean**	**O / D**	**Mean O / D**
Krugersland – opposite alluvial fan A	1.267		
Krugersland – downstream alluvial fan A	0.810	0.639	
Kompanjiesdrift – opposite alluvial fan D	0.310		
Kompanjiesdrift – downstream alluvial fan D	0.312	1.006	
Kompanjiesdrift – opposite alluvial fan E	0.394		
Kompanjiesdrift – downstream alluvial fan E	0.386	0.980	
Jagersbos – opposite alluvial fan J	0.853		
Jagersbos – downstream alluvial fan J	0.813	0.953	0.895

5.8.1.2 Erosional reaches vs non-erosional reaches

In the Krugersland and Kompanjiesdrift wetlands, there are erosional and non-erosional reaches that are associated with erosion control structures. Downstream of erosion control structures, velocity, stream power, and depth values are higher than upstream of the structures where flow is spread across the valley floor (Figures 47, 48, and 49). Of the three variables considered, depth adjusts least (mean E / N = 0.630) to being confined to an erosion gully and in an unconfined non-erosional reach, followed by flow velocity (mean E / N = 0.220), while the difference in stream power shows the greatest response (mean E / N = 0.124) to variation in valley width.

The confinement and concentration of flow within gullies increase velocity, stream power, and depth values compared to reaches that are broad in cross-section and have not eroded (Tables 14, 15 and 16).

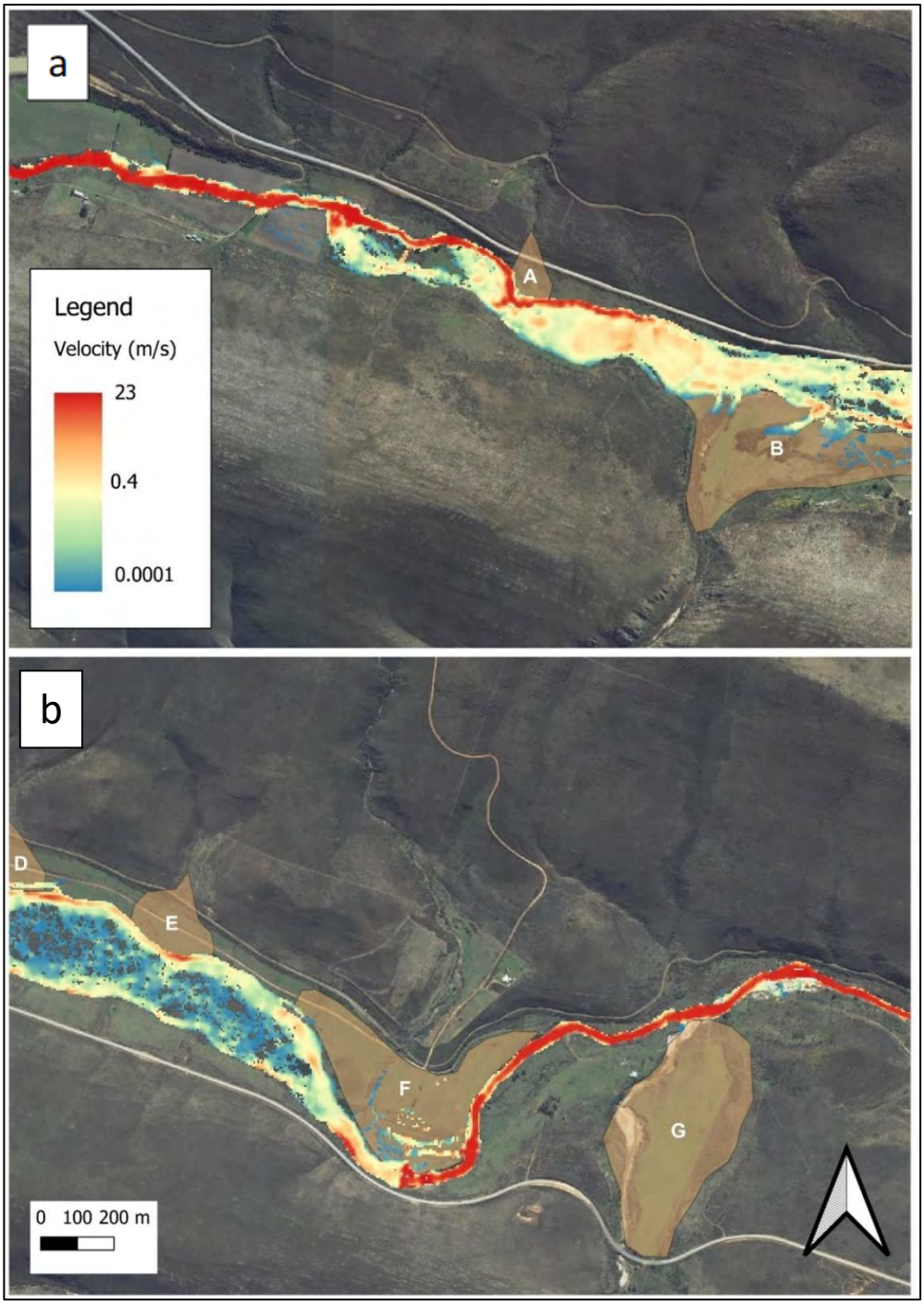

Figure 47: Spatial variation in modelled velocity in erosional and non-erosional reaches of the Krugersland (a) and Kompanjiesdrift (b) wetlands.

Table 14: Mean velocity in erosional reaches associated with erosion control structures (E) and in non-erosional reaches upstream of erosion control structures (N).

Reach	**Mean**	**E / N**	**Mean E / N**
Krugersland – gully downstream of erosion control structures 1, 2 and 3	1.177		
Krugersland – upstream of erosion control structure 4	0.332	0.282	
Kompanjiesdrift – gully downstream of erosion control structures	1.741		
Kompanjiesdrift – upstream of erosion control structures	0.274	0.157	0.220

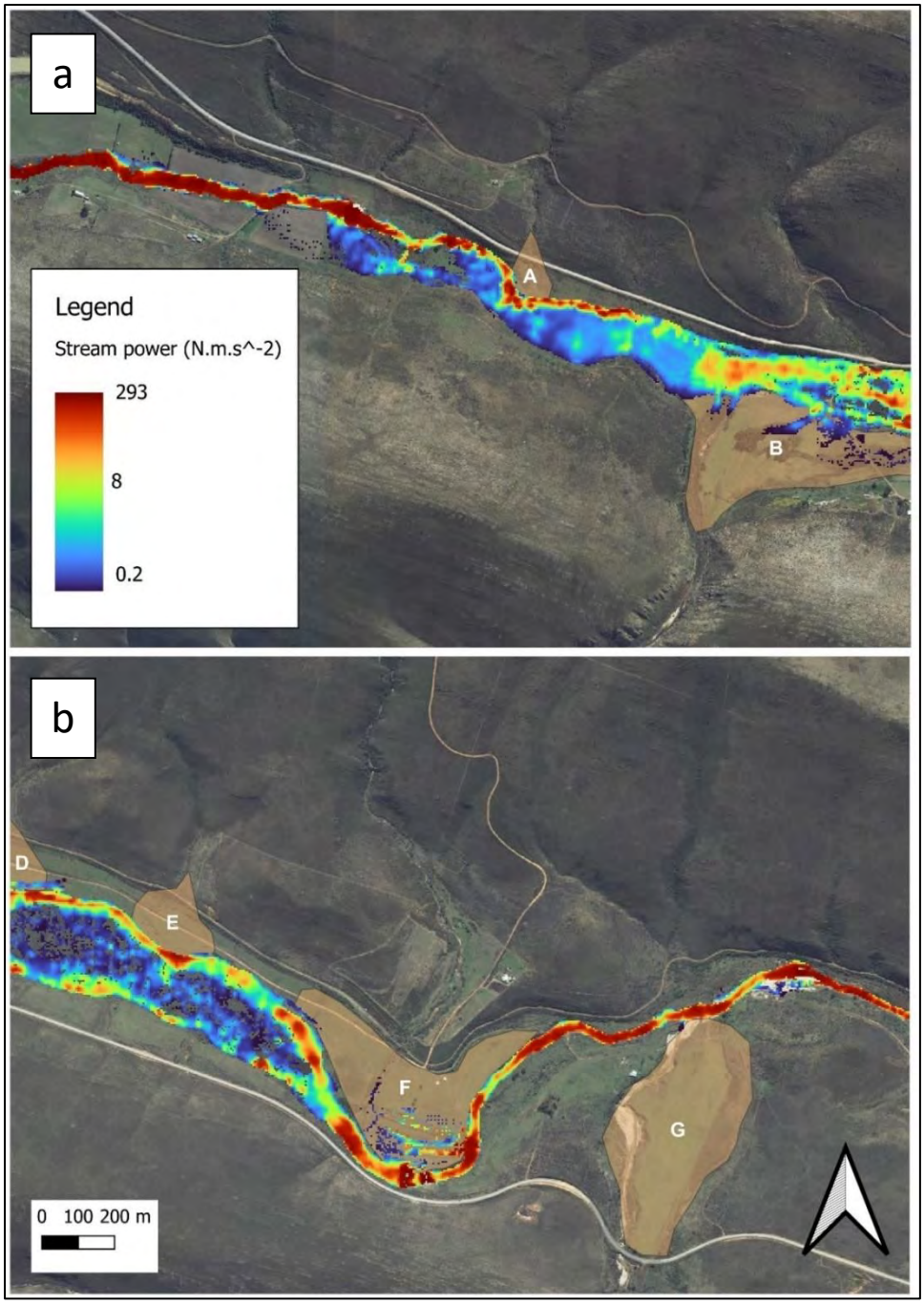

Figure 48: Spatial variation in modelled stream power in erosional and non-erosional reaches of the Krugersland (a) and Kompanjiesdrift (b) wetlands.

Table 15: Mean stream power in erosional reaches associated with erosion control structures (E) and in non-erosional reaches upstream of erosion control structures (N).

Reach	**Mean**	**E / N**	**Mean E / N**
Krugersland – gully downstream of erosion control structures 1, 2 and 3	121.391		
Krugersland –upstream of erosion control structure 4	4.460	0.037	
Kompanjiesdrift – gully downstream of erosion control structures	37.581		
Kompanjiesdrift –upstream of erosion control structures	7.957	0.211	0.124

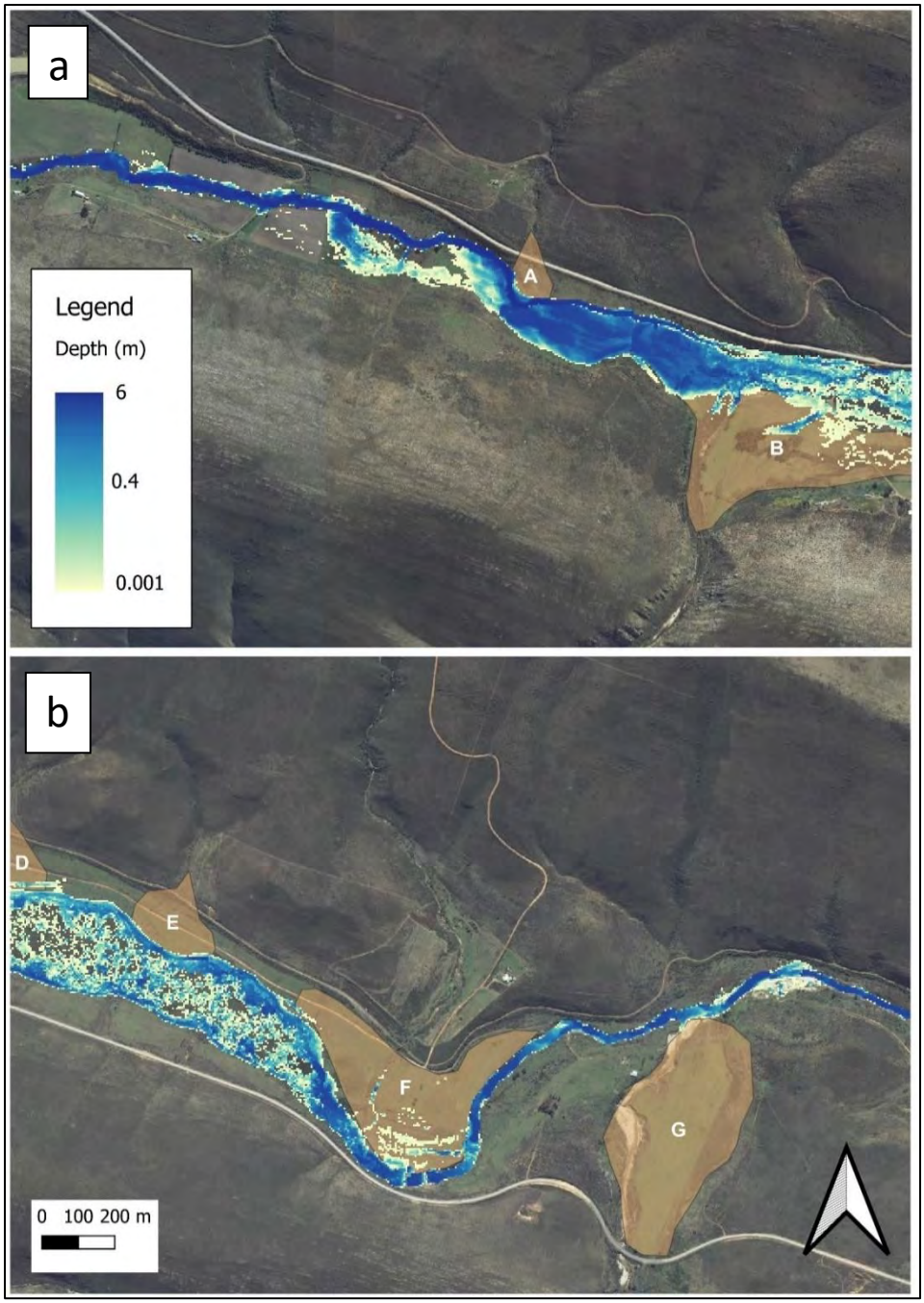

Figure 49: Spatial variation in modelled depth in erosional and non-erosional reaches of the Krugersland (a) and Kompanjiesdrift (b) wetlands.

Table 16: Mean depth in erosional reaches associated with erosion control structures (E) and in non-erosional reaches upstream of erosion control structures (N).

Reach	**Mean**	**E / N**	**Mean E / N**
Krugersland – gully downstream of erosion control structures 1, 2 and 3	0.969		
Krugersland –upstream of erosion control structure 4	0.417	0.430	
Kompanjiesdrift – gully downstream of erosion control structures	0.637		
Kompanjiesdrift –upstream of erosion control structures	0.529	0.830	0.630

5.8.1.3 Upstream vs on floodout features

In the Krugersland wetland, upstream of alluvial fan C and downstream of the erosion control structure opposite alluvial fan B, there is a short erosional gully with a depositional floodout directly downstream of it (Figures 50a, 51a, and 52a). In the Jagersbos wetland, there is a long erosional gully and downstream of it is a large depositional floodout feature (Figures 50b, 51b, and 52b). Velocity, stream power, and depth values on the bed upstream of these floodouts are greater than on the floodouts themselves (Tables 17, 18 and 19). Of the three variables considered, flow velocity adjusts least (mean O / U = 0.703) to being on or upstream of a floodout, followed by water depth (mean O / U = 0.476), while the difference in stream power shows the greatest response (mean O / U = 0.344) to variation in valley width.

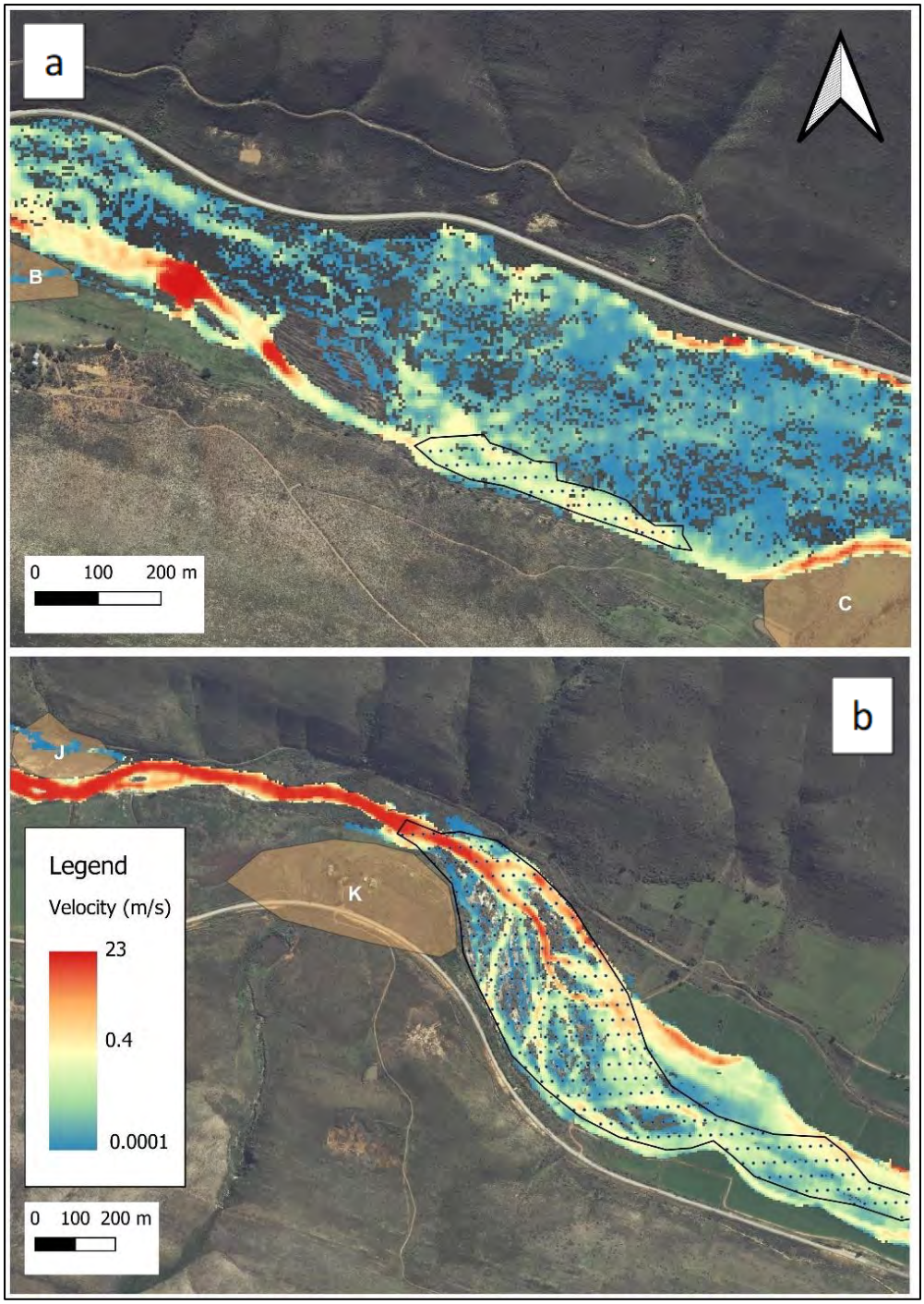

Figure 50: Spatial variation in modelled velocity upstream from and on floodout features in the Krugersland (a) and Jagersbos (b) wetlands.

Table 17: Mean velocity upstream of depositional floodouts (U) and on the floodouts (O).

Reach	**Mean**	**O / U**	**Mean O / U**
Krugersland – upstream of floodout, on gully bed	0.273		
Krugersland – on floodout feature	0.268	0.982	
Jagersbos – upstream of floodout, on gully bed	0.745		
Jagersbos – on floodout feature	0.316	0.424	0.703

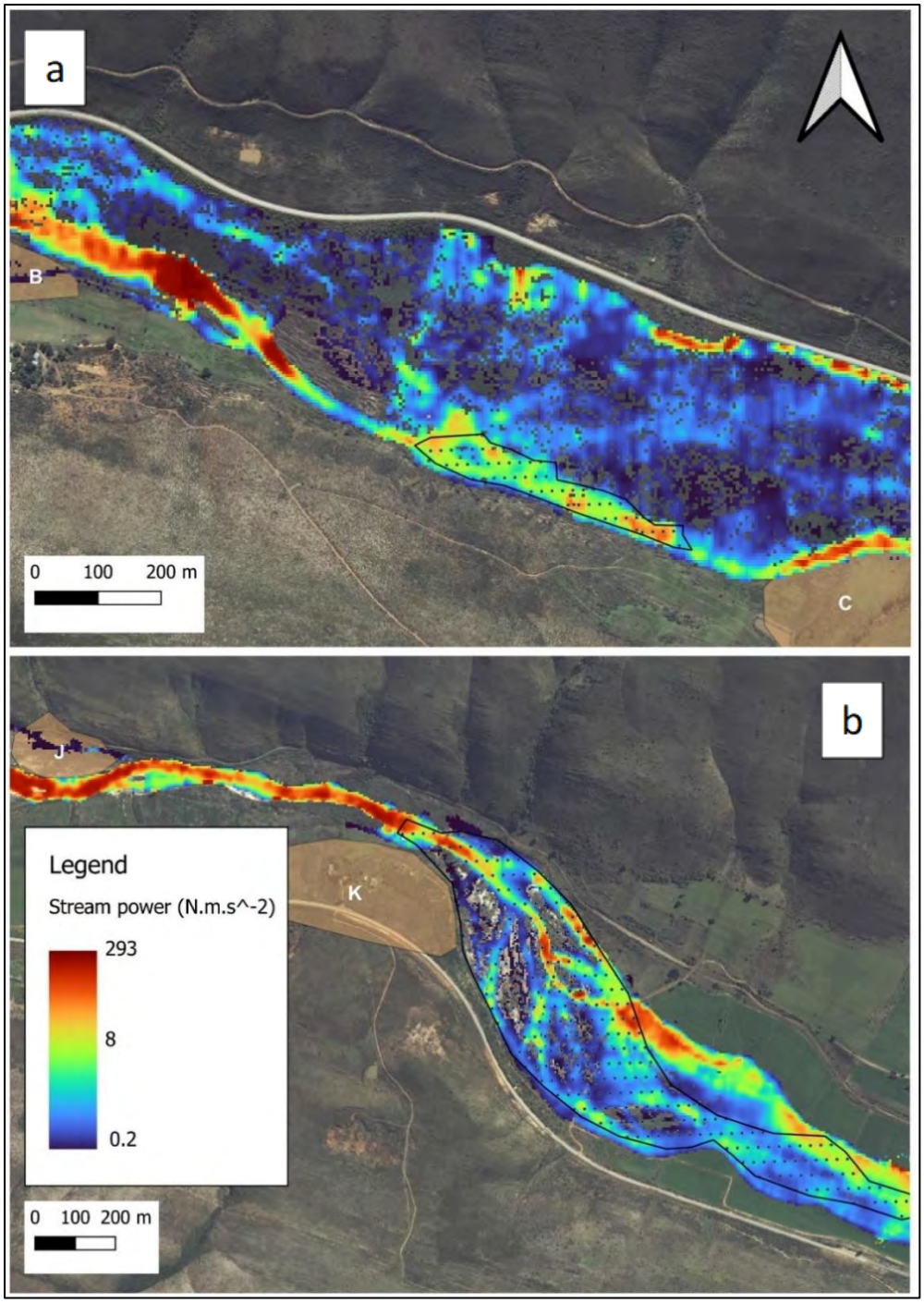

Figure 51: Spatial variation in modelled stream power upstream from and on floodout features in the Krugersland (a) and Jagersbos (b) wetlands.

Table 18: Mean stream power upstream of depositional floodouts (U) and on the floodouts (O).

Reach	**Mean**	**O / U**	**Mean O/ U**
Krugersland – upstream of floodout, on gully bed	9.996		
Krugersland – on floodout feature	5.215	0.524	
Jagersbos – upstream of floodout, on gully bed	27.113		
Jagersbos – on floodout feature	4.504	0.166	0.345

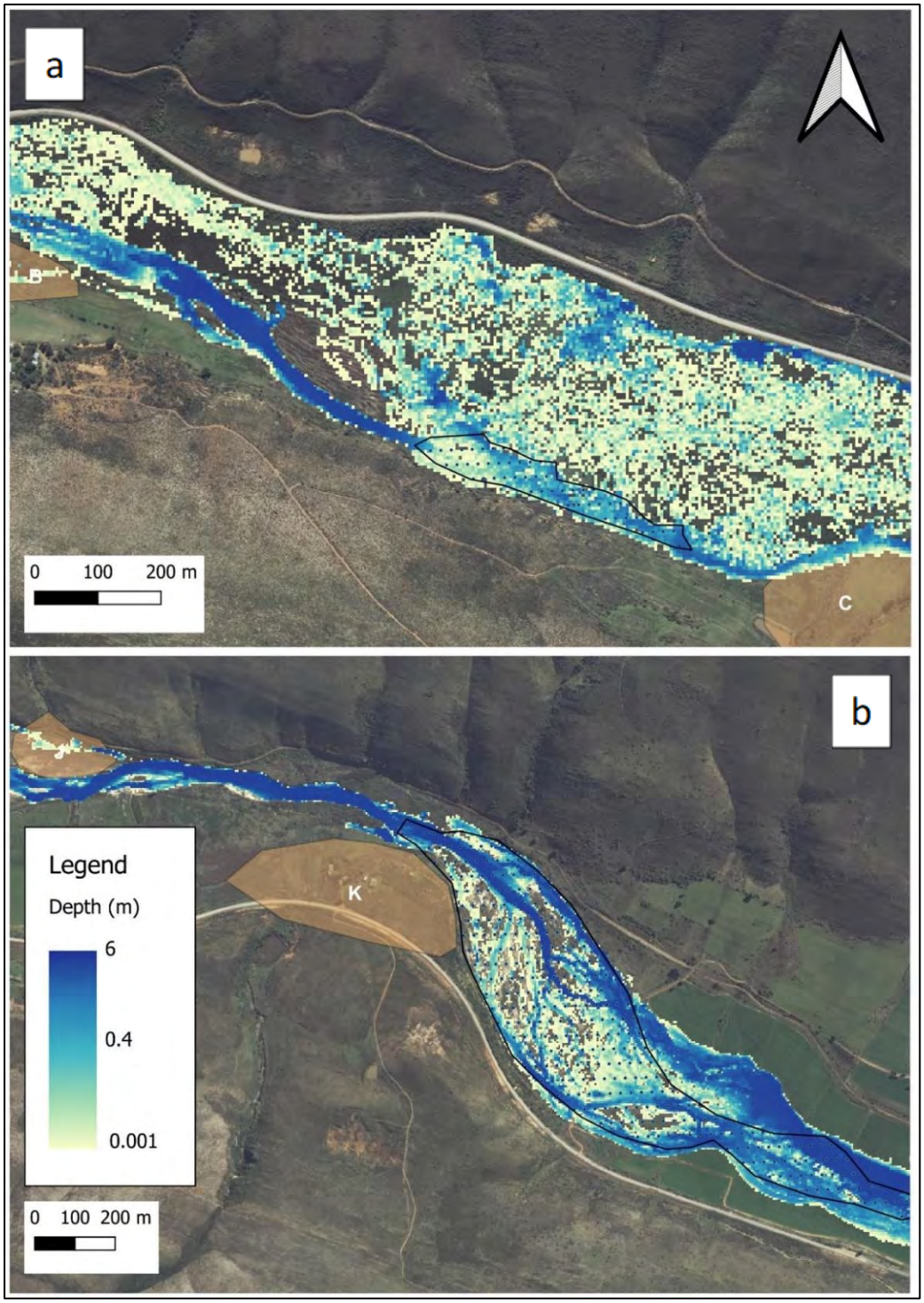

Figure 52: Spatial variation in modelled depth upstream from and on floodout features in the Krugersland (a) and Jagersbos (b) wetlands.

Table 19: Mean depth upstream of depositional floodouts (U) and on the floodouts (O).

Reach	**Mean**	**O / U**	**Mean O / U**
Krugersland – upstream of floodout, on gully bed	0.673		
Krugersland – on floodout feature	0.340	0.505	
Jagersbos – upstream of floodout, on gully bed	1.054		
Jagersbos – on floodout feature	0.470	0.446	0.476

5.9 Sites best-suited to trial new wetland rehabilitation strategies

The high-resolution hydraulic modelling done in this study has indicated the spatial distribution of zones that are suitable for trialling new methods of rehabilitation. By identifying areas in gullies and on floodouts where velocity and stream power are very low, and deposition is likely to occur, rehabilitation practitioners can determine where to plant palmiet seeds or plant fragments so that they have the best possible chance of surviving and proliferating.

A map indicating proposed sites for novel rehabilitation strategies to be trialled was created from the data collected and a better knowledge of palmiet regeneration (Figure 53). Areas that are considered most favourable are localised reaches on depositional features within gullies or areas on the floodout where depositional features are close to water and therefore have a very shallow depth to water below the surface of the sedimentary deposit.

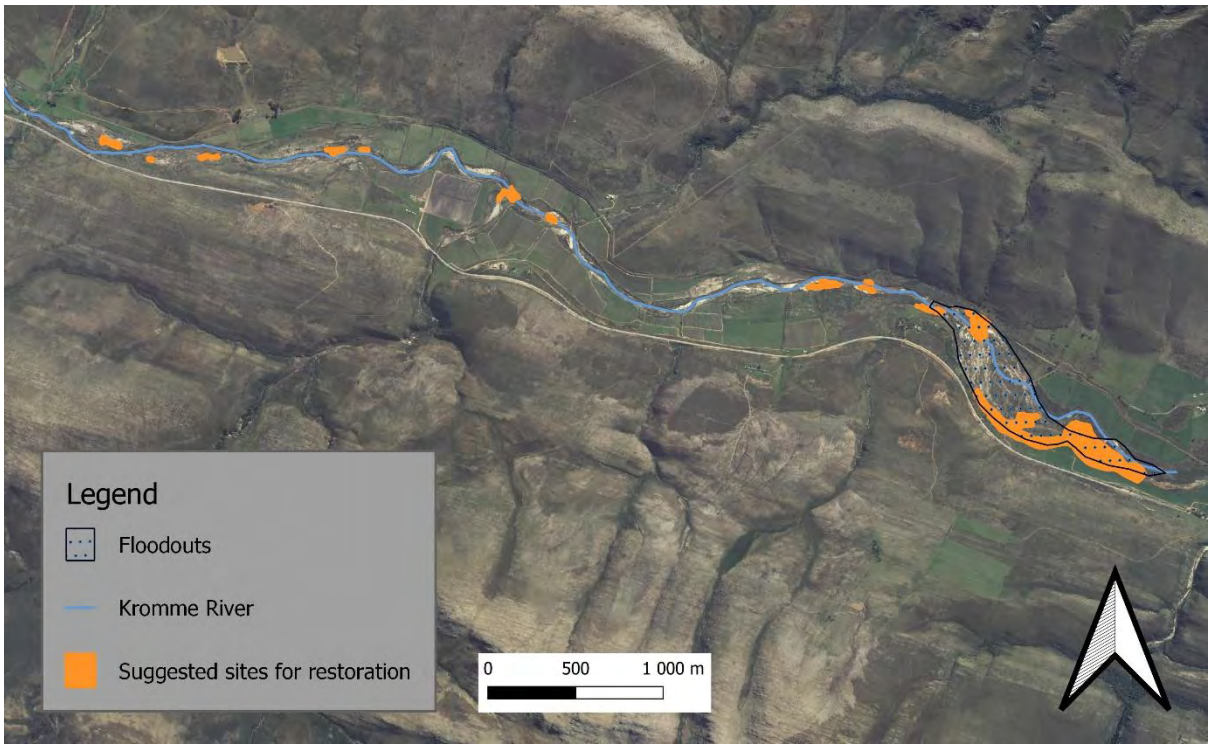

Figure 53: Map of the Jagersbos wetland indicating sites where new wetland rehabilitation strategies involving palmiet can be trialled.

5.10 Model calibration

The intention at the start of the study was to measure hydraulic characteristics in the field and comparing modelled results with measured values for the measured and modelled results. This was not possible because of a regional drought that was the worst in nearly 200 years (Ellery, personal communication). Using rainfall data from Gqeberha, for a period greater than 100 years, the years 2016, 2017, 2018, 2019 and 2020 had extremely low values. The data showed that of the lowest rainfall measured over this period, of the 10 lowest rainfall years, 5 were over the period from 2016

to 2020. Even after this period, monthly rainfall has been well below average in all months since 2016.

As an approach to calibrating the modelled results, the results from this study using HEC-RAS were visually compared with modelled results using an alternative modelling tool – Delft 3D, which was done by an expert, Professor Michael Grenfell. It proved difficult to make accurate comparisons between the images because the modelling by Professor Grenfell was not made available digitally. Furthermore, the scaling of the colour scales was completely different as one was linear (Delft 3D) while the other was logarithmic (HEC-RAS; Figure 54). Furthermore, the Delft 3D model had many zero values across the valley floor while HEC-RAS only showed cells with measurable flow. Given all of this, the best that can be said about calibrating the model produced in this study shows a broad resemblance between the two software packages. This will remain the case until the model is calibrated using measured velocities, stream powers and depths for a flood of known size.

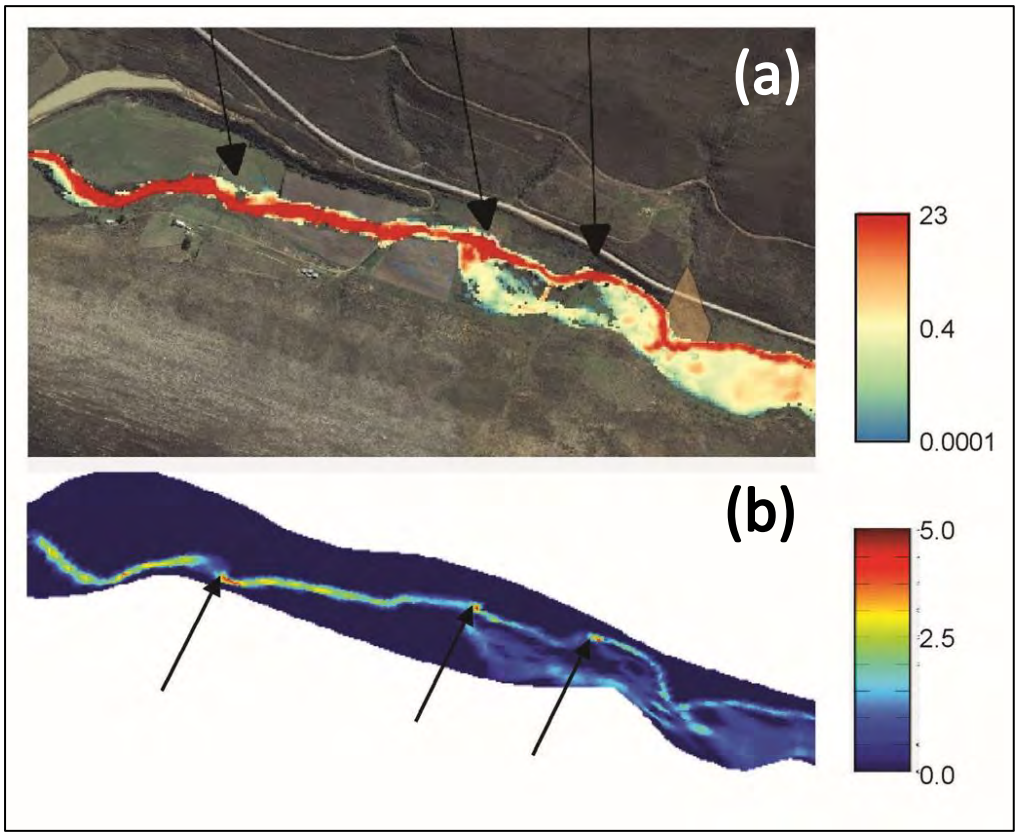

Figure 54: Comparison of model results using HEC-RAS((a); this study)) and Delft 3D (b) undertaken by Professor M Grenfell. The flows were the same magnitude and the elevation data were the same in both studies.

CHAPTER 6: DISCUSSION

6.1 Controls on the formation, structure, and dynamics of the Kromme River wetland

The presence of a valley with a broad, flat valley bottom in the steeply-sloping Cape Fold Mountains reveals the role of geomorphic processes in valley widening and longitudinal slope reduction, creating conditions ideal for wetland formation of valley bottom wetlands. Other geomorphic models of wetland formation, such as those of Tooth *et al*. (2002), McCarthy *et al*. (2011), and Joubert and Ellery (2013) do not seem to apply to the Kromme valley. The Tooth *et al*. (2002) model suggests that in valleys with easily-erodable valley bottoms, a localized resistant lithology, like a dolerite dyke, can lead to lateral erosion upstream of the resistant lithology once a very shallow longitudinal slope has been achieved. Lateral erosion and meander migration plane the valley, creating a landscape where a wetland can form. While the Kromme does have an easily-erodible valley bottom, there is no evidence of a resistant lithology that crosses the river's flow. There is also no evidence of meander migration. For lateral migration to occur, a large sediment input is required (Tooth *et al.*, 2002). The Kromme River does not have a large sediment load because of how much sediment is trapped by palmiet. The geomorphic features that are typically associated with a meandering channel, like alluvial ridges, point bars, and cutoff lakes, are absent from the landscape. There are similarities between the geomorphology of the Kromme River and the Nyl River in terms of the impact of tributary stream sedimentation on the trunk stream (McCarthy *et al*., 2011). However, the model suggested by McCarthy *et al*. (2011) does not account for the formation of the Kromme's wide, flat valley bottom.

The Kromme River has been subject to a large body of research focusing on its geomorphological origin, functioning, and dynamics. The findings of this study support the theories posited by preceding research in the Kromme wetland (Lagesse, 2017, McNamara, 2017, Schlegel, 2017, Pulley *et al.,* 2018). The Kromme seems to have evolved its broad, flat valley-bottom through repeated cut-and-fill cycles that have widened the valley and created a landscape wherein wetlands form (Pulley *et al*., 2018). There is a model for the formation of the Kromme River wetland that has been developed by Lagesse (2017) and Pulley *et al.* (2018; Figure 55). The presence of large tributary alluvial fans that occasionally cross the trunk valley suggests that they may play an important role in wetland formation along the trunk stream, but this study seems to shed further light on this.

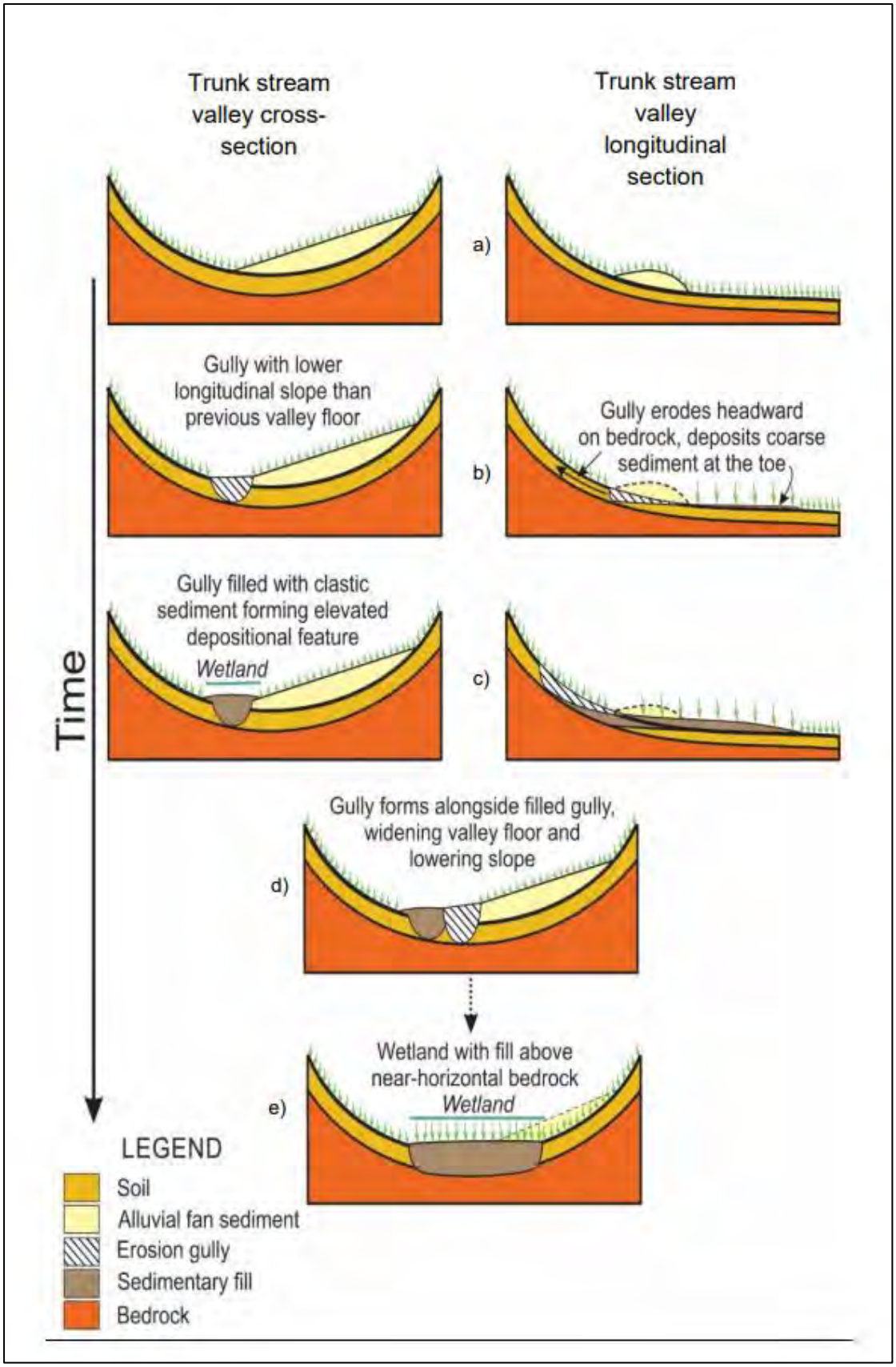

Figure 55: The conceptual model of the mechanism of gully initiation, valley widening, longitudinal slope reduction, and wetland formation in the Kromme wetlands (from Lagesse, 2017, and Pulley *et al*., 2018).

The first phase of the model represents the Kromme valley flanked by steep valley sides with a trunk stream located on the valley floor (cross section, Figure 55a). The valley has a logarithmic longitudinal profile (longitudinal section, Figure 55a). Steeply-sloping tributary streams from the adjacent mountains deposit sediment on the trunk valley floor, forming alluvial fans (Figure 55a). These alluvial fans have an effect on the width of the trunk valley, as well as the longitudinal slope. The tributary alluvial fans impinge the trunk valley bottom, narrowing its width where they enter the valley. This is evident in the cross sections across the valley in the Krugersland, Kompanjiesdrift, and Jagersbos wetlands. Upstream of the alluvial fan, there is a localized decrease in the longitudinal slope of the trunk valley, and downstream of the alluvial fan, there is a localized increase in longitudinal slope (longitudinal section, Figure 55a). This is evident in the longitudinal profiles down the length of the valley in the Krugersland, Kompanjiesdrift, and Jagersbos wetlands.

As the tributary streams deposit more sediment, the alluvial fans increase in size and their effect on valley width and longitudinal slope becomes more pronounced. The reduction in valley width and the localized increase in slope mean that for a given discharge, the flow velocity and stream power are higher in narrow reaches, opposite and directly downstream from alluvial fans. This is reflected in the results of the hydraulic modelling in the Krugersland, Kompanjiesdrift, and Jagersbos wetlands. Eventually, the longitudinal slope downstream of alluvial fans increases to the point where a geomorphic threshold is transgressed. The trunk stream is more vulnerable to erosion once this natural, intrinsic threshold is transgressed.

The second phase of the model discribes what may occur during a large flood event (Figure 55b). When there is a large flood in the catchment, the discharge in the trunk stream increases, and where the flows are concentrated due to the encroachment of alluvial fans, the flow velocity and stream power are higher than in unconfined reaches. Gully erosion is likely to be initiated in the confined reaches. As gullies propagate in an upstream direction, they mobilize large quantities of coarse-grained sediment.

Over long periods of time gully erosion works to lower the slope of the valley floor (Figure 55b). This reduction in slope is evident in the results of this study, as well as in earlier studies in the Kromme River (McNamara, 2017, Schlegel, 2017). The beds of eroded gullies have a lower slope than reaches that have not eroded. For example, in the Kompanjiesdrift wetland, the eroded reach has a slope of -0.69%, whereas the intact wetland upstream has a slope of -0.91%. In the Jagersbos wetland, the same trend is observed as the slope in the eroded reach is -0.22%, whereas the slope of the original valley floor is -0.33%.

The third phase of the model describes what may happen to the sediment generated by gully erosion (Figure 55c). When flow is spread over a broad, flat valley bottom, the flow velocity and stream power are low such that the river cannot transport sediment any further downstream (Ellery *et al.,* 2008). All the coarse-grained sediment is deposited directly downstream of gullies, where the gully loses confinement (McNamara, 2017). The sediment deposited at the toe of the gullies forms wide, elevated depositional features known as floodouts (Tooth and McCarthy, 2007). In the depositional reach of the Jagersbos Basin, there is a fine example of such a floodout. The layer of deposited sediment is thickest at the top of the floodout feature and thins progressively along the length of the floodout (McNamara, 2017). This has the effect of increasing the longitudinal slope locally (Figure 55c). The results of this study reveal that the slope on the Jagersbos floodout is -0.46%, compared to the overall slope of the wetland, which is -0.22%. The floodouts can cover the majority of the width of the valley floor, as was the case in the Kompanjiesdrift wetland as observed during coring of the valley fill in the Kompanjiesdrift basin by Lagesse (2017) and Pulley *et al*. (2018). These studies revealed an extensive layer of sand across the width of the valley and down its length. This is evidence of a floodout feature that formed a long time ago. Today, that sand layer is buried beneath organic-rich sediment and the area that would have been the floodout is covered by dense stands of palmiet. The floodouts provide a suitable environment for palmiet to establish and proliferate, and once this occurs, deposition on the floodout feature is further enhanced because palmiet captures sediment (van Eck 2022, In Prep).

Cross-sections across the floodout in the Jagersbos wetland reveal that the middle of the feature is elevated above the margins. This mounding effect causes flows to be concentrated along the margins of the floodout during a flood event. Because of the localized steepening of the slope and the gently conical form of the floodout, for a given discharge, flow velocity and stream power are higher along the margins of the floodout. Therefore, during a large flood event, when another cycle of gully erosion is initiated, the new gully most likely occurs along the margin of the floodout at the edge of the wetland (Figure 55d). As the new gully erodes, it widens the valley bottom and lowers the slope of the gully bed (Figure 55d). These repeated cycles of cutting and filling have planed the bedrock laterally and widened the floor of the valley, creating conditions where a palmiet wetland can exist (Figure 55e). Erosion is, therefore, a process that is intrinsic to the morphology of the wetland landform. The cut-and-fill cycles in mean that various reaches of the Kromme River alternate between stable and unstable states (McNamara, 2017). At any given time, there are reaches of the Kromme River that are eroding, while deposition is the dominant geomorphic process in other reaches. The periods of instability are characterized by discontinuous gullies that lower the longitudinal slope of the bed, making the reach more stable. While this is happening, deposition

downstream of the gully occurs, which increases the longitudinal slope of the bed, making the reach increasingly unstable. In the long-term, the disconnected way in which sediment flows down the Kromme River and the repeated cut-and-fill cycles that cause alternating periods of stability and instability contribute to the Kromme River's near-perfect graded profile.

The Kromme River generally erodes such that the gully bed is still on valley fill material, but it may erode to bedrock, although this generally happens downstream of erosion-control structures as can be seen in the erosional reach of the Kompanjiesdrift wetland (Figure 56).The widening and planing of the Kromme River valley seems to be mainly a consequence of vertical, rather than lateral erosion. The lateral erosion component for a given cutting cycle is primarily in a single gully. The gully enlarges and widens, but it does not migrate across the valley bottom. The only place along the Kromme River where bedrock is visible is below the erosion control structure at the toe of the Kompanjiesdrift wetland (Figure 56). Widening of the gully has clearly occurred, but the plan form of the gully remains fixed.

Figure 56: A drone image taken at the Kompanjiesdrift wetland, looking up the valley. It shows the erosion control structures and the bedrock that is visible on the bed of the eroded gully below the structure.

Overall, the impact of tributary alluvial fans on the longitudinal slope of the Kromme River is increasingly evident upstream in the study area such that tributary alluvial fan B in the upper (Krugersland) wetland has a striking effect on longitudinal slope, but the effect of tributary alluvial fans becomes less and less evident downstream. The effect of tributary alluvial fans lower down the valley on trunk valley longitudinal slope may, for example, be evident during wetter phases, during which time they may contribute to the initiation of gullies as described by Lagesse (2017) and

Langner (2019), but in general, they do not seem to have the same impact on valley longitudinal form as is the case in Nylsvlei or Wakkerstroom Vlei (McCarthy *et al*., 2011). This also means that gully initiation may be most frequent in the upper part of the study area and lowest in the vicinity of Jagersbos. However, in a general sense, the findings suggest that the overall form of the Kromme River wetland is primarily a consequence of the repeated cycles of cutting and filling, as described by Pulley *et al*. (2018), such that the overall longitudinal form of the wetland is likely to lead to flow characteristics that reflect this.

6.2 Flow characteristics of the Kromme River wetland

Hydraulic modelling of the Kromme wetland revealed likely spatial variation in flow velocity, water depth, and stream power down the length of the valley. Running the model based on sub-catchment inputs led to insights that are difficult to otherwise appreciate due to the challenges of scaling different ranges of velocity across different model simulations. The next step would be to use daily rainfall data from stations across the catchment over a number of years to decades to more correctly achieve realistic simulations under a range of flow conditions. In this case, it would be particularly useful to simulate the 2011 flood event that led to erosion and the associated deposition of the floodout (McNamara, 2017).

A key finding was that flows (velocity, stream power, and stream depth) in gullies in eroded reaches are much higher than in non-eroded reaches where discharge is spread across a broad valley bottom, despite local steepening of slope of depositional features at tributary junctions (McNamara, 2017, Pulley *et al*., 2018). In terms of palmiet establishment and regeneration, this means that areas dominated by depositional processes are likely to be best suited to the establishment of palmiet (see van Eck, 2022, In Prep).

Another key finding from this analysis was that despite a 10-fold increase in discharge down the length of the Kromme in a 1:50 year simulation, there is no significant increase in flow velocity, stream power, or depth in similar geomorphic settings downstream in the study area. Consequently, the kinetic energy of the water in the lower part of the wetland is surprisingly low for the appropriate discharge, again suggesting that the establishment of palmiet is likely to be successful on the floodout at Jagersbos. Without this kind of modelling, it would only be possible to make much more tentative claims regarding this. The reason for the consistency of flow characteristics in similar geomorphic settings down the length of the valley is unlikely to be a result of variation in hydraulic radius as the valley cross-section in similar geomorphic settings does not increase systematically in a downstream direction, and neither does bed roughness. The observed consistency in flow

characteristics must therefore be entirely related to the observed consistent reduction in the slope of the bed that is a product of fluvial processes.

6.3 The Kromme River is a graded stream

In the long-term, rivers work, via erosional and depositional processes, to achieve a state where the energy of flowing water is evenly distributed down their length (Leopold and Bull, 1979, Philips, 2010). Over very long periods, fluvial systems work to minimize the kinetic energy along their course, resulting in a longitudinal profile with a steady decline in slope from the headwaters to the river mouth (Leopold and Bull, 1979). Rivers do this by adjusting their channel morphology in terms of width, depth, and longitudinal slope to accommodate a given discharge and sediment load. In the long term rivers therefore work to achieve a state where neither erosion nor deposition occurs to reduce or increase longitudinal slope respectively (Patton and Schumm, 1975, Ellery *et al.,* 2009). When a river achieves this state, it is called a graded river. The slope along the length of a graded river is appropriate for a given discharge and sediment load, such that hydraulic characteristics like velocity and stream power are relatively constant (Ellery *et al.,* 2009). This would explain why no significant increase in velocity and stream power is observed in the lower reaches of the Kromme River (Jagersbos wetland), where discharge is much greater than in the upper reaches (Krugersland and Kompanjiesdrift).

However, in the short term, rivers work to maintain a uniform slope (Ellery *et al.,* 2009). The erosional events in the Kromme Valley occur because the river is still working to distribute energy optimally along its length. The Kromme River makes geomorphic adjustments when threshold slopes are transgressed, and the river works to adjust the slope through erosion and deposition. If rivers are viewed as integrated systems, it can be appreciated that changes in hydrogeomorphic factors in one reach can lead to changes in another reach. For example, if there is localized steepening of a trunk stream's longitudinal slope due to tributary alluvial fans impinging on the trunk valley, the stream power will increase, initiating erosion, which will lower the slope (Lagesse, 2017). The Kromme River's near-perfect logarithmic longitudinal slope suggests that it is a graded stream that is "appropriate" for the available discharge all the way down the length of wetland examined in this study (Leopold *et al*., 1964, Schumm, 1977, Ellery *et al.,* 2009). In this context, having an "appropriate" slope means that for a given discharge, energy is uniformly distributed down the length of the valley such that neither erosion nor deposition is likely to occur.

6.4 Why is the Kromme Valley so "perfectly" graded?

The Kromme River's longitudinal slope is surprisingly well-graded, as illustrated by the uniformity of hydrological characteristics down its length. Overall, it has a near-perfect concave-up longitudinal

profile. In the last 20 million years following the isostatic uplift of the African Erosion Surface, the river has incised its bed (Ellery *et al.*, 2009). This incision would have initially created a V-shaped valley with relatively steep sides until an appropriate longitudinal slope had been created, following which valley widening would have been initiated through repeated cycles of erosion and deposition (Pulley *et al.*, 2018). Since then, the narrow, steep-sided valley has developed a broad, near-horizontal valley cross-section. Such erosion also leads to progressive and systematic longitudinal slope reduction.

The nature of the sedimentary fill of the Kromme Valley may contribute to the river's graded profile. The valley-fill sequences comprise organic-rich sediments (2 – 5 % organic content; Lagesse, 2017), that overwhelmingly comprise a significant component of sand, with intermittent layers of fine-to-medium sand up to 1 metre thick across the valley. Furthermore, the valley-fill is between 6 and 8 m thick (Lagesse 2017, Pulley *et al*., 2018). The nature and depth of valley-fill sediment make it readily available for transport such that even small irregularities in slope can be adjusted by erosion and deposition.

The hydrological regime in the Kromme catchment is such that lengthy periods of low flows are punctuated by large flood events that increase the discharge for a short time (Rebelo, 2012). The feature of the valley that most constrains the initiation of erosion is the dense cover of the robust perennial plant, palmiet (Grenfell *et al*., 2008, Rebelo, 2012, Sieben, 2012, Barclay 2017, van Eck, 2022, In Prep). The combination of large irregular floods, easily erodible sediment with a large sandy fraction, and gullies having a lower slope than the valley floor results in the river having a high degree of sediment disconnectivity (McNamara, 2017). This means that following an erosional event, large depositional features form as floodouts at the toe of gullies, spreading sandy sediment across the entire valley such that the bulk of sediment generated by erosion is retained within close proximity of its point of generation (McNamara, 2017). These depositional features are favoured sites for palmiet regeneration and mean that natural rehabilitation is likely to be rapid (decades) and associated with vegetation that limits a further cycle of erosion. Because floodouts are conical, future cycles of erosion are likely to occur laterally to them, promoting valley widening.

In conclusion, the Kromme River flows on sandy and organic-rich alluvial fill that is easily entrained and transported during large, episodic flood events. The river can, therefore, adjust its channel morphology fairly easily compared to rivers that flow on more resistant (clay and silt) valley-fill sequences or on bedrock lithologies. This would explain why the Kromme River has been able to achieve and maintain a graded profile.

6.5 The role of palmiet in the Kromme Valley

Palmiet is considered an ecosystem engineer that plays a key role in the functioning and dynamics of wetlands in South Africa (Sieben, 2012). Sieben (2012) suggested that palmiet plays an important role in turning rivers into unchanneled valley-bottom wetlands by altering the hydrology and causing organic sedimentation. Barclay (2017) found that palmiet is central to the geomorphic and fluvial dynamics of the Kromme Wetland and suggested that palmiet has contributed to the creation of a landscape that can host an unchanneled valley-bottom wetland. Job (2014) identified that palmiet plays a similar role in influencing the hydrogeomorphic dynamics of the Goukou Wetland in the Western Cape.

Palmiet has fibrous leaves that remain attached to the plant's stem even after they have died, creating a dense network of roots, stems, and rhizomes that readily trap sediment. Barclay (2017) found that in the Kromme Valley, palmiet grows in three distinct settings: on open bodies of water and along gully margins, on gully beds that have been filled with coarse-grained sediment or are characterised by open water, and on broad, flat valley-bottom habitats, where it forms extensive, dense, monospecific stands. Ongoing research in the Kromme focusing on the regeneration ecology of palmiet has found that the plant colonises open bodies of water, depositional reaches, as well as gully bars and pockets of deposition within erosional reaches (Van Eck, 2022, In Prep).

Palmiet seems to be adapted to the hydrogeomorphic dynamics of the Kromme Valley, as it is a dominant species in both geomorphically stable reaches and in reaches with exposed sediments due to recent disturbance. Its extensive, deep root system and its clonal growth form enable it to proliferate in reaches with relatively high flow velocity and stream power.

Where open bodies of water exist upstream of gullies that have been blocked by sediment from tributary alluvial fans, palmiet colonises from the edges of the areas of open water (Barclay, 2017). It encroaches over the water surface, eventually forming a dense, monospecific stand covering the entire ponded area (Job 2014, Barclay, 2017). This blocks the channel of open water, slowing the flow and promoting sedimentation (Job, 2014, Barclay, 2017, Van Eck, 2022, In Prep)

Within erosional gullies, pockets of deposition exist in the form of marginal gully bars (Barclay, 2017, Van Eck, 2022, In Prep). These provide a suitable habitat for palmiet to colonize, which happens readily following a flood because it propagates vegetatively from plant fragments produced by a flood. Because of palmiet's life history strategies (deep roots and clonal growth form) it can proliferate on the beds of gullies. As palmiet spreads within the gullies, it traps sediment, helping to fill the gully (Barclay, 2017, Van Eck, 2022, In Prep).

Van Eck (2022, In Prep) suggested that palmiet plays a key role in the filling phase of the cut-and-fill cycles that characterise the Kromme Valley. In depositional reaches with a floodout feature, such as in the Jagersbos wetland, palmiet colonises areas of open water along the thalweg of distributary streams on the floodout. As it proliferates on the floodout, it traps sediment, enhancing deposition in an upstream direction, progressively filling the gully upstream of the floodout (McNamara, 2017, Van Eck, 2022, In Prep). As sedimentation along the thalweg progresses, the stream anastomoses. As the channel moves across the width of the floodout, palmiet follows. This eventually leads to the entire width of the valley bottom being dominated by dense, monospecific stands of palmiet, forming an unchanneled valley bottom wetland (Barclay, 2017, Van Eck, 2022, In Prep).

In this way, palmiet facilitates the stabilization of disturbed reaches. The diffuse flow caused by palmiet leads to further deposition that steepens the slope of the bed locally. When a threshold slope is transgressed, a new cycle of gully erosion is initiated, ushing in another period of instability in the reach.

In this way, palmiet exerts a key control on the hydrogeomorphic functioning and dynamics of the Kromme Wetlands. The Kromme Valley appears to be a self-organizing landscape in which vegetation, hydrology, and geomorphological processes work together to create a river with a near-perfect logarithmic longitudinal profile along which energy is fairly uniformly distributed.

6.6 Implications for current wetland rehabilitation work in the Kromme Valley

The value of the Kromme wetlands (in terms of ecosystem services they provide) has long been recognized (Rebelo, 2012, De Haan, 2016). Rehabilitation work in the Kromme wetlands was first proposed in the mid 1990s (De Haan, 2016). The main causes of wetland degradation in the Kromme valley were throught to be land use and land cover changes, like poor farming practices and the construction of roads and bridges across the wetland (Rebelo, 2012). These changes were thought to promote the initiation of gully erosion by altering runoff patterns and increasing peak flows (Rebelo *et al.,* 2015). Gully erosion in the Kromme valley was equated to wetland degradation because gullies can drain certain wetland areas (De Haan, 2016). The rehabilitation strategy, therefore, focused on arresting gully erosion along the floor of the Kromme valley.

Between 2002 and 2013, 11 concrete and gabion erosion-control structures were constructed (De Haan, 2016). The purpose of the structures was to stabilize erosional headcuts in gullies and decrease the transport of sediment to ensure sustained flows into the wetlands and promote the re-saturation of drained areas of wetland (De Haan, 2016). The ultimate goal was to conserve the dominant vegetation in these wetlands, with a fairly singular focus on palmiet.

This approach hinges on two key assumptions that have not been fully considered. They are that: a) if no structure is installed, the erosional nick-point will erode a gully through the intact portion of wetland, thereby draining it, and (b) erosion is inherently harmful to wetlands, and the process of erosion must be halted. These assumptions are made without considering the broader context of the wetland – the geomorphic processes that have led to the origin, structure, functioning, and dynamics of valley floors. While structural interventions are successful in halting further erosion, they may have other impacts that have not been considered. Interrupting the movement of sediment downstream of the structure can enhance erosion below the structure and instill a state of stasis upstream of the structure that is more stable than it would be naturally.

Of course land use and land cover changes influence erosion, but considering the recent findings about the Kromme River wetlands' origin and evolution, it seems that erosion in this setting is inevitable and has occurred naturally for tens- to hundreds-of-thousands of years. Thus, attempting to halt the erosion may be futile and could result in undesirable outcomes.

De Haan (2016) investigated the impact of the erosion-control structures in the Kromme wetlands on the water table. It was found that the structures did successfully increase saturation of the wetland upstream and promote diffuse flow across the valley bottom. The structures were successful in preventing erosional headcuts from migrating further upstream (De Haan, 2016, Tanner *et al.*, 2019). For example, the erosional headcut downstream from the Kompanjiesdrift wetland has not migrated since the erosion control structure was built in 2003 (Tanner *et al.*, 2019). However, the gully downstream of this erosion control structure has widened significantly over the last two decades, in some areas by a factor of three (De Haan, 2016, Tanner *et al.*, 2019). This is likely due to the effect of the structure on the movement of sediment. Sediment is trapped behind the erosion-control structure, decreasing the movement of bedload sediment below the structure. This de-stabilizes the stream bed downstream, leading to increased erosion below the structure (De Haan, 2016, Tanner *et al.*, 2019), with limited chances of filling in ways that are natural.

The results of the hydraulic modelling carried out in this study demonstrate the impact of the erosion control structures on flow velocity and stream power. In the Krugersland and Kompanjiesdrift wetlands, flow velocity and stream power are significantly higher in eroded reaches below erosion control structures. These changes to the flow do not promote the establishment and growth of palmiet within erosional gullies.

From the latest research on the regeneration ecology of palmiet, it is becoming increasingly clear that the plant relies on the formation of depositional features to proliferate (Van Eck, 2022, In Prep). If erosion is halted and sediment cannot be deposited downstream, palmiet's regeneration niche

may thus be lost. Because palmiet seems to establish on depositional features that are formed due to erosion, halting erosion may negatively affect palmiet recruitment. If the goal of rehabilitation is to conserve palmiet wetlands in the Kromme, structural interventions such as those currently used may be counterproductive. For example, between 2003 and 2013, the extent of the palmiet wetland upstream of the erosion control structure in Kompanjiesdrift has decreased (De Haan, 2016).

6.7 New strategies for wetland rehabilitation in the Kromme Valley

The hydrogeomorphic dynamics of the Kromme Valley (the repeated cycles of cutting and filling over the last 20 million years) have created a valley with a broad, flat valley floor and a low longitudinal slope. The erosion and deposition are the very things that have created a valley where a wetland can form. The model outputs strongly suggest that sediment deposition by tributary alluvial fans leads to a localized increase in flow velocity and stream power and the initiation of natural erosion gullies. Natural gully erosion in the Kromme valley is likely enhanced by anthropogenic activities, but because erosion seems to be a process that is inherent to the system, halting all erosion completely through the construction of hard structures may be problematic in the long-term. Rehabilitation strategies should aim to work with the natural dynamics of a system rather than against them. Interventions should seek to mimic and enhance natural hydrogeomorphic dynamics.

More recently, Working for Wetlands has shifted its approach to wetland rehabilitation, favoring innovative “soft” interventions over large and costly “hard” interventions, like concrete and gabion structures (Nieuwoudt *et al*., 2018). Effective interventions that involve the use of vegetation need to be developed.

Palmiet is an excellent candidate to use in new rehabilitation strategies as its regeneration niche mean that it readily colonises depositional features – both by vegetative propogation and by seeds (van Eck, 2022, In Prep). Furthermore, given that palmiet is an ecosystem engineer, the plant has a pronounced effect on wetlands’ hydrogeomorphic processes. A possible new rehabilitation strategy could aim to enhance the recruitment and growth of palmiet downstream of an erosional headcut, thereby increasing the rate of deposition and promoting natural infilling of the gully in an upstream direction.

6.8 Optimal locations to trial new rehabilitation strategies

Considering that palmiet naturally colonizes newly exposed sediments on gully beds and on floodout features (Van Eck, 2022, In Prep), these areas seem to be suitable locations to put new rehabilitation strategies involving palmiet, to the test. To give palmiet the best possible chance to establish, it should be planted in reaches with low flow velocity and stream power so that young plants are not at risk of being uprooted and washed downstream during high discharge flood events. Furthermore,

its regeneration requires that the water table is close to the land surface (< 1 m; van Eck, 2022, In Prep).

It is suggested that hydraulic modelling is a valuable tool for determining the optimal locations to test new wetland rehabilitation strategies. It allows areas that are suitable for palmiet recruitment and growth to be identified and mapped. Such mapping may be a valuable part of planning future wetland rehabilitation projects.

The results of the modelling done in this study indicate that the Jagersbos wetland may be the best area to begin testing new wetland rehabilitation strategies that involve palmiet. It is more suitable than the Krugersland and Kompanjiesdrift wetlands because there are very few areas of bare sediment exposed in these wetlands and the kinetic energy of the water in the Jagersbos wetland is surprisingly low for the discharge. High-resolution hydraulic modelling is valuable because it allows for the identification of specific sites within the Jagersbos wetland where conditions are most suitable for the establishment of palmiet. It enables wetland practitioners to produce maps relatively quickly and easily. This type of mapping would greatly support the planning of rehabilitation work. Less time and resources could be wasted if palmiet is only planted in areas where it is unlikely to be uprooted and washed downstream during large floods.

6.9 LiDAR vs conventional topographic surveying

The insights that have been gained through the high-resolution hydraulic modelling done in this study are valuable in planning wetland rehabilitation interventions. However, LiDAR surveys are costly, and it would be impractical to suggest that wetland rehabilitation practitioners need to fund such a survey each time they plan rehabilitation strategies in a wetland. Is it possible for the same level of insight to be gained with conventional topographic surveying techniques at a much lower cost?

Previous research in the Kromme Wetland determined the topography of the valley by means of surveying using a Differential GPS (DGPS; Lagesse, 2017, McNamara, 2017, Schlegel, 2017, Pulley *et al.,* 2018, Langner, 2019). Conducting topographic surveys in palmiet wetlands is challenging given the tall, dense vegetation that has sharp, serrated leaf margins. Walking across the wetland with a DGPS rover, measuring surveys points every 5 to 20 m, takes a long time and considerable physical effort. To get the level of topographic detail required for accurate modelling using conventional surveying techniques is therefore extremely difficult.

In previous studies, detailed topographic surveys were only conducted along a limited length of the Kromme River. For example, in the Kompanjiesdrift wetland, a 2-km reach was surveyed along 8

transects across the valley floor. In the Jagersbos wetland, a 1.4-km reach was surveyed along 11 transects. To enhance the detail of the topographic data and create a DTM with a suitable resolution for modelling, geo-referenced orthophotographs (1:10 000 scale) with 10-m contour lines were used to get supplemental survey points (Lagesse, 2017, McNamara, 2017, Pulley *et al.,* 2018). This allowed hydraulic modelling to be done with a 20 x 20 m computational grid (Schlegel, 2017).

In this study, obtaining the topographic data by means of LiDAR survey meant that a much higher-resolution DTM could be created. The LiDAR sensors measure on average 5.5 data points per square meter. This level of detail would be nearly impossible using conventional topographic surveying techniques with a DGPS. The entire 23-km reach of the upper Kromme River was surveyed in a single day using LiDAR. In terms of efficiency and accuracy, a LiDAR survey is infinitely better than a conventional topographic survey.

However, due to constraints in computing capabilities, running a model with a computational grid cell size of 1 x 1 m or 2 x 2 m was impractical. The large size of the input data results in very long simulation times when running the model and requires a lot of computing power. For this reason, the modelling in this study was done with a computational grid cell size of 5 x 5 m. This was still a much higher and more accurate resolution than that at which previous hydraulic modelling work was done in the Kromme (Schlegel, 2017).

Small differences in elevation within the wetland, especially those with extant stands of palmiet, are difficult to measure with conventional surveying techniques, and they do not show up on topographic maps with 10 m contour lines. Therefore, the level of topographic detail captured in the LiDAR survey was significantly greater. The modelled outputs demonstrate a high degree of spatial variability over short distances of less than 20m.

Conventional topographic surveying seems to produce data with a high enough resolution to appreciate the larger-scale cross-sectional morphology of the valley and geomorphic features, like floodouts and gullies. Important characteristics, such as the mounding effect caused by depositional floodouts, and the fact that they cause local steepening of the slope downstream were still apparent in low-resolution cross-sections (McNamara, 2017).

However, to visualize differences in flow velocity, stream power, and depth at a small spatial scale using high-resolution topographic data seems to be required. If the goal of modelling is to identify the optimal locations to establish palmiet within a gully that is less than 20 m wide, or on a floodout feature where significant changes in hydraulic characteristics happen over short distances, a DTM with a resolution of at least 10 x 10 m is necessary.

Currently, the highest resolution DEM that covers the whole of South Africa is the Stellenbosch University Digital Elevation Model (SUDEM). SUDEM has a resolution of 5 m x 5m. The vertical accuracy is 2 to 15 m and the horizontal accuracy is 10 to 30 m. This is a reasonable resolution to derive a computational grid for hydraulic modelling purposes, and may be sufficient to investigate valley morphology.

If hydraulic modelling to determine optimal sites for rehabilitation work is to be recommended as an approach to wetland rehabilitation, it is further recommended that SUDEM is used by wetland practitioners as a topographic input to the model. Obtaining SUDEM is much more cost-efficient than procuring a LiDAR dataset – it costs R 6 000 for a 300 km^2 area, R 7 500 for a 1:50 000 map sheet, and R 18 750 for a quarter-degree square. This is roughly 16 times cheaper than the cost of a LiDAR survey!

6.10 Limitations of the model

Model calibration was challenging because of the lack of data for observed water surface elevation and flood extent in recent years. The study area has experienced a severe drought over the last decade, and the modelled discharge has not been observed for a long time. Therefore, it was not possible to collect data for water surface elevation or flood extent for a discharge of 45 cumecs. While the model seemed well-calibratedbased on and independent software tool and expert input, the lack of observed flow data was a major limiting factor in the calibration process.

The rainfall data used to build the model was averaged from 1978 to 2019. Overall, the mean annual rainfall seems to be decreasing, possibly due to climate change. The model does not account for climate variability, which is another limitation. Farmers along the Kromme River abstract water for irrigation. The model also does not account for this.

CHAPTER 7: CONCLUSION

Wetland formation has traditionally been attributed to mainly hydrological factors, with climatic and geomorphic factors being viewed as externalities that only have a minor effect on the evolution of a wetland environment (Gosselink and Turner, 1978, Mitsch and Gosselink, 2015). However, a growing body of research is recognizing the central role of geomorphology in wetland formation, structure, and dynamics (McCarthy and Ellery, 1995, Tooth *et al.,* 2002, Tooth *et al.,* 2004, Grenfell *et al.,* 2008, Grenfell *et al.,* 2010, McCarthy *et al.,* 2011, Lagesse, 2017, Pulley *et al*., 2018). This study formed a part of this body of research, as it investigated how geomorphic processes in the Kromme River valley effect the functioning and dynamics of the unchannelled valley-bottom wetlands. Developing a thorough understanding of the origin, structure, functioning, and dynamics of a particular wetland is essential in order to plan effective and sustainable rehabilitation interventions that result in positive effects. It is important to determine the geomorphic processes, like erosion and deposition, that are inherent in a wetland system, so that rehabilitation interventions can be designed to work with natural dynamics rather than against them (Ellery, *et al.,* 2009).

There are two key geomorphic requirements for the formation of a wetland. Firstly, wetlands require a valley with a near-horizontal floor to form, and, secondly, they form in valleys with a gentle longitudinal slope (Tooth, *et al.,* 2002*,* 2004). The Kromme River valley has a broad, near-horizontal floor, and its longitudinal slope decreases systematically in a downstream direction. The results of this research support the model of wetland formation proposed by Lagesse (2017) and Pulley *et al*. (2018), whereby repeated cut and fill cycles have widened and planed the Kromme River valley and lowered the longitudinal slope to create a landscape where a wetland can form. The LiDAR topographic survey provided detailed insight into the longitudinal profile and morphology of the valley, and strongly suggest that other geomorphic models of wetland formation, such as those proposed by Tooth *et al*. (2002), McCarthy *et al*. (2011), and Joubert and Ellery (2013) are unlikely to apply to the Kromme wetlands.

The high-resolution topographic dataset and aerial imagery were used to identify geomorphic features like tributary alluvial fans, erosion gullies, and depositional floodouts in the wetlands, and the geomorphic processes that created these features were inferred. The steep tributary streams that enter the Kromme River valley deposit sediment on the trunk valley bottom, forming alluvial fans that reduce the width of the valley floor. The alluvial fans affect the longitudinal slope of the trunk valley. Upstream of the alluvial fans, the slope is locally reduced, and downstream of the alluvial fans the slope increases locally. In between the alluvial fans the valley is broad and flat in cross-section. During large flood events, gully erosion may be initiated in the reaches that are

confined by alluvial fans. The longitudinal slope on the gully bed is lower than the original slope of the valley floor. The sediment generated at the erosional nickpoint is deposited a short distance downstream, at the toe of the gully where the valley floor loses confinement, forming a floodout feature. This increases the longitudinal slope locally. The effect of the tributary alluvial fans on the longitudinal slope of the valley is most striking in the upper Krugersland wetland but becomes less and less evident downstream. This means that gully initiation may be most frequent in the upper part of the study area and lowest in the vicinity of Jagersbos.

The hydraulic model built using the high-resolution topographic data (DTM) was able to demonstrate the effect of the valley morphology on stream hydraulics. Stream power was a useful variable to model because it is directly related to a streams ability to entrain, transport, and deposit sediment (Bagnold, 1960, 1966, 1977, 1980). Sediment transport is a key consideration to determine which reaches along a river are prone to erosion or deposition (Gartner, 2016). In zones with very high stream power, erosion is likely to be a dominant process and in zones with low stream power, depositional processes are likely to dominate

The model outputs showed detailed spatial variation in flow velocity, stream power, and water depth along the 23-km-long reach of the valley that was surveyed. Flow velocity and stream power were generally lowest in unconfined reaches where flow is spread across a broad valley bottom and were much higher in confined reaches. This supports the theory by Lagesse (2017) and Pulley *et al*. (2018) that gully erosion may be initiated in confined reaches where alluvial fans enter the valley. Downstream of gullies where the valley loses confinement the river does not have sufficient stream power to transport the sediment generated by erosion, therefore it is deposited, forming a floodout. In the Krugersland and Kompanjiesdrift wetlands, the unconfined reaches are densely vegetated with palmiet, which promotes diffuse flow across the width of the valley bottom. However, in the Jagersbos wetland, the unconfined reach represents a wide, sandy depositional floodout. Even though the floodout has a higher longitudinal slope than the bed of the eroded gully upstream from it, stream power is significantly lower on the floodout compared to the gully.

A key finding was that despite a 10-fold increase in discharge down the length of the Kromme River in a 1:50 year simulation, there is a lesser increase in flow velocity, stream power, or water depth in similar geomorphic settings downstream in the study area. The reason for the consistency of flow characteristics in similar geomorphic settings down the length of the valley is unlikely to be a result of variation in hydraulic radius as the valley cross-section in similar geomorphic settings does not increase systematically in a downstream direction, and neither does bed roughness. The observed

consistency in flow characteristics must therefore be entirely related to the observed consistent reduction in the slope of the bed that is a product of fluvial geomorphic processes.

Given the likely origin of the Kromme River valley-bottom wetlands, and the geomorphic processes that characterize the system, wetland rehabilitation interventions that disrupt sediment flux are unlikely to have the desired effect in the long term. It is suggested that rehabilitation in these wetlands should focus more on enhancing palmiet recruitment on the beds of erosion gullies and on depositional floodouts. Palmiet is a key biogeomorphic agent in the system, so this type of approach could mimic the natural dynamics of the system by enhancing deposition within gullies and on floodouts. Getting palmiet to establish in these zones could increase the rate at which gullies are filled from their toe, as is the natural geomorphic dynamic in the Kromme River valley. Knowing the spatial variation in velocity, stream power, and depth in a reach of wetland where rehabilitation strategies are being planned is important as it indicates where erosional and depositional processes are likely to be dominant during a large flood event, and, hence, where the best places are to propagate palmiet. The hydraulic modelling that was done in this study enabled the mapping of zones most appropriate for testing new wetland rehabilitation techniques that employ palmiet.

A major limitation of the model is that it was only calibrated using computed flow data. It was not possible to collect observed flow data because the study area has been affected by a severe drought over the last decade and a measurable discharge that could be modelled has not occurred since the inception of this study. It is recommended that the model be better calibrated before model outputs are used to make decisions about wetland rehabilitation interventions. Nevertheless, this study has demonstrated the value of using high-resolution remotely sensed topographic data to investigate the origin, structure, functioning, and dynamics of a wetland. This could support wetland rehabilitation practitioners in selecting the most appropriate type of intervention for a particular system.

References

Antevs, E. 1952. Arroyo-cutting and filling. *The Journal of Geology*, 60(4), pp. 375–385.

Avni, Y. 2005. Gully incision as a key factor in desertification in an arid environment, the Negev highlands, Israel. *Catena*, 63, pp. 185–220.

Bagnold, R.A. 1960. Sediment discharge and stream power – a preliminary announcement: US Geological Survey, Circular 421.

Bagnold, R.A. 1966. An approach to the sediment transport problem from general physics: US Geological Survey, Professional Paper 422.

Bagnold, R.A., 1977. Bed load transport by natural rivers. *Water resources research*, 13(2), pp. 303-312.

Bagnold, R.A., 1980. An empirical correlation of bedload transport rates in flumes and natural rivers. *Proceedings of the Royal Society of London. A. Mathematical and Physical Sciences*, 372(1751), pp. 453-473.

Bailey, A.K. and Pitman, W.V. 2016. Water resources of South Africa, 2012 STUDY: Book of maps. *WRC Report* TT 382/08. Water Research Commission, Pretoria.

Balling, R.C. and Wells, S.G. 1990. Historical rainfall patterns and arroyo activity within the Zuni River drainage basin, New Mexico. *Annals of the Association of American Geographers*, 80(4), 603-617.

Barclay, A. 2017. *Ecosystem engineering by the wetland plant Palmiet: Does it control fluvial form and promote diffuse flow in steep-sided valleys of the Cape Fold Mountains*. Grahamstown: Rhodes University (MSc Thesis) [pdf].

Bekkaddour, T., Schlunegger, F., Vogel, H., Delunel, R., Norton, K. P., Akcar, N. and Kubik, P. 2014. Paleo-erosion rates and climate shifts recorded by Quaternary cut-and-fill sequences in the Piso valley, central Peru. *Earth and Planetary Science Letters*, 390, 103– 115.

Bizzi, S. and Lerner, D. N. 2015. The use of stream power as an indicator of channel sensitivity to erosion and deposition processes. *River Research and Applications*, 31(1)1, pp. 16-27.

Bocco, G. 1991. Gully erosion: processes and models. *Progress in physical geography*, 15(4), pp. 392-406.

Bork, H.R. 2003. State-of-the-art of erosion research-soil erosion and its consequences since 1800 AD. In: Boix-Fayos, C., Dorren, L. and Imeson, A.C. (Eds.) Briefing Papers of the first SCAPE Workshop, pp. 11-14.

Botha, G.A., Wintle, A.G. and Vogel, J.C. 1994. Episodic late quaternary palaeogully erosion in northern KwaZulu-Natal, South Africa. *Catena,* 23, pp. 327–340.

Boucher, C. and Withers, M. 2004. Palmiet. Prionium serratum, a Cape river plant. *Veld and Flora (South Africa)*.

Bracken, L.J., Turnbull, L., Wainwright, J., and Bogaart, P. 2015. Sediment connectivity: a framework for understanding sediment transfer at multiple scales. *Earth Surface Processes and Landforms*, 40(2), 177–188.

Brierley, G. and Fryirs, K. 1999. Tributary-trunk stream relations in a cut-and-fill landscape: a case study from Wolumla catchment, New South Wales, Australia. *Geomorphology*, 28(1–2), 61–73.

Brunner, G.W. 2016. HEC-RAS River Analysis System: Hydraulic Reference Manual, Version 5.0. US Army Corps of Engineers–Hydrologic Engineering Center, 547.

Brunner, G., Savant, G. and Heath, R.E. 2020. *Modeler Application Guidance for Steady vs Unsteady, and 1D vs 2D vs 3D Hydraulic Modeling*. California, USA: Hydrologic Engineering Center.

Bull, W.B. 1979. Threshold of critical power in streams. *Geological Society of America Bulletin*, 90(5), pp. 453-464.

Buraas, E.M., Renshaw, C.E., Magilligan, F.J. and Dade, W.B. 2014. Impact of reach geometry on stream channel sensitivity to extreme floods. *Earth Surface Processes and Landforms*, 39(13), pp. 1778-1789.

Burrough, S.L., Thomas, D.S.G., Orijemie, E.A. and Willis, K.J. 2015. Landscape sensitivity and ecological change in western Zambia: The long-term perspective from dambo cut-and-fill sediments. *Journal of Quaternary Science*, 30(1), pp.44-58

Carnicelli, S., Benvenuti, M., Ferrari, G. and Sagri, M. 2009. Dynamics and driving factors of late Holocene gullying in the Main Ethiopian Rift (MER). *Geomorphology*, 103(4), pp. 541-554.

Chang, H.H. 1979. Minimum stream power and river channel patterns. *Journal of Hydrology*, 41(3-4), pp. 303-327.

Chow, V .T. 1959. *Open-Channel Hydraulics*. New York: McGraw-Hill.

Cooke, J.A. and Johnson, M.S. 2002. Ecological restoration of land with particular reference to the mining of metals and industrial minerals: A review of theory and practice. *Environmental Reviews*, 10(1), pp. 41-71.

Cooper, A., Murray, R. and McCann, T. 1991. The environmental effects of blanket peat exploitation. Ireland: University of Ulster.

Costabile, P., Costanzo, C., Ferraro, D., Macchione, F. and Petaccia, G. 2020. Performances of the new HEC-RAS version 5 for 2-D hydrodynamic-based rainfall-runoff simulations at basin scale: Comparison with a state-of-the art model. *Water*, 12(9), p.2326.

Coulthard, T.J. and van de Wiel, M.J. 2013. Numerical modelling in fluvial geomorphology. In: Shroder, J. and Wohl, E. (Eds.), Treatise on Geomorphology. *Fluvial Geomorphology*, 9, pp.694–710. San Diego, California: Academic Press.

De Haan, V. 2016. *The effects of erosion-control structures and gully erosion on groundwater dynamics along the Kromrivier, Eastern Cape, South Africa*. Stockholm University, Stockholm, Sweden (MSc Thesis) [pdf].

Dennis, I. and Pretorius, J. 2006. *Groundwater reserve determination for the Kromme/Seekoei catchments*. Final Report, Project No. 2005-18. Pretoria: Department of Water Affairs and Forestry.

De Vente, J., Poesen, J. and Verstraeten, G. 2005. The application of semi-quantitative methods and reservoir sedimentation rates for the prediction of basin sediment yield in Spain. *Journal of Hydrology*, 305(1), pp.63–86.

Dini, J. and Bahadur, U. 2016. South Africa's national wetland rehabilitation programme: Working for wetlands. In: C.M. Finlayson et al. (Eds.), The Wetland Book. Dordrecht, The Netherlands: Springer.

Driver, A., Sink K.J., Nel, J.N., Holness, S., Van Niekerk, L., Daniels, F., Jonas Z., Majiedt, P.A., Harris, L., Maze, K. 2012. National biodiversity assessment 2011: an assessment of South Africa's biodiversity and ecosystems. *Synthesis report*. Pretoria: South African National Biodiversity Institute and Department of Environmental Affairs.

Eitel, B., Eberle, J. and Kuhn, R. 2002. Holocene environmental change in the Otjiwarongo thornbush savanna (Northern Namibia): evidence from soils and sediments. *Catena*, 47, pp.43–62.

Ellery, W.N., Grenfell, M.C., Grenfell, S.E., Kotze, D., McCarthy, T.S., Tooth, S., Grundling, P.L., Beckedahl, H., le Maitre, D. and Ramsay, L. 2009. WET-Origins: Controls on the distribution and dynamics of wetlands in South Africa. *WRC Report* No TT334/09.

Ellery, W.N., Grenfell, S.E., Grenfell, M.C., Humphries, M.S., Barnes, K., Dahlberg, A. and Kindness, A. 2012. Peat formation in the context of the development of the Mkuze floodplain on the coastal plain of Maputaland , South Africa. *Geomorphology*, 141–142, pp.11–20.

Ellery, W.N. and Ellery, K. 2022, In Prep. *The Okavango Delta as a peatland landscape.* In: Eckardt, F. (Ed.): Landscapes and Landforms of Botswana. World Geomorphological Landscapes. Switzerland: Springer.

Ellery, W.N., Langner, W., Glenday, J.,Grenfell, S.E., Grenfell, M.C., Tanner, J., Job, N., Kotze, D.C. 2022, In Prep. Controls on the origin and distribution of palmiet wetlands in South Africa: understanding the landscape and hydrological settings of wetlands. Submitted to *Wetlands Ecology and Management*.

Fryirs, K.A. and Brierley, G.J. 1998. The character and age structure of valley fills in Upper Wolumla Creek catchment, South Coast, New South Wales, Australia. *Earth Science Reviews*, 23, pp.271– 287.

Fryirs, K.A., Brierley, G.J., Preston, N.J. and Kasai, M. 2007. Buffers, barriers and blankets: the (dis)connectivity of catchment-scale sediment cascades. *Catena*, 70(1), pp. 49–67.

Fryirs, K.A. and Brierley, G.J. 2012. *Geomorphic analysis of river systems: an approach to reading the landscape*. United States of America: John Wiley and Sons.

Fryirs, K.A. 2013. (Dis)Connectivity in catchment sediment cascades: a fresh look at the sediment delivery problem. *Earth Surface Processes and Landforms*, 38(1), pp. 30–46.

Gartner, J.D., Dade, W.B., Renshaw, C.E., Magilligan, F.J. and Buraas, E.M. 2015. Gradients in stream power influence lateral and downstream sediment flux in floods. *Geology*, 43(11), pp.983-986.

Gartner, J.D. 2016. Stream power: Origins, geomorphic applications, and GIS procedures. *Water Publications*. [Online] Available: https://scholarworks.umass.edu/water_publications/1 [15/1/2021].

Gilbert, G.K. and Murphy, E.C. 1914. The transportation of debris by running water, No. 86. US Government Printing Office.

Gosselink, J. G., and Turner, R. E. 1978. The role of hydrology in freshwater wetland ecosystems. In: R. E. Good, D. F. Whigham, and R. L. Simpson (Eds.), Freshwater wetlands-ecological processes and management potential, pp. 63–78. New York: Academic Press.

Graf, W.L. 1983. Downstream changes in stream power in the Henry Mountains, Utah. *Annals of the Association of American Geographers*, 73(3), pp.373-387.

Grenfell, M.C., Ellery, W.N., Garden, S.E., Dini, J. and Van der Valk, A.G. 2007. The language of intervention: A review of concepts and terminology in wetland ecosystem repair. *Water SA*, 33(1), pp. 43-50.

Grenfell, M.C., Ellery, W. and Grenfell, S.E., 2008. Tributary valley impoundment by trunk river floodplain development: a case study from the KwaZulu-Natal Drakensberg foothills, eastern South Africa. *Earth Surface Processes and Landforms*, 33(13), pp. 2029–2044.

Grenfell, M.C., Ellery, W.N. and Grenfell, S.E., 2009. Valley morphology and sediment cascades within a wetland system in the KwaZulu-Natal Drakensberg Foothills, Eastern South Africa. *Catena*, 78(1), pp. 20–35.

Grenfell, S.E., Ellery, W.N. and Grenfell, M.C. 2010. Sedimentary facies and geomorphic evolution of a blocked-valley lake: Lake Futululu, northern Kwazulu-Natal, South Africa. *Sedimentology,* 57(5), pp. 1159–1174.

Grenfell, M.C. 2015. Modelling Geomorphic Systems: fluvial virtual rivers*. Geomorphological Techniques. British Society for Geomorphology*, 4, pp.1–12.

Grenfell, S.E., Grenfell, M.C., Ellery, W.N., Job, N. and Walters, D. 2019. A genetic geomorphic classification system for southern African palustrine wetlands: global implications for the management of wetlands in drylands. *Frontiers in Environmental Science*, *7*, pp.174.

Gull, K. 2012. *Water supply in the Eastern Cape: an economic case study of land rehabilitation in the Kromme River Catchment*. Cape Town: University of Cape Town. (MComm. Thesis) [pdf].

Gumbricht, T., McCarthy, T.S. and Merry, C.L. 2001. The topography of the Okavango Delta, Botswana, and its tectonic and sedimentological implications. *South African Journal of Geology*, 104, pp.243–64.

Hagberg, T.D. 1995. *Relationships between hydrology, vegetation and gullies in montane meadows of the Sierra Nevada.* United States of America: Humboldt State University. (MSc Thesis) [pdf].

Haigh, L., Illgner, P., Wilmot, J., Buckle, J., Kotze, D. and Ellery, F. 2009. The wetland rehabilitation project in the Kromme River Wetlands, Eastern Cape. In: Breen, C., Dini, J., Ellery, W., Mitchell, S. and Uys, M. (Eds). WET-Outcome evaluate: An evaluation of the rehabilitation outcomes at six wetland sites in South Africa. *WRC Report* TT343/09, 109–168. Water Research Commission, Pretoria.

Harvey, A. M. 2001. Coupling between hillslopes and channels in upland fluvial systems: implications for landscape sensitivity, illustrated from the Howgill Fells, northwest England. *Catena*, 42(2–4), pp. 225–250.

Harvey, A. M. 2012. The coupling status of alluvial fans and debris cones: a review and synthesis. *Earth Surface Processes and Landforms*, 37(1), 64–76.

Henderson, P.M. 1966. *Open-channel flow*. New York: MacMillan Publishing. pp. 522.

Hjulström, F. 1935. *Studies of the morphological activity of rivers as illustrated by the River Fyris.* Sweden: The Geological institution of the University of Upsala (Doctoral dissertation) [pdf].

Hooke, J. 2003. Coarse sediment connectivity in river channel systems: a conceptual framework and methodology. *Geomorphology*, 56(1–2), pp. 79–94.

Jansen, F. and van Veen, J. 2014. *Proposal for rehabilitation of the Upper Peatland Basin*. [Online] Available: http://data.saeon.ac.za/saeon/documents/presence-network/kromme-catchment/reports/. [22/08/21].

Job, N. 2014. *Geomorphic origin and dynamics of deep, peat-filled, valley bottom wetlands dominated by Palmiet (Prionium serratum) – a case study based on the Goukou Wetland, Western Cape*. Grahamstown: Rhodes University (MSc Thesis) [pdf].

Joubert, R. and Ellery, W.N. 2013. Controls on the formation of Wakkerstroom Vlei , Mpumalanga province , South Africa. *African Journal of Aquatic Science*, 38 (2), pp.135–151.

Kirby, E., and Whipple, K. 2001. Quantifying differential rock-uplift rates via stream profile analysis. *Geology*, 29(5), pp.415–418.

Kirkby, M.J. and Bracken, L.J. 2009. Gully processes and gully dynamics. *Earth Surface Processes and Landforms*, 34, pp.1841–1851.

Knapp, R.T. 1938. Energy-balance in stream-flows carrying suspended load. *Eos, Transactions American Geophysical Union*, 19(1), pp.501–505.

Kondolf, G.M., Piégay, H., Schmitt, L. and Montgomery, D.R. 2016. Geomorphic classification of rivers and streams. *Tools in fluvial geomorphology*, pp.133-158.

Kotze, D. and Ellery, W. 2009. WET-OutcomeEvaluate: An evaluation of the rehabilitation outcomes at six wetland sites in South Africa. *WRC Report* No. TT 343/08.

Lagesse, J. 2017. *Discontinuous gully erosion as a mechanism of wetland formation: a case study of the Kompanjiesdrif Basin, Krom River, Eastern Cape, South Africa*. Grahamstown: Rhodes University (MSc Thesis) [pdf].

Lane, E.W. 1955. Design of stable channels. *Transactions of the American society of Civil Engineers*, 120(1), pp.1234-1260.

Lane, S.N. 2001. More floods, less rain: changing hydrology in a Yorkshire context. *The Yorkshire and Humber Regional Review*, 11(3), pp. 18–19.

Langner, W. 2019. *A conceptual model of the initiation of gully erosion in an unchanneled valley-bottom wetland: A case study of the Kromrivier, Eastern Cape, South Africa*. Grahamtown: Rhodes University (Honours Thesis) [pdf].

Lea, D.M. and Legleiter, C.J. 2016. Mapping spatial patterns of stream power and channel change along a gravel-bed river in northern Yellowstone. *Geomorphology*, 252, pp.66-79.

Leopold, L.B., Wolman, M.G. and Miller, J.P. 1964. *Fluvial processes and geomorphology*. San Francisco: Freeman.

Leopold, L.B. and Maddock, T. 1953. *The hydraulic geometry of stream channels and some physiographic implications*. Washington: US Government Printing Office.

Leopold, L.B. and Bull, W.B. 1979. Base level, aggradation, and grade. *Proceedings of the American Philosophical Society*, 123(3), pp.168-202.

Liu, H., Zhang, S., Li, Z., Lu, X. and Yang, Q. 2004. Impacts on wetlands of large-scale land-use changes by agricultural development: the small Sanjiang Plain, China. *AMBIO: A Journal of the Human Environment*, 33(6), pp.306–310.

Lizias, K. and Felix, C. 2013. Wetlands and Urban Growth in Bindura, Zimbabwe. *Greener Journal of Environment Management and Public Safety*, 2(6), pp. 195–199.

Lyons, R., Tooth, S. and Duller, G.A.T. 2013. Chronology and controls of donga (gully) formation in the upper Blood River catchment, KwaZulu-Natal, South Africa: Evidence for a climatic driver of erosion. *The Holocene*, 23(12), 1875–1887.

Magilligan, F.J. 1992. Thresholds and the spatial variability of flood power during extreme floods. *Geomorphology*, 5(3-5), pp.373-390.

McCabe, A.M. and Dardis, G.F. 1989. Sedimentology and depositional setting of late Pleistocene Drumlins, Galway Bay, Western Ireland. *Journal of Sedimentary Research*, 59(6), pp.944–959.

McCarthy, T.S., Green, R.W. and Franey, N.J. 1993. The influence of neo-tectonics on water dispersal in the northeastern regions of the Okavango swamps, Botswana. *Journal of African Earth Sciences* 17, pp. 23–32.

McCarthy, T.S. and Ellery, W.N. 1995. Sedimentation on the distal reaches of the Okavango fan, Botswana, and its bearing on calcrete and silcrete (ganister) formation. *Journal of Sedimentary Research* A65, pp. 77–90.

McCarthy, T. S., Barry, M., Bloem, A., Ellery, W. N., Heister, H., Merry, C. L., Rother H. and Sternberg, H. 1997. The gradient of the Okavango fan, Botswana, and its sedimentological and tectonic implications. *Journal of African Earth Sciences*, 24, pp. 65–78.

McCarthy, T.S., Smith, N.D., Ellery, W.N. and Gumbricht, T. 2002. The Okavango Delta – semiarid alluvial-fan sedimentation related to incipient rifting. In: *Renaut, R.W. and Ashley, G.M., editors, Sedimentation in continental rifts, SEPM (Society for Sedimentary Geology) Special Publication 73*, pp. 179–93.

McCarthy, T.S. and Rubidge, B. 2005. *The story of Earth and Life: A southern African perspective on a 4.6-billion-year journey*. Cape Town: Struik Publishers.

McCarthy, T.S., Arnold, V., Venter, J., and Ellery, W.N. 2007. The collapse of Johannesburg's Klip River wetland. *South African Journal of Science*, 103, pp. 391–397.

McCarthy, T. S., Tooth, S., Jacobs, Z., and Ellery, W. N. 2011. The origin and development of the Nyl River floodplain wetland, Limpopo Province, South Africa: Trunk-tributary river interactions in a dryland setting. *The South African Geographical Journal*, 93, pp. 172–190.

McNamara, S. 2017. *The influence of landscape disconnectivity on the structure and function of the Krom river, Eastern Cape, South Africa*. Grahamstown: Rhodes University (MSc Thesis) [pdf].

Middleton, B.J. and Bailey, A.K. 2008. Water resources of South Africa: book of maps. *Water Resources*.

Mieth, A. and Bork, H. 2005. History, origin and extent of soil erosion on Easter Island (Rapa Nui). *Catena*, 63, pp. 244–260.

Mitsch, W.J. and Gosselink, J.G. 1993. *Wetlands, Second Edition*. New York: Van Nostrand Reinhold, pp. 722.

Mitsch, W.J. and Gosselink, J.G. 2015. *Wetlands, Forth Edition*. New Jersey: John Wiley and Sons, Ltd, pp. 600.

Mucina, L. and Rutherford, M.C. (Eds). 2006. The vegetation of South Africa, Lesotho and Swaziland. *Strelitzia 19*. South African National Biodiversity Institute, Pretoria.

Nanson, G.C. and Croke, J.C. 1992. A genetic classification of floodplains. *Geomorphology*, 4(6), pp. 459-486.

Nelson, M.S. and Rittenour, T.M., 2014. Middle to late Holocene chronostratigraphy of alluvial fill deposits along Kanab Creek in southern Utah. *Geology of Utah's Far South: Utah Geological Association, Publication*, 43, pp. 97-116.

Ngetar, N.S. 2011. *Causes of wetland erosion at Craigieburn, Mpumalanga Province, South Africa*. University of KwaZulu-Natal (MSc Thesis) [pdf].

Nieuwoudt, H., Grundling, P.L., Du Toit, L. and Tererai, F. 2018. Pietersieliekloof wetland rehabilitation project–Investing in the future. *Water Wheel*, 17(2), pp. 26-28.

Nsor, C.A. and Gambiza, J. 2013. Land use changes and their impacts on the vegetation of the Krom River Peat Basin, South Africa. *Science Journal of Environmental Engineering Research*, pp. 1–12.

Nyssen, J., Poesen, J., Veyret-Picot, M., Moeyersons, J., Haile, M., Deckers, J., Dewit, J., Naudts, J., Teka, K. and Govers, G. 2006. Assessment of gully erosion rates through interviews and measurements: a case study from Northern Ethiopia. *Earth Surface Processes and Landforms*, 31(2), pp. 167–185.

Patton, P.C. and Schumm, S.A. 1975. Gully Erosion, Northwestern Colorado: A threshold phenomenon. *Geology*, 3(2), pp. 88–90.

Patton, P. C. and Schumm, S. A. 1981. Ephemeral-stream processes: Implications for studies of Quaternary valley fills. *Quaternary Research*, 15, pp. 24–43.

Phillips, J. D. 2010. The job of the river. *Earth Surface Processes and Landforms, 35*(3), pp. 305–313.

Poesen, J., Nachtergaele, J., Verstraeten, G. and Valentin, C. 2003. Gully erosion and environmental change: importance and research needs. *Catena*, 50(2–4), pp. 91–133.

Prosser, I.P. and Slade, C.J. 1994. Gully formation and the role of valley-floor vegetation, southeastern Australia. *Geology*, 22(12), pp.1127-1130.

Pulley, S., Ellery, W.N., Lagesse, J.V., Schlegel, P.K., McNamara, S.J. 2018. Gully erosion as a mechanism for wetland formation: An examination of two contrasting landscapes. *Land Degradation and Development*, 29(6), pp. 1756-1767.

Rebelo, A.G., Boucher, C., Helme, N., Mucina, L. and Rutherford, M.C. 2006. Fynbos biome. In: Mucina, L. and Rutherford, M.C. (Eds). The Vegetation of South Africa, Lesotho, and Swaziland. Pretoria: South African National Biodiversity Institute, pp. 53–219.

Rebelo A.J. 2012. *An ecological and hydrological evaluation of the effects of restoration on ecosystem services in the Krommerivier system, South Africa*. University of Stellenbosch (MSc Thesis) [pdf].

Rebelo A.J., le Maitre D.C., Esler K.J. and Cowling R.M. 2015. Hydrological responses of a valley-bottom wetland. to land-use/land-cover change in a South African catchment: making a case for wetland restoration. *Restoration Ecology*, 23, pp. 829–842.

Rebelo A.J. 2018. *Ecosystem Services of Palmiet Wetlands: The Role of Ecosystem Composition and Function*. University of Antwerp and University of Stellenbosch. (PhD Thesis) [pdf].

Rebelo A.J., Emsens W.J., Meire P. and Esler K.J. 2018. The impact of anthropogenically induced degradation on the vegetation and biochemistry of South African palmiet wetlands. *Wetlands Ecology and Management*, 26, pp. 1157–1171.

Riddell, E.S., Everson, C., Clulow, A. and Mengistu, M. 2013. The hydrological characterisation and water budget of a South African rehabilitated headwater wetland system. *Water SA*, *39*(1), pp.57-66.

Rubey, W.W. 1933. Equilibrium-conditions in debris-laden streams. *Eos, Transactions American Geophysical Union*, 14(1), pp. 497–505.

Russell, W., Sieben, E., Braack, M., Ellery, W., Kotze, D., Mitchell, S., Brooker, C. and Breen, C. 2009. WET-RehabMethods national guidelines and methods for wetland rehabilitation. *WRC Report*, (341/09).

Schlegel, P.K. 2017. *Spatial Variation In Modelled Hydrodynamic Characteristics Associated With Valley Confinement In The Kromme River Wetland: Implications For The Initiation Of Erosional Gullies.* Grahamstown: Rhodes University (MSc Thesis) [pdf].

Schneider, V.R. and Arcement, G.J. 1989. *Guide for Selecting Manning's Roughness Coefficients for Natural Channels and Flood Plains*. US Geological Survey Water-Supply Paper No. 2339(38), pp. 22.

Schumm, S.A. and Hadley, R.F. 1961. *Progress in the application of landform analysis in studies of semiarid erosion*. US Geological Survey Circular No. 437, pp. 1–18

Schumm, S.A. 1973. Geomorphic thresholds and complex response of drainage systems. *Fluvial geomorphology*, 6, pp. 69-85.

Schumm, S.A., 1977. *The fluvial system*. United States of America, New York: John Wiley and Sons.

Schumm, S.A. 1979. Geomorphic thresholds: the concept and its applications. *Transactions of the Institute of British Geographers*, 4(4), pp. 485–515.

Schumm, S.A. 1981. Evolution and response of the fluvial system, sedimentologic implications. In: F. G. Ethridge, R. M. Flores (Eds.). Recent and ancient nonmarine depositional environments: models of exploration. SEPM Society for Sedimentary Geology.

Sieben, E.J.J. 2012. Plant functional composition and ecosystem properties: the case of peatlands in South Africa. *Plant Ecology*, 213, pp. 809–820.

Sieben, E.J.J., Khubeka S.P., Sithole S., Job N.M. and Kotze D.C. 2018. The classification of wetlands: integration of top-down and bottom-up approaches and their significance for ecosystem service determination. *Wetlands Ecology and Management*, 26, pp. 441–458.

Snyder, N.P., Nesheim, A.O., Wilkins, B.C. and Edmonds, D.A. 2013. Predicting grain size in gravel-bedded rivers using digital elevation models: Application to three Maine watersheds. *Bulletin*, 125(1-2), pp.148-163.

Streeter, V.L. 1971. *Fluid mechanics*. New York: McGraw-Hill Book Co., 5th ed., pp. 705.

Streever, W.J. 1999. *An International Perspective on Wetland Rehabilitation*. The Netherlands: Kluwer Academic Publishers, pp. 338.

Tanner, J.L., Smith, C., Ellery, W.N. and Schlegel, P. 2019. Palmiet wetland sustainability: a hydrological and geomorphological perspective on system functioning. *WRC Report*, (2548/1/18).

Tebebu, T., Abiy, A., Dahlke, H., Easton, Z., Zegeye, A., Tilahun, S., Collick, A., Kidnau, S., Moges, S., Dadgari, F. and Steenhuis, T. 2010. Surface and subsurface flow effect on permanent gully formation and upland erosion near Lake Tana in the Northern Highlands of Ethiopia. *Hydrology and Earth System Sciences*, 14(11), pp. 2207-2217.

Toerien, D.K. 1986. 1:250 000 3324 Port Elizabeth geological map. Council for Geoscience, Pretoria.

Tooth, S., McCarthy, T.S., Brandt, D., Hancox, P.J. and Morris, R. 2002. Geological controls on the formation of alluvial meanders and floodplain wetlands: the example of the Klip River, Eastern Free State, South Africa. *Earth Surface Processes and Landforms*, 27, pp. 797–815.

Tooth, S., Brandt, D., Hancox, P.J. and McCarthy, T.S. 2004. Geological controls on alluvial river behaviour: a comparative study of three rivers on the South African Highveld. *Journal of African Earth Sciences*, 38, pp. 79–97

Tooth, S. and McCarthy, T.S. 2007. Wetlands in drylands: Geomorphological and sedimentological characteristics, with emphasis on examples from southern Africa. *Progress in Physical Geography*, 31(1), pp. 3–41.

Tooth, S., McCarthy, T.S., Rodnight H., Keen-Zebert A., Rowberry M.D., Brandt D. 2010. Geomorphological dynamics of South African floodplain wetlands and the implications for management planning. Association of American Geographers Annual Meeting, 14-18 April 2010, Washington DC, United States of America.

Tooth, S., Hancox, J., Brandt, D., Mccarthy, T. S., Jacobs, Z., and Woodborne, S. 2013. Controls on the genesis, sedimentary architecture, and preservation potential of dryland alluvial successions in stable continental interiors: Insights from the incising Modder River, South Africa. *Journal of Sedimentary Research*, 83, pp. 541–561.

Valentin, C., Poesen, J. and Li, Y. 2005. Gully erosion : Impacts, factors and control. *Catena*, 63(2), pp. 132–153

van Eck, C. 2022, In Prep. *The regeneration of palmiet (Prionium serratum) following geomorphic disturbance: a case study of the Kromme wetland*. Grahamstown: Rhodes University (MSc thesis) [PDF].

Wainwright, J. and Mulligan, M. 2013. *Environmental modelling: finding simplicity in complexity*. United Kingdom: John Wiley and Sons.

Walsh, R.P.D. and Lawler, D.M. 1981. Rainfall seasonality: description, spatial patterns and change through time. *Weather*, 36(7), pp.201-208.

Wasson, R.J., Caitcheon, G., Murray, A.S., McCulloch, M. and Quade, J. 2002. Sourcing sediment using multiple tracers in the catchment of Lake Argyle, Northwestern Australia. *Environmental Management*, 29 (5), pp. 634–646.

Wohl, E., 2004. Limits of downstream hydraulic geometry. *Geology*, 32(10), pp. 897-900.

Womack, W.R. and Schumm, S.A. 1977. Terraces of Douglas Creek, northwestern Colorado: an example of episodic erosion. *Geology*, 5(2), 72–76.

APPENDIX 1

GEOsense

Palmiet Wetland near Kareedouw
Lidar survey

Document No:	**1**
Revision:	0
Author:	HC de Wet (S0472)
Effective Date:	04/11/2019

Notice

Document enquiries can be directed to:

Attention: HC de Wet
E-Mail: Hennie@promap.co.za
Mobile: +27 (0) 82 573 1335

CONTENTS

1. Introduction

Geosense was appointed to perform an aerial LiDAR survey of the Palmiet wetlands near Kareedouw. The project was flown on the **4th Nov 2019**, between 9:50 am and 10:45 am.

1.1 Survey Area

Figure 1.1 below shows the area of interest (study area – 1 282ha).

Figure 1.1 Study areas for LiDAR survey

1.2 Flight Specifications

The following flight specifications were applied during the survey:

- Survey took place with a fixed wing aircraft
- Flying height – 700 meters over study areas
- Flying speed – 110 knots
- Scan Rate – 300 KHz
- Point density p/m² - approximately 5.5 points per sqm

2. Survey control

The projection for the whole survey area was Hartebeesthoek Transverse Mercator, Central Meridian 25. Ellipsoidal heights were converted to orthometric heights using the SAG2010 geoid model.

Geosense was asked to survey the control for the survey. See 2.1.1 below. These were used to check the position of the survey. Three points were placed along the route and pre-marked.

T120 (ME-AL) Melkhoutkraal was held as a fixed point in the network and T194 (Joubertina) as a check point. See the network report in the appendix.

2.1 Coordinates Used During Post Processing

Base-Station Coordinates on the day of flying:

Hartebeesthoek Geographical			
Name	Lat	Long	Ellipsoidal height
KAR3	-33 53 52.01987	24 07 09.18216	332.613

Table 2.1.1 Control point coordinates surveyed by Promap

Name	Easting	Northing	Ellipsoidal height	Orthometric height SAG2010
JOUBERTINA T194	104 459.085	3 744 353.692	779.817	749.861
KAR1	92 644.881	3 748 754.548	470.364	440.614
KAR3	81 469.482	3 752 672.671	332.613	303.031
KAR4	72 810.013	3 755 155.526	303.721	274.370
ME-AL T120	70 172.763	3 756 020.828	349.513	320.200

3. Equipment used

3.1 Aerial lidar systems

Promap uses the advanced Riegl systems:
Harrier 68i & Rollei/PhaseOne 60 MegaPixel Camera.

3.2 GPS receivers

GPS base station is deployed on day of flight, and can be any of the following: Trimble R4/5800, Trimble 5700 and Geomax zenith 10.

4. Overview and Workflows

4.1 Team Responsible for the Aerial Survey (Expertise & Qualifications)

Mnr. Willie de Winnaar

- Pilot/CPL rating,
- 1 year with ProMap

Mnr. Armand Swanepoel

- System Operator in Aircraft
- 5 years with ProMap

Mnr. Hennie de Wet

- Surveyor/LiDAR Processing,
- SAGC #S0472, Nat. Dip. Surveying – CPUT,
- 32 years of experience, 1 year with ProMap

Mnr. Janco vd Merwe

- Technical Director/Project Manager/QC,
- SAGC# PGP0186,
- Nat. Dip. Cartography - TUT,
- B.Sc. Honors Geo-Informatics -UP,
- Project Management Principals (PMP) – UP
- 10 years at ProMap/Geosense

5. Processes and Workflow of Project/Program

5.1 Workflow followed during Aerial Survey project/program

5.1.1 Flight planning:
The flight is planned according to the project requirements and the system to be used.
GCP positions will be determined. Managers will do the quality control.

5.1.2 Mission/data capture:
If required, GCP's will be established.
Base station is setup in advance and operator also serves as weather observer.
The mission is flown; quality control is done in the air using the lidar capture software.

5.1.3 Post processing:
The raw field data is downloaded.
IMU/GPS processing is done to obtain trajectory, QC done on trajectory (RMS X, Y and Z).
Raw lidar data is processed using system specific software that combines the trajectory and field lidar data.
Manager does a quality control check on the trajectory and raw lidar.

5.1.4 Production:
Lidar point cloud is imported into a project and filtered into ground and non-ground.
From the ground a DTM is extracted for the processing of the images in TerraPhoto.
Tie points are run to determine inter image orientation as well as tie points with known points to check the position of the survey. The ortho rectification of the images is done and image tiles created.
Quality control is done on the lidar point cloud using the control.
The classification of the ground points are manually checked to ensure that there are no holes in the data set.
Quality control then done by manager.

DTM is extracted from the ground points using algorithms to ensure accurate surfaces.

6. Accuracies

Accuracies obtained are dependent on the GPS data logged in the air and ground and can vary on a day to day basis.

The accuracy of the trajectory is stated as North position Error RMS, east position Error RMS and down position Error RMS.

Accuracy of the lidar point cloud over bare ground is: XY <10cm and Z<5cm.

7. Quality Control

7.1 Combined solution result from post processing (IMU/GPS accuracies)

Figure 4.1 IMU/GPS solution (trajectory)

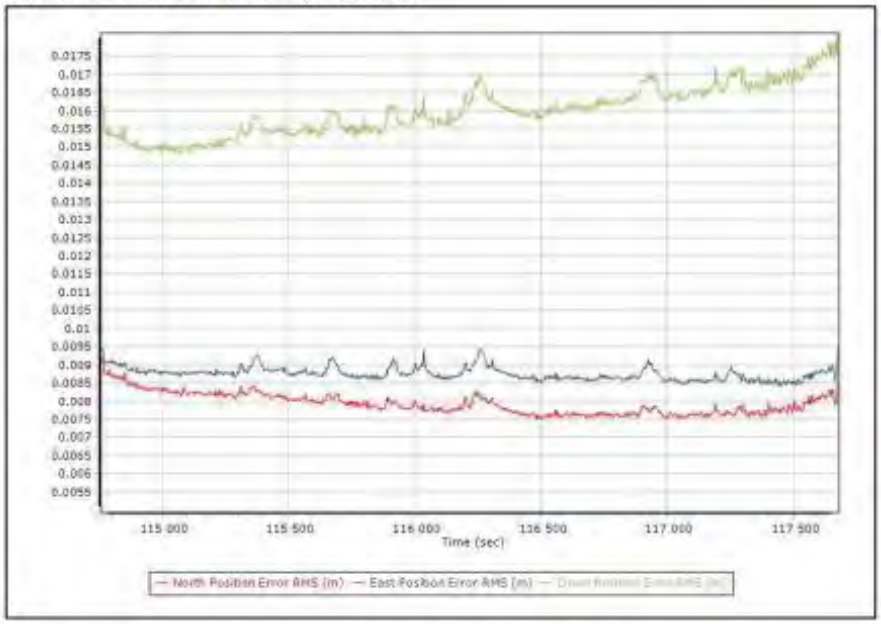

From the graph above it is apparent that the RMS values for the X, Y and Z respectively were below 20mm. This RMS values can be seen as a direct correlation to the accuracy of the aerial survey data.

7.2 Trajectory Plot

Figure 7.2 Trajectory/Flight plan of the aerial survey that took place on the 4th of November 2019.

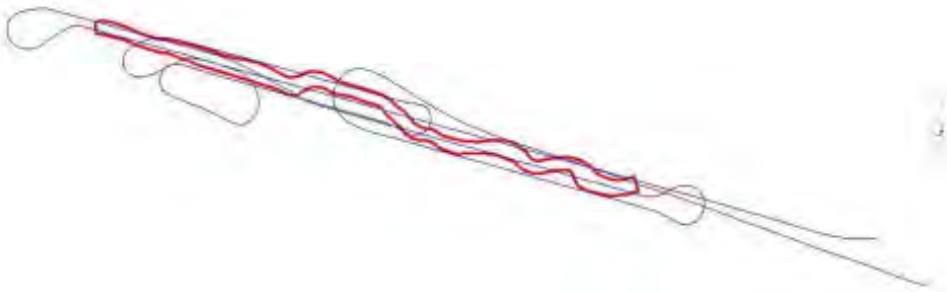

In total 6 lines were flown in clear weather conditions

7.3 Number of GPS Satellites

Figure 7.3 Indication of the number satellites during the mission

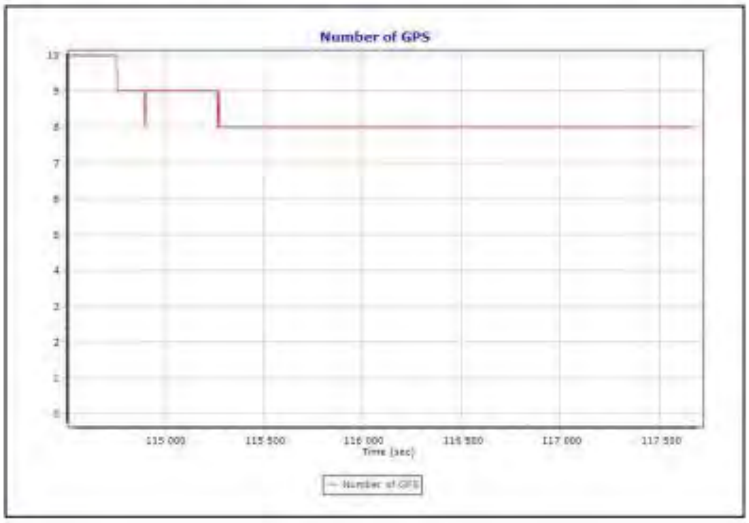

7.4 PDOP

Figure 7.4 Indication of the PDOP during the mission

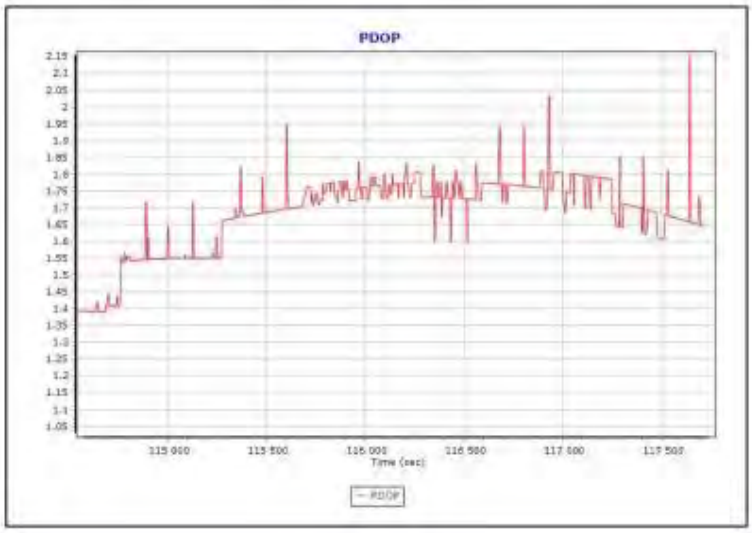

7.5 DTM compared to mine control points (dz)

Table 7.5 RMS value (LiDAR)

It is clear that the RMS values for all three surfaces are below 4cm when compared to the control points.

Number	Easting	Northing	Known Z	Laser Z	Dz
KAR1	-92644.880	-3748754.548	440.614	440.630	+0.016
KAR3	-81469.482	-3752672.671	303.031	303.000	-0.031
KAR4	-72810.013	-3755155.526	274.370	274.370	-0.000

Average dz	-0.005
Minimum dz	-0.031
Maximum dz	+0.016
Average magnitude	0.016
Root mean square	0.020
Std deviation	0.024

7.6 Photo Tie-point adjustment report known XY

Table 7.6 Average mismatch (Imagery)

Average mismatch	4.5027 cm
Start average	4.5027 cm
Final average	4.2896 cm

Known point comparison

Number	Easting	Northing	Elevation	Dx	Dy	Dz
1	-92644.883	-3748754.544	470.542	+0.013	-0.063	-0.024
2	-81469.484	-3752672.669	332.622	+0.011	+0.058	+0.003
3	-72810.012	-3755155.527	303.551	-0.030	-0.009	+0.011
Average from known to tie point				-0.002	-0.005	-0.003

8. Deliverables

- DTM of study area in ascii format per block reference
- Non-ground points in ascii format per block reference
- Images in ECW and Geotif format per block reference
- All lidar in las format per block reference
- 0.5m contours in dgn, dxf and dwg format
- Block reference file in dgn, dxf and dwg format
- Survey report

Appendix:

```
                ************************************************
                * NETWORK - WEIGHTED GNSS NETWORK ADJUSTMENT     *
                *                                                *
                * (c) Copyright NovAtel Inc., (2019)             *
                *                                                *
                * Version: 8.80.2720                             *
                *                                                *
                *Kareedouw_Network_2.net
                ************************************************

DATE(m/d/y): Wed.  11/13/19   TIME:  7:48:22

*****************************************************************

  DATUM:            'WGS84'
  GRID:             WG25
  SCALE_FACTOR:     0.2321
  CONFIDENCE LEVEL: 39.40 %   (Scale factor is 1.0009)


*****************************************************************
    INPUT CONTROL/CHECK POINTS
*****************************************************************

STA_ID     TYPE    -- LATITUDE --  -- LONGITUDE --  ELLHGT -   H2-SD   V-SD
JOUBERTIN  CHK-3D -33 49 14.77600   23 52 18.10630    779.456
ME-AL      GCP-3D -33 55 43.60210   24 14 27.85450    349.513 0.00500 0.00500


*****************************************************************
    INPUT VECTORS
*****************************************************************

SESSION NAME           VECTOR(m)    ------ Covariance (m) [unscaled] ------
                        DX/DY/DZ          standard deviations in brackets
KAR1 to JOUBERTIN (1)  7311.2617   1.9863e-04 (0.0141)
                      -9629.6662   7.1646e-05  6.6355e-05 (0.0081)
                       3584.2309  -8.1086e-05 -3.7990e-05  8.7366e-05 (0.0093)

KAR1 to KAR3 (1)      -6691.7768   2.2108e-04 (0.0149)
                       9210.8081   8.6542e-05  7.7025e-05 (0.0088)
                      -3260.7840  -1.1663e-04 -5.3094e-05  1.1947e-04 (0.0109)
```

```
KAR1 to KAR4 (1)       -11549.6863   4.9071e-05 (0.0070)
                        16499.6551   2.0201e-05  2.0776e-05 (0.0046)
                        -5363.4863  -2.1008e-05 -1.0726e-05  2.3963e-05 (0.0049)

KAR4 to JOUBERTIN (1)  18860.9562   1.9463e-04 (0.0140)
                       -26129.3166   7.7127e-05  7.3939e-05 (0.0086)
                         8947.7216  -7.8862e-05 -3.9375e-05  8.4621e-05 (0.0092)

KAR4 to KAR3 (1)        4857.9080   2.0150e-04 (0.0142)
                       -7288.8506   7.9514e-05  7.0510e-05 (0.0084)
                        2102.7087  -1.0699e-04 -4.9039e-05  1.1031e-04 (0.0105)

ME-AL to KAR1 (1)      13045.0022   1.8316e-04 (0.0135)
                       -18711.4881   5.1873e-05  7.1765e-05 (0.0085)
                         6123.5080  -1.0586e-04 -2.5015e-05  1.2368e-04 (0.0111)

ME-AL to KAR4 (1)       1495.3154   5.1778e-05 (0.0072)
                       -2211.8214   1.5460e-05  2.0958e-05 (0.0046)
                         760.0091  -3.0278e-05 -7.4394e-06  3.7449e-05 (0.0061)



*****************************************************************
    OUTPUT VECTOR RESIDUALS (East, North, Height - Local Level)
*****************************************************************
```

SESSION NAME	-- RE -- (m)	-- RN -- (m)	-- RH -- (m)	- PPM -	DIST (km)	- STD - (m)
KAR1 to JOUBERTIN (1)	0.0011	0.0032	0.0032	0.368	12.6	0.0090
KAR1 to KAR3 (1)	-0.0005	0.0007	-0.0023	0.207	11.8	0.0098
KAR1 to KAR4 (1)	0.0017	-0.0024	0.0015	0.159	20.8	0.0047
KAR4 to JOUBERTIN (1)	-0.0014	-0.0033	-0.0037	0.152	33.4	0.0091
KAR4 to KAR3 (1)	0.0005	-0.0006	0.0021	0.251	9.0	0.0094
ME-AL to KAR1 (1)	0.0071	-0.0043	0.0068	0.455	23.6	0.0094
ME-AL to KAR4 (1)	-0.0020	0.0014	-0.0023	1.195	2.8	0.0051
RMS	0.0030	0.0026	0.0035			

$ - This session is flagged as a 3-sigma outlier

```
*****************************************************************
    CHECK POINT RESIDUALS (East, North, Height - Local Level)
*****************************************************************

STA. NAME     -- RE --    -- RN --    -- RH --
                 (m)         (m)         (m)
JOUBERTIN       0.0231      0.0688      0.3610
              ---------------------------------
RMS             0.0231      0.0688      0.3610

*****************************************************************
    CONTROL POINT RESIDUALS (ADJUSTMENT MADE)
*****************************************************************

STA. NAME     -- RE --    -- RN --    -- RH --
                 (m)         (m)         (m)
ME-AL          -0.0000      0.0000      0.0000
              ---------------------------------
RMS             0.0000      0.0000      0.0000

*****************************************************************
    OUTPUT STATION COORDINATES (LAT/LONG/HT)
*****************************************************************

STA_ID       -- LATITUDE --   -- LONGITUDE --  - ELLHGT -   ORTHOHGT
JOUBERTIN  -33 49 14.77377    23 52 18.10720    779.8170   749.8611
KAR1       -33 51 41.55098    23 59 55.77220    470.3644   440.6138
KAR3       -33 53 52.01987    24 07 09.18216    332.6126   303.0310
KAR4       -33 55 14.87624    24 12 45.44108    303.7205   274.3703
ME-AL      -33 55 43.60210    24 14 27.85450    349.5130   320.1997


*****************************************************************
    OUTPUT STATION COORDINATES (GRID)
*****************************************************************

STA_ID        - EASTING -    - NORTHING -  - ELLHGT -   ORTHOHGT
                    (m)            (m)         (m)        (m)
JOUBERTIN   -104459.0854 -3744353.6918    779.8170   749.8611
KAR1         -92644.8805 -3748754.5483    470.3644   440.6138
KAR3         -81469.4824 -3752672.6708    332.6126   303.0310
KAR4         -72810.0126 -3755155.5255    303.7205   274.3703
ME-AL        -70172.7628 -3756020.8275    349.5130   320.1997
```

```
*****************************************************************
    OUTPUT VARIANCE/COVARIANCE
*****************************************************************
                                                 2
STA_ID      SE/SN/SUP  --------- CX matrix (m )-----------
            (39.40 %)  (not scaled by confidence level)
              (m)           (ECEF, XYZ cartesian)
JOUBERTIN     0.00565   5.7733e-05
              0.00580   1.1635e-05  3.7165e-05
              0.00945  -1.4988e-05 -5.9431e-06  4.1905e-05

KAR1          0.00536   3.9061e-05
              0.00538   4.5873e-06  3.0658e-05
              0.00680  -7.5798e-06 -2.3165e-06  3.3990e-05

KAR3          0.00564   5.9340e-05
              0.00574   1.2576e-05  3.7509e-05
              0.00981  -1.8645e-05 -7.3537e-06  4.5221e-05

KAR4          0.00527   3.4745e-05
              0.00528   2.9233e-06  2.8927e-05
              0.00633  -5.6335e-06 -1.4166e-06  3.1882e-05

ME-AL         0.00500   2.5000e-05
              0.00500   2.7285e-20  2.5000e-05
              0.00500  -1.8190e-20  1.8190e-20  2.5000e-05



*****************************************************************
    VARIANCE FACTOR = 1.0002

    Note: Values < 1.0 indicate statistics are pessimistic, while
          values > 1.0 indicate optimistic statistics. Entering this
          value as the network adjustment scale factor will bring
          variance factor to one.
*****************************************************************
```